2020-04-27

Electrical Characterization and Annealing of DNA Origami Templated Gold Nanowires

Tyler Richard Westover
Brigham Young University

Electrical Characterization and Annealing of DNA Origami Templated Gold Nanowires

Tyler Richard Westover

A thesis submitted to the faculty of
Brigham Young University
in partial fulfillment of the requirement for the degree of

Masters of Science

Robert C. Davis, Chair
Richard R. Vanfleet
Adam T. Woolley

Department of Physics and Astronomy
Brigham Young University

Abstract

Electrical Characterization and Annealing of DNA Origami Templated Gold Nanowires

Tyler Richard Westover
Department of Physics and Astronomy, BYU
Masters of Science

DNA origami templates have been studied due the versatility of shapes that can be designed and their compatibility with various materials. This has potential for future electronic applications. This work presents studies performed on the electrical properties of DNA origami templated gold nanowires. Using a DNA origami tile, gold nanowires are site specifically attached in a "C" shape, and with the use of electron beam induced deposition of metal, electrically characterized. These wires are electrically conductive with resistivities as low as 4.24×10^{-5} Ω-m. During moderate temperature processing nanowires formed on DNA origami templates are shown to be affected by the high surface mobility of metal atoms. Annealing studies of DNA origami gold nanowires are conducted, evaluating the effects of atom surface mobility at various temperatures. It is shown that the nanowires separate into individual islands at temperatures as low as 180° C. This work shows that with the use of a polymer template the temperature at which island formation occurs can be raised to 210° C. This could allow for post processing techniques that would otherwise not be possible.

Keywords: DNA origami, electrical characterization, gold nanowires, polymer coated anneal

Acknowledgements

I would like to first thank my wife and children for their understanding love and support as I have worked through this degree. For the time they spent at home during class breaks, so I could continue to work in the lab. Their patience with the long days that sometimes turned into long nights at the lab while collecting data. I would also like to thank the rest of my family for their support and encouragement throughout this whole process, and their attempts to understand my explanations of what I was doing for my research.

I would also like to thank the students that I worked with and the other students in the lab that allowed for conversations about the research into the development of methods to overcome hurdles. Especially the other grad students for their help in the writing process with editing and encouragement.

I would like to give thanks to my research advisors Dr. Davis, Dr. Harb and Dr. Woolley for asking hard questions while I presented data that pushed for further understanding. For their help with new ideas and insight into what experiments to try next and when to not worry about something that only happened once. You were able to help me develop and grow as a researcher.

I would like to thank Brigham Young University for the research facilities provided, especially the microscopy department their staff to help train and teach me as I used the equipment in new ways.

Table of Contents

List of Figures

List of Tables

Chapter 1: Introduction

Research has been growing in the field of bottom up manufacturing as a technique that allows for the formation of new structures that would not be possible through top down manufacturing. One such nanoscale technique is DNA origami. DNA origami is named after its resemblance to Japanese paper folding. Pioneered by Rothemund[1], DNA origami involves taking a large single stranded DNA (scaffold strand) and short complementary DNA stands (staple strands) and mixing them in a warmed buffer solution. The attachment of complementary base pairs found in the staple and scaffold strands is termed DNA hybridization. DNA is most stable in a double helix configuration; the scaffold strands hybridize with complementary staple strands allowing a short local double helix to be formed. The base pairs of each half of the staple stands are designed to be complementary with two or more different locations on the scaffold strand, effectively stapling these two scaffold strand locations together. This process happens for each of the staple strands resulting in the folding of the scaffold into complex two or three dimensional shapes[2-8]. Two dimensional origami structures typically have lateral dimensions of about 100 nm[9].

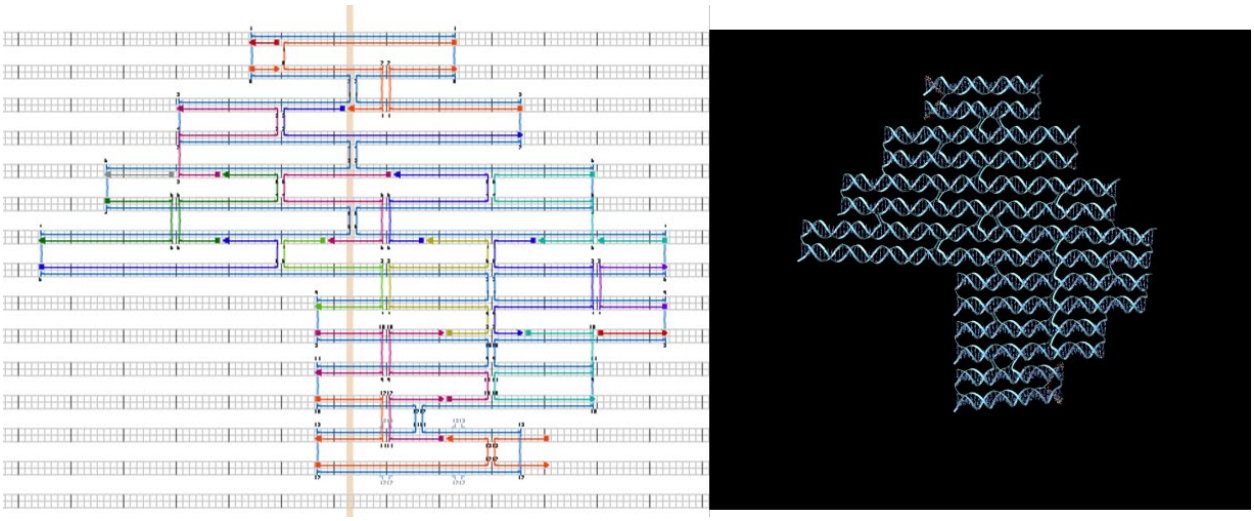

Figure 1. *Computer modeling software used to design and determine the required staple strands for a Pac-Man design. Left CaDNAno allows for pattern design though placement of staple strands. Using visualization software like Maya (right) the final design can be imaged.*

The most common scaffold strand, M13mp18, is 7249 nucleotides long[10] and comes from M13, a virus that infects bacteria. Staple strands are much shorter ranging from 22 to 32 nucleotides. The complexity of the origami shape determines how many different staple strands are required, with typical counts being around 200. Staple strands are custom synthesized and are commercially available. DNA origami computer modeling programs such as CaDNAno can be used to quickly determine the required staple strand sequences (see **Figure 1**). Other programs are used to analyze the robustness of the constructed structure for example, CanDo provide simulation through finite element modeling, and OxDNA simulates using molecular dynamics (see **Figure 2**). The robustness of the structure can be influenced by the staple strand length and placement. Various research groups have utilized DNA origami technology to make complex devices such as tiles[11-12], tubes[13-14], cages[6, 15], switches[16-18] and logic[19].

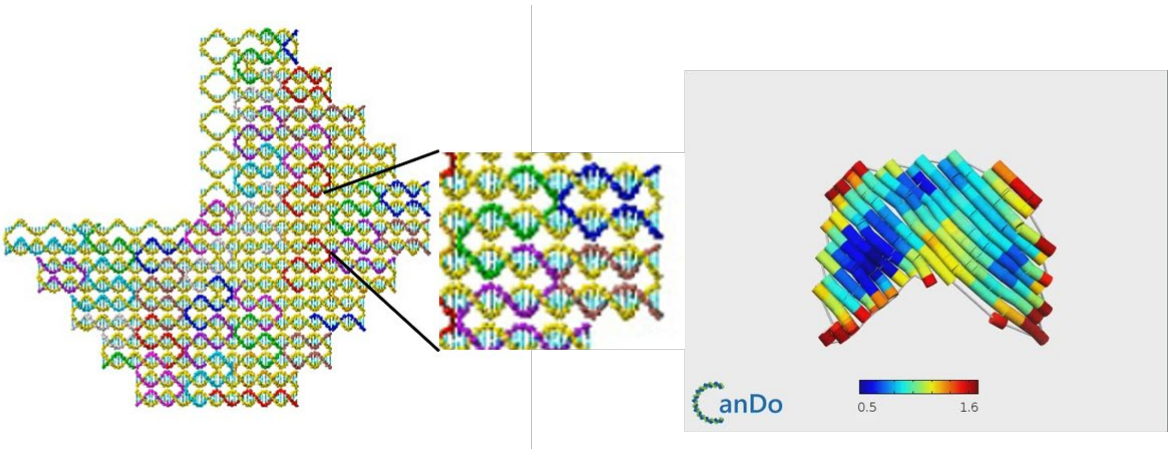

Figure 2*. Visualization tools allow for the stability analysis of DNA origami patterns. On the left OxDNA uses molecular dynamics to check stability on what we called a Pac-Man design using DNA. On the right is a stability simulation of the same design using CanDo.*

The appeal of DNA for designing and building complex nanoscale structures is due to the large number of base paring combinations, a 10 base pair long staple strand, which is typical, can have 4^{10} possibilities which is 1048576 combinations. This results in one unique staple strand for each location on the scaffold. This can be used to attach other nanostructures to specific sites on the origami surface. The site specific nature on DNA of binding nanostructures to origami has been utilized for various applications including: medical, plasmonic[20-21] and electrical[22]. For example, metal particles and rods have been functionalized, by having small strands of DNA attached, allowing for site specific attachment to DNA origami (illustrated in **Figure 3**). Even different materials can be attached to the same DNA origami template[23]. In addition to hybridization, other approaches to attach nanostructures to origami include chemical and electrostatic bonding that allow for direct nanorod attachment are not site specific[24-25]. Various electronic materials that have been attached to DNA origami include Au[3, 22, 24-28], Ag[4, 21], Cu[21, 24, 29-30], Ni[31], Pd[32-33], Te[34] and carbon nanotubes[35]. The size of the nanowires can vary from a few hundred nanometers to several microns. Nanowires formed in this manner have been found to be

conductive, but with resistivities 2-3 orders of magnitude higher than that of the bulk material[22, 26, 36-37].

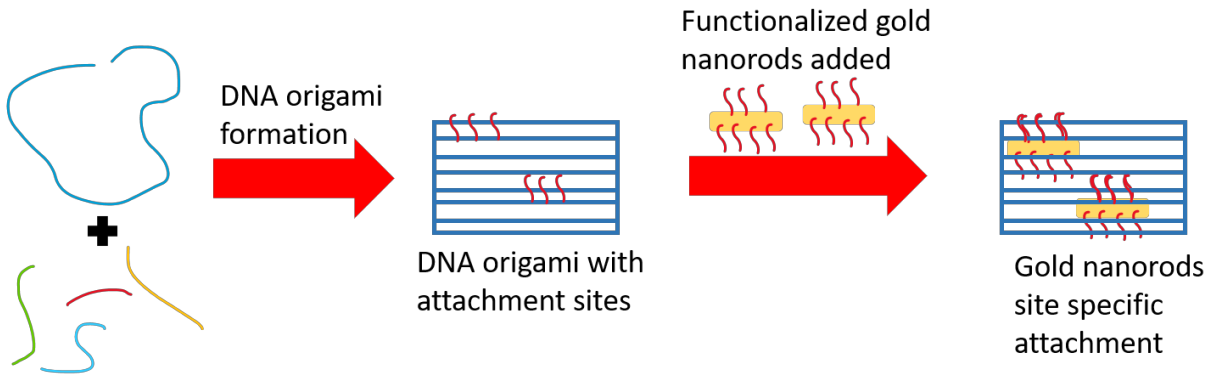

Figure 3. *Schematic representation of the attachment of functionalized gold nanorods. Using a scaffold and staple strands a DNA origami shape can be constructed with free attachment sites. When complementary DNA is attached to gold nanorods the nanorods will site specifically attach.*

Nanowires used in our research are designed to be 400 nm in length. These wires are placed randomly on a substrate, making electrical connections to the nanowires difficult to pattern. The method we employ for contacting these nanowires is electron beam induced deposition (EBID)[12, 38]. Performed in a scanning electron microscope (SEM), this technique uses the electron beam to locally decompose a precursor gas, depositing metal atoms in pre-determined patterns[39-40]. Precursors are typically organometallics solids or liquids that when heated slightly, becoming a gas. With the use of an incorporated gas injection system, the gas is released into the SEM close to the desired write location. As the electron beam is raster scanned in a desired pattern, the electron beam breaks the bonds of the organometallic gas, leaving metal atoms behind as depicted in ***Figure 4***.

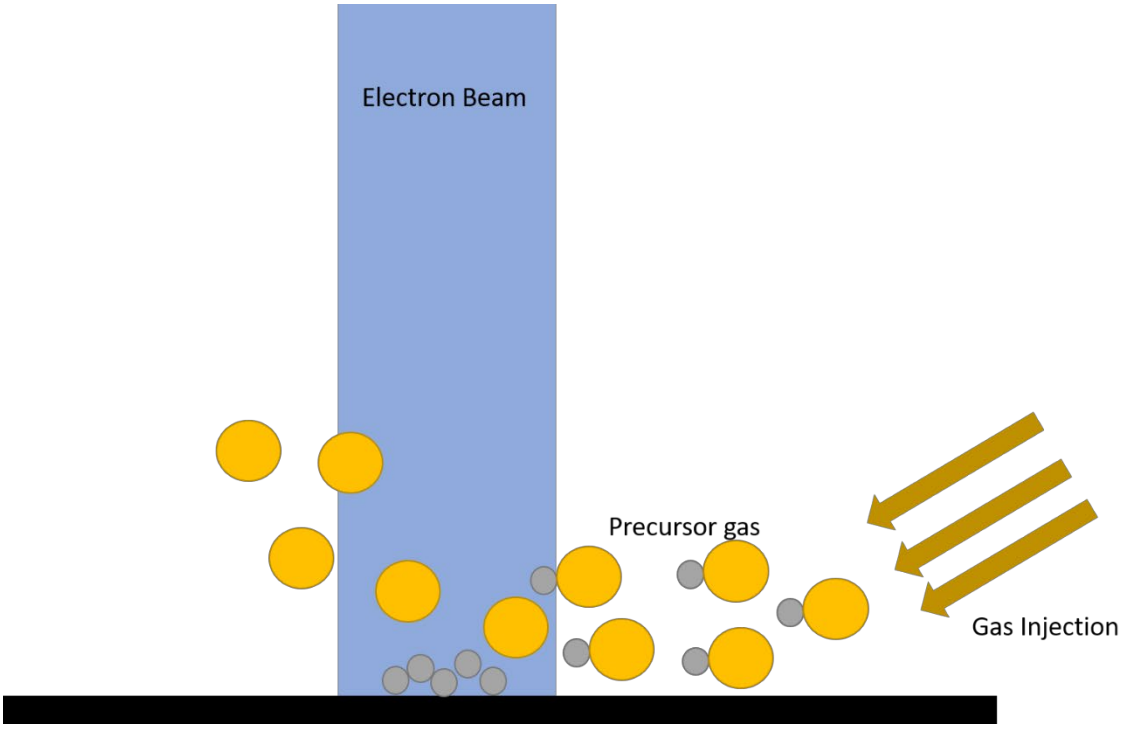

Figure 4. *Cartoon of the electron beam induced deposition process. An organometallic precursor gas is injected into the scanning electron microscope chamber close to the surface of the substrate. The electron beam interacts with the gas molecules breaking off the metal atoms (silver) and releasing the volatile organics (yellow).*

In a process similar to 3D printing but at a much smaller scale, nanoscale two and three dimensional patterns can be created via EBID through the use of computer aided design and control available with the SEM[41]. The resolution of the EBID structures is limited by secondary scattering events but can result in lines below 10 nanometers in width. Electrons from the primary beam interact with the organometallic bonds or the surface and scatter resulting in secondary electrons can interact with molecules outside of the direct beam, which results in features slightly larger than the primary beam diameter. Some of these secondary electrons go further out creating a "halo" around the structure as seen in **Figure 5**. This can lead to

conductive areas outside the proposed area. The size of the "halo" is influenced by the height of the patterned structures due to longer exposure times.

A primary challenge with EBID is that carbon, within the organometallic gas and in the SEM chamber, is deposited at the same time as the metal atoms resulting in high resistivity carbon metal alloys[39, 42-43]. Various in-situ and post processing methods, along with carbon free precursor gases have been developed to decrease the carbon content and related high resistivity[44-47]. One such method for platinum deposition involves post processing EBID structures by exposing to an electron beam in the presence of water vapor[45]. Carbon atoms are moved toward the surface of the matrix allowing for the formation an underlying layer of pure platinum. This method has been shown to result in significant improvements in conductivity.

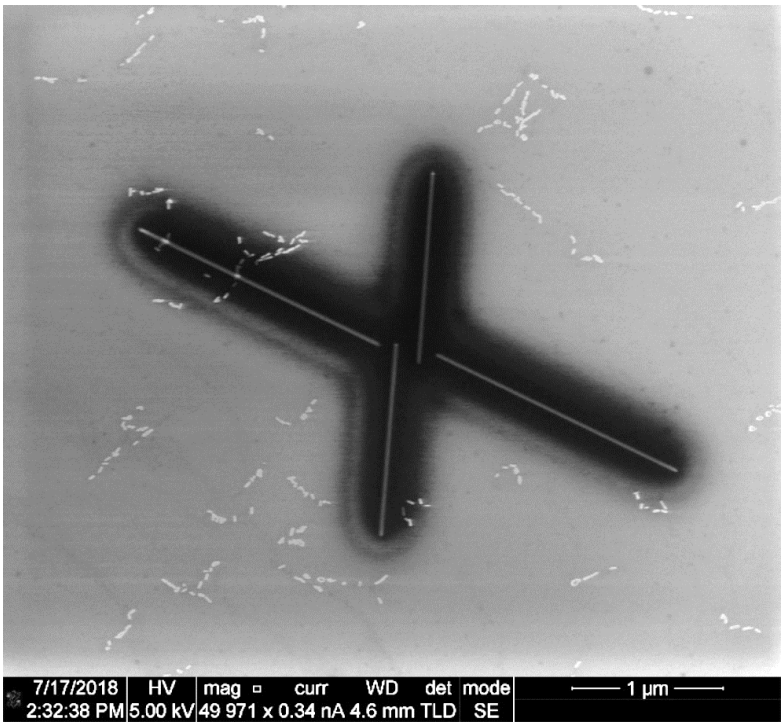

Figure 5. *EBID traces written with tungsten. A visible "halo" surrounds the EBID traces. Although there is significant "halo" visible was found to be non-conductive. The small light structures are DNA origami templated gold nanowires.*

A challenge directly related to nanowire fabrication and its use, is the Rayleigh instability. The Rayleigh instability, originally describing the stability of an infinitely long liquid cylinder, hypothesizes that the cylinder, when perturbed, will spontaneously separate into a series of equally spaced spheres as seen in **Figure 6**. The spacing between spheres is calculated to be 8.89R, where R is the radius of the original cylinder. The specific spacing of 8.89R yields the minimum surface area, resulting in greater stability. A radius perturbation in a nanowire will grow in amplitude until complete spherical separation. This instability is known to occur in nanowires at temperatures far below the melting point of the material[48-50]. Various factors can influence the temperatures when this effect begins to manifest including crystallinity and the size of the wires[51-53].

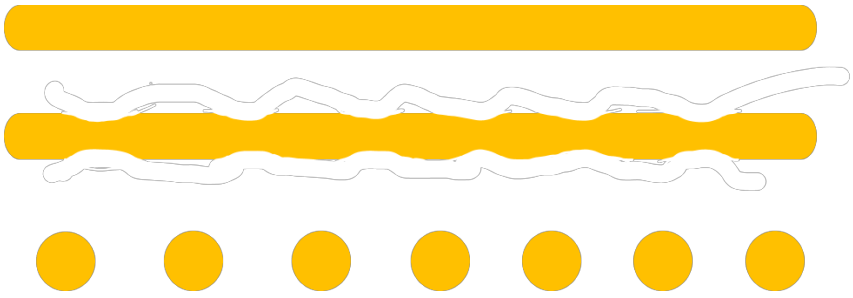

Figure 6. *Illustration of the Rayleigh instability in a gold nanowire. The nanowires begin as a continuous cylinder but develop a perturbation eventually separating into a series of equally spaced spheres.*

The Rayleigh instability can impact the structure of nanowires during various processing techniques which require elevated temperatures. Nanowires are especially susceptible to the morphological instability[49]. The Rayleigh separation of gold nanowires studied here is observed to happen below 180° C. Various important manufacturing processes happen around 200° C including plasma enhanced chemical vapor deposition of silicon dioxide, silicon nitride[54], silicon oxinitride[55], WO_3[56] and ZnO[57] among others[58-59]. In this work we will present a technique that

suppresses the Rayleigh instability allowing for the retention of nanowire morphology up to 210° C.

This thesis is divided up based on the different projects performed and the equipment required for each. Chapter two shows the results of some preliminary work done to characterize the "halo" surrounding EBID tungsten traces. Chapter three and four are separate journal articles that have been submitted for publication. Chapter five summarizes conclusions on the work as a whole and introduces some future directions. At the end of the thesis an appendix is included of standard operating procedures containing process details.

Chapter three is a paper published in Langmuir titled "Four Point Probe Electrical Measurements on Templated Gold Nanowires Formed on Single DNA Origami Tiles". In this paper Tyler Westover and Basu Aryal were equal contribution first authors. The authors used site specific attachment of gold nanorods to create a C-shaped pattern on a single DNA origami tile. These C shaped patterns were connected in a four-point configuration using EBID platinum, that was purified, to determine the resistivity.

Chapter four is a manuscript submitted for review in Langmuir at the time of writing titled "Impact of Polymer-Constrained Annealing on the Properties of DNA Origami Templated Gold Nanowires". Tyler Westover is the first author of this paper. It is shown that with the use of a polymer overcoat, the separation into isolated spheres due to the Rayleigh instability can be delayed until a higher temperature with the same annealing conditions. Electrical connections were patterned using EBID tungsten which did not require a purification step due to the makeup of the organometallic precursor.

The appendix has four separate standard operating procedures (SOPs) that were vital to this work. The first is a modified SOP for thermal evaporation of chrome/gold using a home

built thermal evaporator. This is included because the typical SOP and equipment training only involves one material. For this work gold was deposited but will not adhere to silicon dioxide without an adhesion layer. Chromium was used as an adhesion layer as it bonds to both gold and silicon dioxide. This all must be done without breaking vacuum in the thermal evaporator. The second SOP is a step by step guide to performing electron beam induced deposition (EBID). The third SOP is how to perform purification of platinum traces. If EBID platinum is to be used for electrical measurements it must first be purified to reduces its resistivity. The fourth SOP is a guide for the operation of the in house four-point probe station.

Chapter 2: Four-Point Probe Electrical Measurements on Templated Gold Nanowires Formed on Single DNA Origami Tiles

The following is the text from a published paper in Langmuir authored by Basu R. Aryal, Tyler R. Westover, Dulashani R. Ranasinghe, Diana G. Calvopiña, Bibek Uprety, Robert C. Davis, John N. Harb and Adam T. Woolley. Equal author contributions are attributed to Basu Ayral and Tyler Westover. The author contributions were as follows: Basu Aryal designed and assembled the DNA origami tiles, deposited and electroless plated the gold nanorods; Tyler Westover performed the electron beam deposition of platinum, purification of the platinum and the electrical characterization; Dulashani and Diana assisted Basu in DNA tile formation and nanorod synthesis and deposition; Bibek formulated the gold rod growth and electroless plating processes; Robert Davis, John Harb and Adam Woolley advised and directed the project along with giving guidance for overcoming obstacles as they appeared. Reproduced with permission from "Four-Point Probe Electrical Measurements on Templated Gold Nanowires Formed on Single DNA Origami Tiles, Basu R. Aryal, Tyler R. Westover, Dulashani R. Ranasinghe, Diana G. Calvopiña, Bibek Uprety, John N. Harb, Robert C. Davis, and Adam T. Woolley, Langmuir ***2018*** 34 *(49), 15069-15077" Copyright 2018 American Chemical Society.*

Four Point Probe Electrical Measurements on Templated Gold Nanowires Formed on Single DNA Origami Tiles

Basu R. Aryal[a,*], Tyler R. Westover[b,*], Dulashani R. Ranasinghe[a], Diana G. Calvopiña[a], Bibek Uprety[c], John N. Harb[c], Robert C. Davis[b], Adam T. Woolley[a]

[a] Department of Chemistry and Biochemistry, Brigham Young University, Provo, UT 84602

[b] Department of Physics and Astronomy, Brigham Young University, Provo, UT 84602

[c] Department of Chemical Engineering, Brigham Young University, Provo, UT 84602

[*]Equal author contribution

Correspondence: Adam T. Woolley, phone: 801-422-1701; email: atw@byu.edu

Abstract

Bottom-up nanofabrication is increasingly making use of self-assembled DNA to fabricate nanowires and potential integrated circuits, although yields of such electronic nanostructures are inadequate, as is the ability to reliably make electrical measurements on them. In this paper, we report improved yields and unprecedented conductivity measurements for Au nanowires created on DNA origami tile substrates. We created several different self-assembled Au nanowire arrangements on DNA origami tiles that are approximately 70 nm x 90 nm, through anisotropic growth of Au nanorods attached to specific sites. Modifications to the tile design increased yields of the final desired nanostructures as much as six fold. In addition, we measured the conductivity of Au nanowires created on these DNA tiles (~130 nm long, 10 nm diameter and 40 nm spacing between measurement points) with a four-point measurement technique that utilized electron beam induced metal deposition to form probe electrodes. These nanowires formed on single DNA origami tiles were electrically conductive, having resistivities as low as 4.24×10^{-5} Ω m. This work

demonstrates the creation and measurement of inorganic nanowires on single DNA origami tiles as a promising path toward future bottom-up fabrication of nanoelectronics.

Introduction

Nanofabrication is well-known for generating functional structures at the nanometer scale, with particular emphasis on electronic devices and integrated circuits.[60] Current commercial nanofabrication makes use of traditional, well-established, top-down techniques. In addition, other emerging lithographic techniques, such as soft,[61] nanoimprint[62] and block copolymer,[63] are becoming increasingly important. Typical top-down approaches require increasingly complex patterning processes and tools,[60, 64] therefore, alternative techniques, including bottom-up methods, are in demand to provide improvements in quality, speed, and/or cost.[65-66]

DNA-based methods are promising bottom-up alternatives that may be particularly well suited for complex 3D nanofabrication.[67-71] DNA molecules are robust, versatile and highly effective materials for creating precise, high-quality nanostructures in a variety of shapes[65, 72-73] owing to self-assembly enabled by complementary base pairing. Exploiting these simple base-pair rules, Rothemund[1] created DNA origami by designing and folding a longer single-stranded DNA with the help of oligonucleotide staple strands to produce complex 2D and, eventually, 3D designs.[9, 74] Since then, researchers have fabricated a wide range of DNA structures including tiles,[1] ribbons and tubes,[14, 25] and various dynamic systems such as switches,[18] walkers[75] and circuits.[76] In addition, Ke et al.[11] demonstrated scaffold-free techniques that utilize “DNA bricks” to fabricate multiple shapes. Hence, the unique properties of DNA enable nanofabrication of components, devices and systems at relatively low cost, with low energy consumption and without the need for complex patterning tools.[22, 26-27, 66]

Over the past few years, there has been interest in assembling inorganic nanostructures through the use of biological molecules. DNA is a popular substrate to which metals or semiconductors can be attached, providing a fundamental framework for the creation of functional nanodevices.[77-78] These materials attach to DNA via chemical/electrostatic interaction or base pairing to specific sites.[27] Various materials have been bound to DNA templates including Au,[3, 22, 24-27, 79] Ag,[4, 21] Cu,[21, 24, 29-30] Ni,[80] Pd,[32-33] Te,[81] and carbon nanotubes[35, 82] through site-specific or non-site-specific placement. Site-specific attachment permits molecularly directed placement of select components at particular locations on predesigned DNA templates. Such controlled localization of materials on DNA substrates facilitates fabrication of wires and, ultimately, more complex circuits.

Spherical nanoparticles have generally been used as the seeding materials for metallization on DNA templates. Such particles grow isotropically during plating, enlarging the diameter and ultimately resulting in nanowires that consist of a large number of individually interconnected particle grains. In work done previously by our group, Uprety et al.[25] reported the fabrication of continuous wires on DNA origami using Au nanorod seeds, and compared the results to wires similarly formed on DNA from plated nanoparticles. We found that seeded Au nanorods contributed to anisotropic growth in the length direction with minimum increase in nanowire width/diameter. Two-point conductance measurements were performed on nanowires formed on DNA origami templates ~430 nm long. In a more recent study, we formed different arrangements of metal nanostructures by site-specific deposition of Au nanorods on DNA tiles and subsequent electroless plating; however, yields for fabricated designs were lower than desired.[27] In addition, although the nanowires appeared to be continuous, their lengths were too small to allow conductance measurement using electron beam patterned electrodes as we did previously for longer nanowires.[25]

This paper addresses several deficiencies in previous work by describing methods used to improve yields and to perform four-point probe electrical measurements on Au nanowires fabricated on individual DNA origami tile templates. These DNA tiles (~70 nm x 90 nm) were formed with standard origami methods using an M13mp18 scaffold, where staple strands were extended to provide sticky end attachment points for DNA-coated Au nanorods. We report improved formation yield results for three different shapes, a "plus," a "cross" and a "C-shaped" structure formed on DNA tile surfaces by seeding with Au nanorods followed by electroless deposition as illustrated schematically in Figure 7. These structures are too small for conductance measurements to be made using contact electrodes formed by electron beam lithography patterning and liftoff as we have previously done.[22, 24-26, 78] Thus we instead demonstrate electrical measurements that utilize electron beam induced deposition (EBID) of conductive metal contacts, which enable inorganic structures smaller than a single templating DNA origami tile to be characterized electrically. The EBID approach further enables the use of a four-point probe measurement technique to eliminate the influence of contact resistances to which the previous two-point method was susceptible. These key advances offer a clear path forward for the creation and electrical characterization of increasingly complex electronic structures on individual DNA origami tiles.

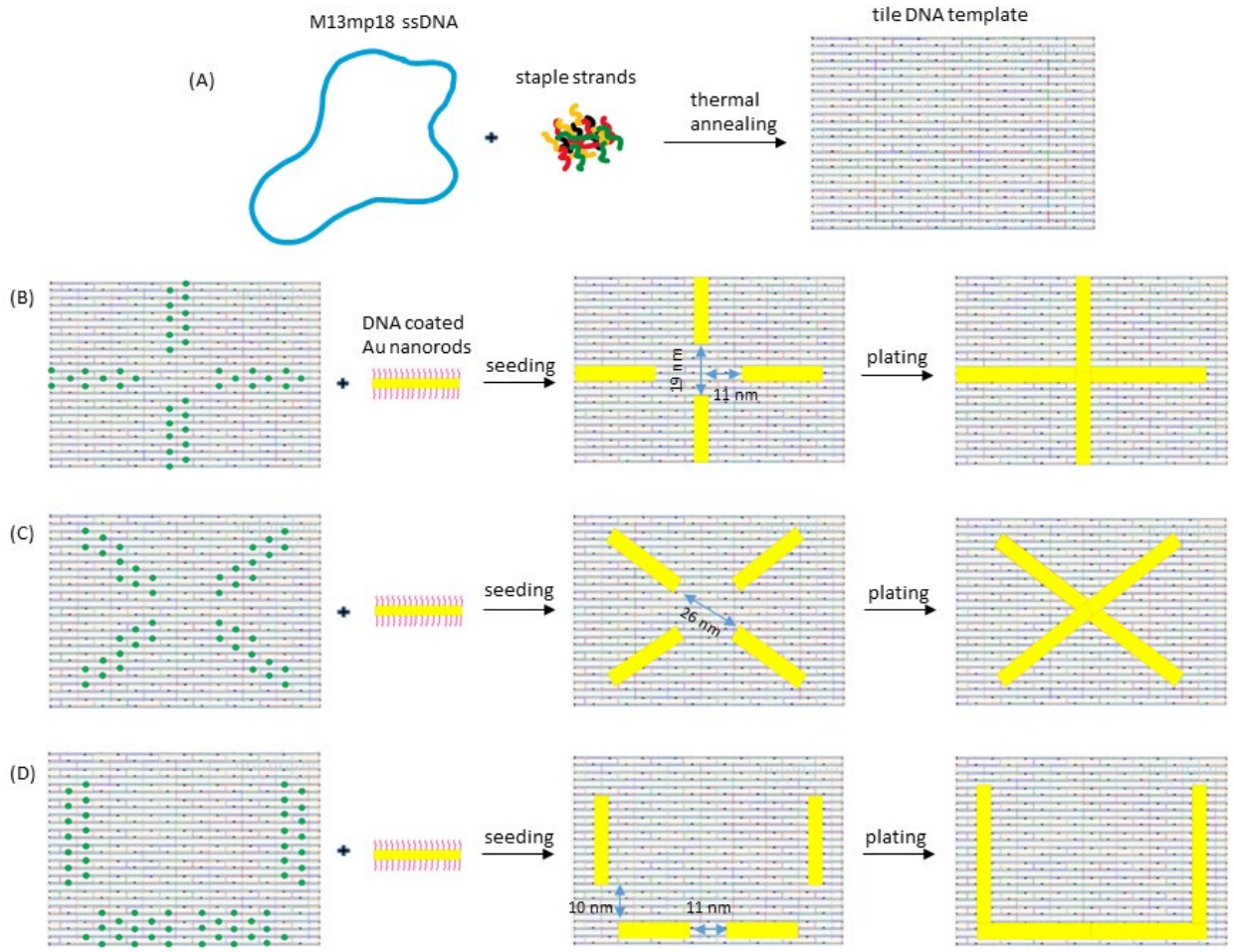

Figure 7. *Schematic diagram of (A) folding single-stranded DNA into tile DNA origami where green dots represent protruding sticky end sequence sites on the staple strands. Site-specific placement of DNA-coated Au nanorods on tile DNA templates to create (B) plus, (C) cross and (D) C shapes through seeding and plating.*

Experimental Section

Chemicals and Materials. All chemicals utilized were similar to those reported by Uprety et al.[27] M13mp18 single-stranded DNA was purchased from New England Biolabs (Ipswich, MA). Staple strands for DNA origami folding were obtained from Eurofins MWG Operon (Huntsville, AL). The dry staple strands were diluted in water to prepare solutions of desired concentrations. For coating DNA on Au nanorods, single-stranded DNA having a thiol group attached to the 5' end

was purchased from Eurofins MWG Operon with PAGE purification and diluted to 1 mM in water. Tris(hydroxymethyl) aminomethane (Tris base) was purchased from Fisher Scientific (Fair Lawn, NJ). Ethylenediaminetetraacetic acid (EDTA) was purchased from Life Technologies (Carlsbad, CA). Acetic acid, hydrochloric acid (HCl), magnesium chloride ($MgCl_2$), and magnesium acetate ($MgAc_2.4H_2O$) were obtained from EMD Chemicals (Gibbstown, NJ). For preparing 10× TAE-Mg^{2+} (pH 8.3) buffer, 400 mM Tris base, 200 mM acetic acid, 10 mM EDTA, and 125 mM $MgAc_2 \cdot 4H_2O$ were used. Cetyl trimethylammonium bromide (CTAB) (H5882, 98%), ascorbic acid and chloroauric acid ($HAuCl_4$) were purchased from Sigma-Aldrich (St. Louis, MO). Silver nitrate was obtained from Mallinckrodt Chemicals (Phillipsburg, NJ). Bis(*p*-sulfonatophenyl) phenylphosphine dihydrate dipotassium salt (BSPP) was purchased from Strem Chemicals (Newburyport, MA). Sodium borohydride ($NaBH_4$) was from Acros (Newark, NJ). Tris(2-carboxyethyl)phosphine (TCEP) was purchased from Alfa Aesar (Ward Hill, MA). Water (18.3 MΩ cm) for aqueous solution preparation as well as rinsing was processed with a Barnstead EASYpure UV/UF purification system (Dubuque, IA).

Gold Nanorod Synthesis and DNA-coated Gold Nanorod Preparation. Au nanorod synthesis followed a reported method used previously in our lab,[83] except the gold reduction time was increased to 4.5 hr to synthesize nanorods of appropriate length (25-30 nm). Coating Au nanorods with DNA also followed a published method,[84] except we used 0.1 M instead of 1 M NaCl during DNA reaction with the Au nanorods.

DNA Origami Design. The tile DNA origami template utilized 6812 of the 7249 bases in the M13mp18 scaffold as reported previously.[27] We designed plus, cross and C shapes where Au nanorods were captured on tile surfaces. The staple strands for capturing Au nanorod seeds had an additional length of 10 adenine nucleotides on the 3′ end. Figure 7 schematically illustrates tile

DNA assembly and linking of Au nanorods to tile DNA templates. Further information about specific staple strand sequences is included in the Appendix

DNA Origami Folding. The tile DNA origami structures were constructed by folding M13mp18 DNA with staple strands in a TECHNE TC-3000 thermal cycler. A mixture of M13mp18 scaffold (2 nM) and staple strands (40 nM of each staple strand) in 10× TAE-Mg^{2+} buffer was initially heated to 95°C for 3 min and then cooled to 4°C over 1.5 hr.[27]

Deposition of Tile DNA Origami onto Si Wafers. The deposition method of tile DNA origami onto Si wafers is similar to what our group previously reported in the literature.[24-25] Oxidized Si wafers (1 cm x 1 cm) were plasma cleaned in a Harrick Plasma Asher (PDC-32G) for 30 s at 18 W. Then, 3 μL of DNA origami (1 nM) in 10× TAE-Mg^{2+} buffer was added to the central region of a cleaned surface and left to adsorb for 25 min at 20°C in a humid chamber. The wafers were then rinsed by gently adding water drops for 9-10 s. The surfaces were then dried with flowing filtered air and imaged using a MultiMode Atomic Force Microscope (MMAFM-2, Bruker, Santa Barbara, CA).

Seeding and Plating Nanorods on DNA Origami. Seeding was done as described by Uprety et al.,[27] except we rinsed the surface with water instead of magnesium acetate solution. In brief, a Au nanorod seeding solution was pipetted onto a Si wafer surface that had DNA tiles previously deposited, and was left for 1 hr in a humid chamber, then rinsed and dried under flowing air. Plating also followed a published approach we adapted,[25] except the rinsing was done with water only. In short, Au plating solution was applied on the seeded DNA tiles for 30 min at room temperature, and after plating the samples were rinsed and dried as was done in the seeding step.

Atomic Force Microscopy (AFM) Imaging. DNA on Si wafers was imaged by AFM using 'Peak Force' tapping mode using ScanAsyst automatic image optimization technology with Bruker silicon tips on nitride cantilevers (ScanAsyst-Air and ScanAsyst-Air HD).

Scanning Electron Microscopy (SEM) Imaging. DNA samples seeded and plated with Au nanorods were imaged by SEM in ultra-high-resolution mode on a FEI Helios Nanolab 600, in high-vacuum mode on a Philips XL30 ESEM FEG, or on a ThermoScientific Verios UC G4 SEM.

Electrical Contact Patterning. Gold contact pads were formed using a lift-off process as follows. A 1 μm thick polymer layer with 100 μm patterned square holes was formed on 1x1 in^2 silicon chips by depositing AZ3312 (Merck kGaA) photoresist, exposing in a Karl Suss MA150 contact aligner, and developing in AZ300MIF (Merck kGaA). Following the lithography step, 7 nm of chromium (as an adhesion layer) and 50 nm of gold were sequentially evaporated onto the silicon substrate using a custom thermal evaporator. The photoresist was lifted off by immersing the substrate in 1-methyl-2 pyrrolidinone (Sigma-Aldrich) in an ultrasonic bath for 5 min. The substrates were rinsed in flowing distilled water for 5 s and dried with nitrogen.

Metal contact traces were made from the metallized DNA origami to the 100 μm gold pads using EBID of platinum in a FEI Helios Nanolab 600. EBID is a direct write process typically done in a dual beam scanning electron microscope.[38] The electron beam is scanned in the desired pattern in the presence of an organometallic gas released through a gas injection needle close to the surface. The electron beam decomposes the gas, depositing metal on the surface under the beam. The resulting deposit is not pure metal but a metal carbon mix that results in high resistance metal traces. Geier et al.[45] found that EBID written platinum lines can be purified after writing yielding much more conductive traces.

Platinum traces were written at 10 kV and 86 pA. The particular writing parameters were tuned to yield conductive traces while minimizing conductive overspray. Fine platinum traces (~25 nm wide) were written to make direct contact to the metalized origami structure using the line dose setting with target height of 200 nm. Larger traces were written to connect the fine platinum traces to the 100 μm gold pads using the area dose setting with a target 250 nm width and 250 nm height. Due to the low conductance of the as-deposited platinum, which had a significant carbon impurity, we used a subsequent purification step,[45] by exposing the EBID features to an electron beam for 8 min/μm^2 in a Philips XL30 ESEM FEG using low vacuum mode at 0.5 Torr.

Electrical measurements. A micromanipulator probe station was used to contact the 100 μm gold pads for two-point and four-point resistance measurements. A DL Instruments 1211 current preamplifier was used to detect current, and data were collected using a National Instruments DAQ and a custom LabVIEW program. Applied voltages were between 0 and 1 volt.

Yield Calculations and Determination. From AFM images of DNA samples on silicon wafers, the tiles were classified as 'well-formed', 'small defects' or 'deformed' based on their appearance in the AFM data. The yield percentage for each category of tile DNA was determined by counting the number of each tile classification out of the total tiles for all three tile types. SEM images of seeded and plated tile DNA samples were used to compute the yield values for seeded and plated structures. Seeded structures for all three designs were categorized as 'well-seeded', 'misaligned', 'missing 1 rod' and 'missing >1 rod'. The yields were calculated from the number of structures of a given category out of the total tiles observed. Overall yields for all three structures were determined from the yields calculated for different batches of samples.

Results and Discussion

Figure 8 shows AFM images of assembled tile DNA deposited onto Si wafers. In the large area image (Figure 8A), almost half of the tiles were 'well-formed'; some tiles had small defects and others were more deformed. The zoomed in image (Figure 8B) clearly displays well-formed tile DNA origami. These results show that we had good overall assembly and surface placement yields for the tiles. Additional AFM images are in the SI, Figure 14; a more quantitative yield assessment is given later in this paper.

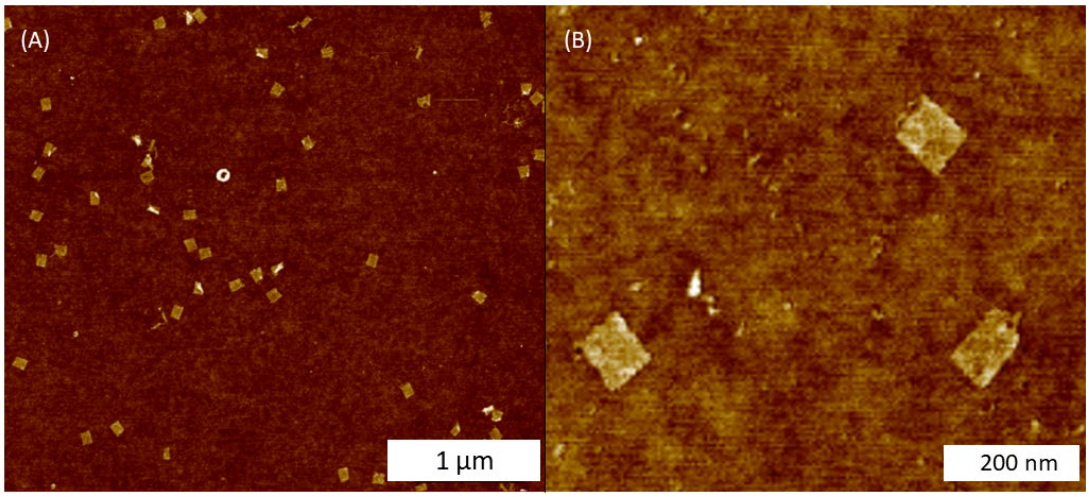

Figure 8. *AFM images of self-assembled tile DNA templates. (A) Large area and (B) zoomed in images. The height scale is 5 nm.*

SEM images of Au nanorod seeded tiles were obtained for the plus, cross, and C designs, as shown in Figure 9. The darker rectangular features in the background are the DNA tiles, whereas the Au nanorods appear as brighter features in Figure 9. Inspection of the plus design (Figure 9A) demonstrated that many DNA tiles had the correct arrangement of four Au nanorods. Additionally, some tiles had four Au nanorods, but they were not properly positioned to create plus structures; similarly, some tiles had just three Au nanorods (missing one) and still others were missing more than one Au nanorod. Additional SEM images and AFM data are in the SI, Figure 15. Figure 9B

shows a zoomed in view of the plus design, in which the gaps between nanorods are more clearly visible than in the Au nanorod seeded large area image.

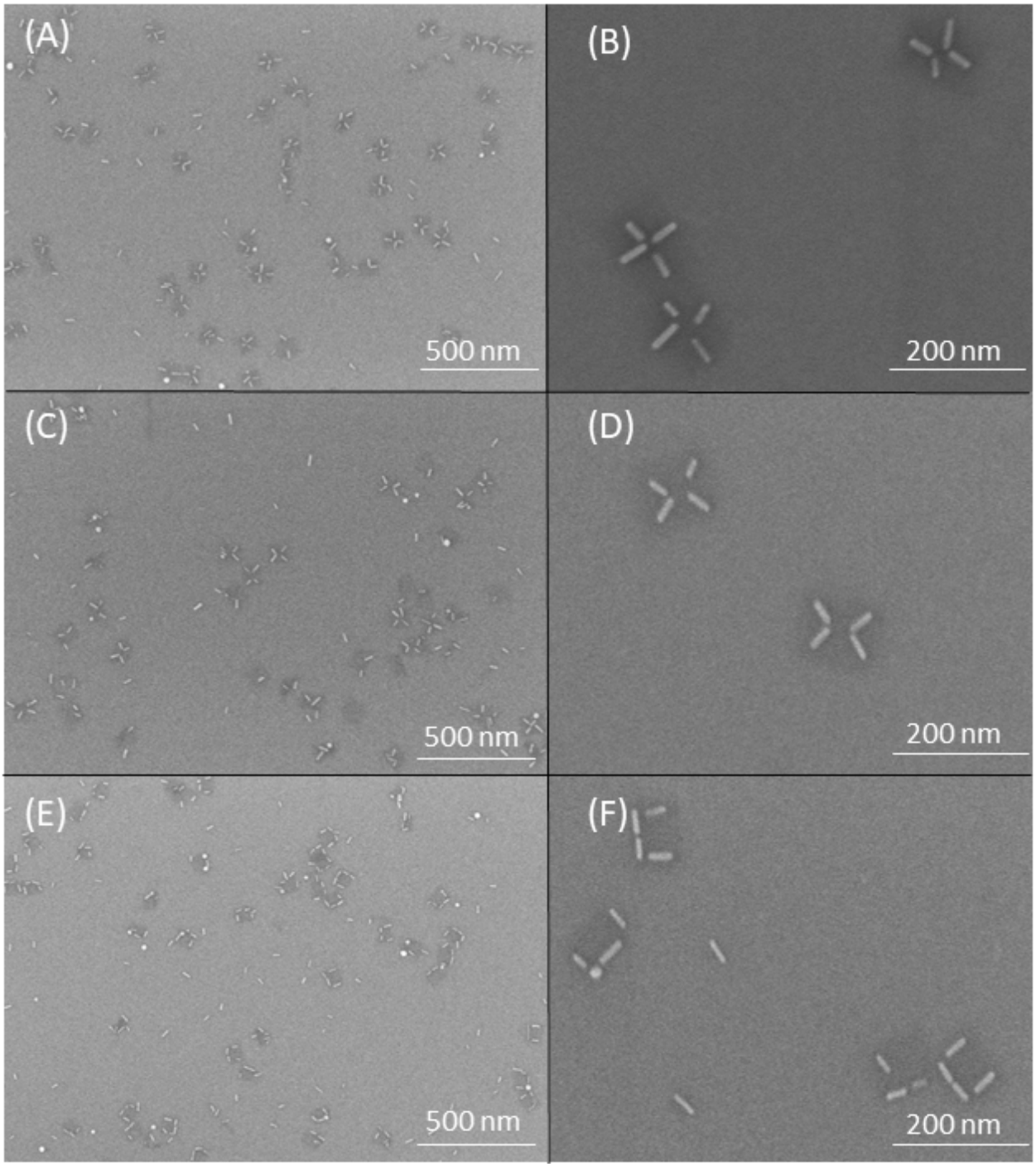

Figure 9. *SEM images of tile DNA origami after seeding with Au nanorods. (A-B) Plus arrangement. (C-D) Cross arrangement. (E-F) C arrangement.*

Figure 9C-D corresponds to Au nanorod seeded cross-shaped structures. Many of the DNA tiles (rectangular darker areas) had perfectly aligned Au nanorods that yielded cross structures. Similar to the plus structures, some tiles had four Au nanorods, but with incorrect orientation, others were missing one rod, and still others were missing more than one rod. Additional SEM images and AFM data on cross structures are provided in the SI, Figure 16. Figure 9D gives a close view of cross structures with visible spaces in between the diagonally placed nanorods on the tiles.

Figure 9E-F shows the C-shape on tiles after Au nanorod seeding. Many well-formed C shapes were found in the large area image while some of the tiles had misaligned Au nanorods, a few had just three (missing one), and some tiles were missing more than one nanorod. More SEM images and AFM data of C shapes are included in the SI, Figure 17. The zoomed-in image (Figure 9F) shows some DNA tiles with four Au nanorods attached to give a C shape. Additional structures with missing nanorods or a nanoparticle instead of one of the nanorods are also visible. We hypothesize that the seeded structures for the three designs are closely dependent on how the tiles landed on the Si wafers during deposition. Thus, well-formed tiles facilitated well-seeded structures whereas incomplete plus, cross, and C structures on tiles likely resulted from tiles having small defects or incomplete assembly. As seen in Figure 9, nearly all DNA tiles had Au nanorods on them, even though the sticky end sequences all protrude from just one face of the DNA origami. We believe that either the protruding sticky ends cause nearly all the DNA tiles to deposit with the protruding sequences facing up, or the sticky ends are long enough to pass through to the top side even if the tiles deposit with the protruding sequences facing down.

Yield calculations were performed for DNA tiles as well as all on the three structures after seeding, and Figure 10 presents the consolidated results. Figure 10A demonstrates that almost 50% of the tiles were well formed, with 24% having small defects and 27% being deformed. Lack of planar

landing on the surface due to inherent tension/twist in these DNA origami tiles[85] might have caused folding at corners of tiles leading to small defects. Some deformed structures could be caused by improper folding of M13mp18 DNA with staple strands. Tile DNA assembly did not utilize the full length of the M13mp18 DNA, so the remaining unutilized scaffold bases resulted in a short tail on one edge of the tile that could connect tiles end-to-end.[1] In order to separate those tiles from each other, the DNA origami was mixed well before deposition, which might have deformed some tiles. To overcome this problem, the use of the full length of the scaffold DNA for assembly would help to form independent tiles without the more thorough mixing step that could deform the structures.

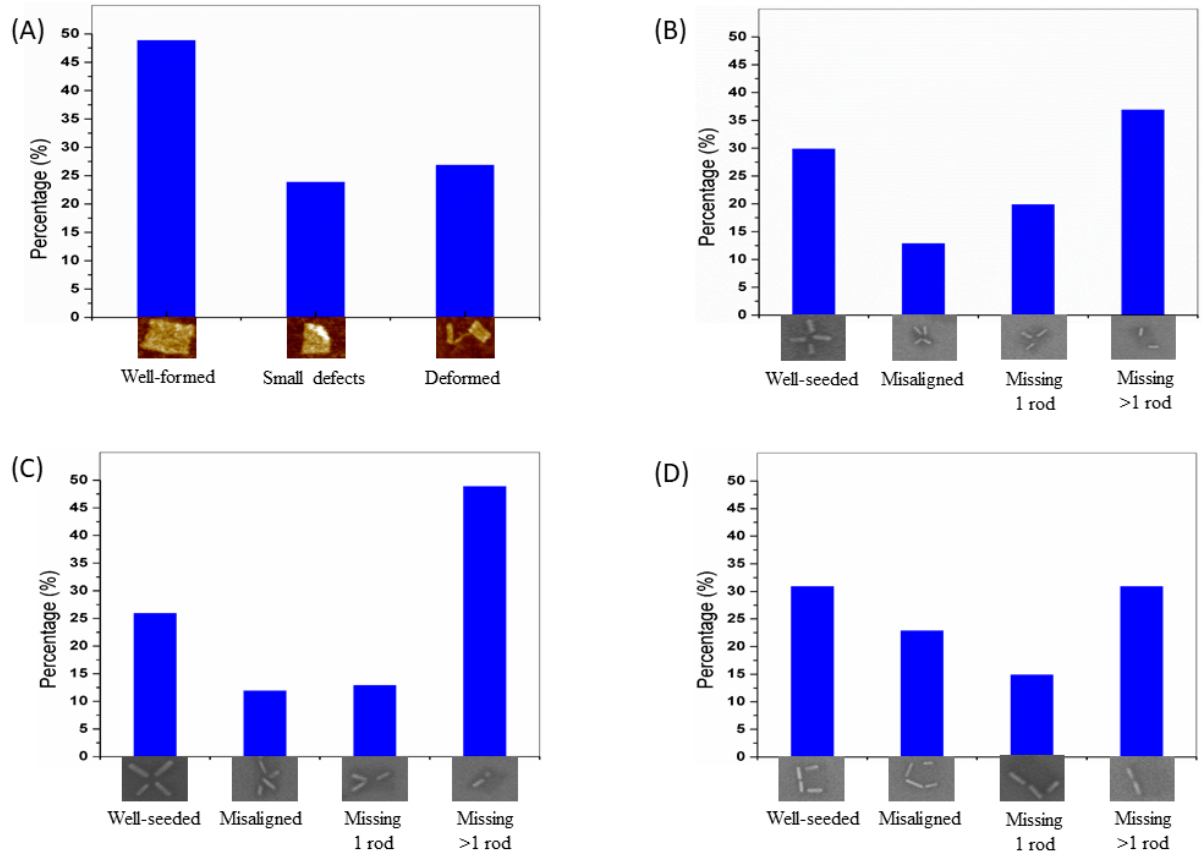

Figure 10. *Yield percentages for unseeded and seeded tiles, (A) Tile DNA origami after deposition onto a Si wafer (n = 364). Yield results for (B) plus (n = 283), (C) cross (n = 318) and (D) C arrangements (n = 345) after seeding with Au nanorods.*

We also determined the yield of seeded structures from the SEM images. Figure 10B shows the yield of seeded plus structures which were classified as 'well-seeded' (i.e., all four nanorod seeds were placed with the correct alignment), 'misaligned', 'missing 1 rod' or 'missing >1 rod'. The yield percentage for the well-seeded tiles was ~30%; however, >35% of the tiles were missing more than one Au nanorod. The yield of well-formed tiles on surfaces limits yields in subsequent seeding steps, as well-seeded structures can only be generated on well-formed tiles. Tiles that have small defects are more likely to result in tiles with misaligned nanorods or with a missing nanorods. Similarly, structures missing more than one nanorod may result from deformed or poorly assembled tiles. Figure 10C gives the yield for different arrangements of Au nanorods in a cross structure. We found that 26% of the tiles had a well-seeded cross design with a similar percentage of tiles having a misaligned or a missing Au nanorod. For this design, nearly half of the tiles were missing more than one Au nanorod. Figure 10D shows the yield for C shapes on seeded tiles. Quantitative analysis of seeding results showed well-seeded C shapes for 31% of tiles, with over 20% of tiles having four Au nanorods, but with one misaligned. About 15% were missing one Au nanorod and over 30% were missing more than one nanorod. Overall, well-seeded yields for the three structures were similar (~30%). In contrast, overall yields for Au nanorod-seeded structures in the previous studies were <10%.[27] Since only 50% of tiles were well-formed and could thus result in well-seeded structures, the yield of correctly seeded structures from well-formed tiles could be considered as >60%, a major improvement over prior work with Au nanorod seeding.[27] These favorable yields for correctly seeded structures open up possibilities for studying plating and making electrical measurements.

Our new tile designs for these three structures have better yields than those we published earlier,[27] because of changes to the DNA origami design for the seeding step. The most important change

was that we increased the number of attachment points for each Au nanorod on the tiles. Each Au nanorod attachment site on tiles had 2 or 3 rows of sticky end DNA sequences protruding (see Figure 7). In previous designs, 1 or 2 rows of sticky end DNA were provided for capturing DNA-functionalized Au nanorods. We compared the yields between one vs. two rows of attachment sites for the cross structure. For a single row of attachment points, the yield for well-seeded structures was <5% (see the SI, Figure 18); importantly, two rows of attachment points improved yields to ~30% (Figure 10) as noted above.

The seeded structures for plus, cross and C shapes were plated to connect the Au nanorods. Figure 11A shows a large area SEM image of plated plus structures in which the Au nanorods appear to be connected in most structures. Figure 11B contains zoomed-in plated plus structures without visible gaps in between nanorods. Comparing the seeded plus structures in Figure 9A-B with similar shapes after electroless deposition in Figure 11A-B, the gaps between Au nanorods are mostly filled in. We previously observed that during plating, the Au nanorods grew anisotropically, with elongation about four times greater than widening.[27] This anisotropic growth allowed the plated nanorods to fill the gaps and provide continuous structures. Similar to the plus structures, plated cross and C shapes (Figure 11C-D and E-F, respectively) were also analyzed. The gaps between nanorods are largely filled in, as observed in the zoomed images with nanowires that appear connected, in contrast to the seeded structures in Figure 9C-F. For all three types of structures after plating, an increase occurred in width and length of plated nanorods. The widths of plated nanorods were measured (n = 25) from the three types of structures, and the average was 11.3 ± 1.2 nm. Likewise, the end-to-end lengths of the C-shaped plated structures were measured on well-plated C shapes (n = 20), and the average (± standard deviation) was 127 ± 14 nm. The overall yield for plated plus, cross and C structures in zoomed SEM images that gave clear views

was calculated (n = 76). Well-plated structures with no visible gaps in the SEM data comprised 39% of the total, whereas 61% of the structures had small gaps visible in the SEM images. C-shapes had the fewest observable gaps in the SEM data compared to plus and cross shapes; this trend is consistent with the smaller designed gap size in the C-shape DNA origami (see Figure 7). These overall yields for plated structures were improved compared to previous studies;[27] the improved yield is especially promising for electrical characterization, due to greater availability of well-plated structures on wafer surfaces.

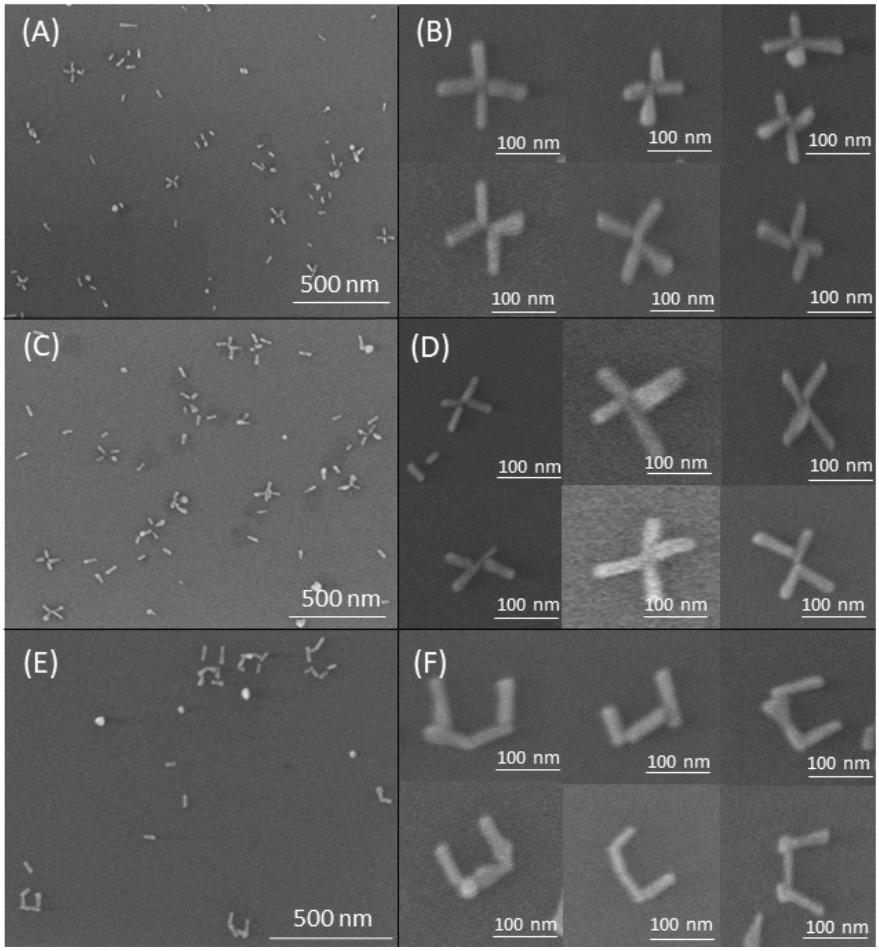

Figure 11. *SEM images of plated structures. (A-B) plus shapes, (C-D) cross shapes, and (E-F) C shapes.*

Upon completion of electroless plating on tiles, electrical characterization was performed to determine the continuity and conductance of the wires. EBID platinum traces were written to make contact to metallized DNA origami structures. Platinum traces with widths <25 nm were created, allowing four contacts to a single C-shape nanowire on a DNA origami tile (Figure 12). Indeed, this is the first work to perform four-point electrical characterization on a nanowires on individual DNA origami tiles that are smaller than 100 nm x 100 nm.

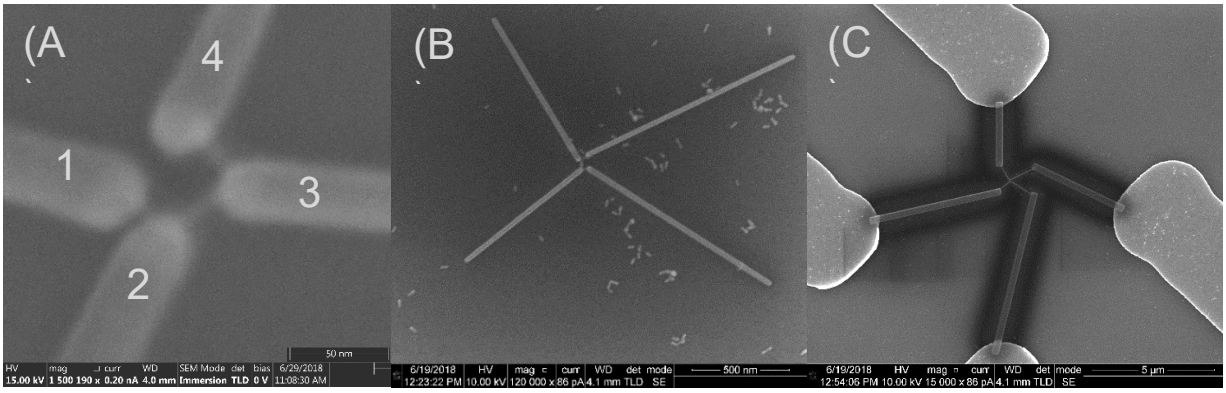

Figure 12. *SEM images of EBID connections. (A) C-shaped Au nanowire with four distinct platinum contacts; two point measurements were performed using leads 1 and 4. When performing four point measurements leads 2 and 3 measured voltage. (B) Larger view of Pt contacts to nanowire. (C) Completed Pt pattern connecting the nanowire to Au pads.*

EBID writing of conductive platinum wires has shortcomings that need to be taken into account in the characterization process. A key issue is that the as-written platinum is highly resistive. Thus, an EBID line can have a resistance >10 MΩ, making four-point measurement interpretation challenging as the lead resistance is comparable to the input resistance of the measurement device. This high resistance is due to the large amount of carbon that is co-deposited with the platinum.[45] The EBID metal purification technique of Geier et al.[45] reduces this problem to a major extent. We found post-purification EBID platinum lines to have resistances of ~100 kΩ, multiple orders of

magnitude less than the input resistance of our measurement hardware. However, this contact lead resistance still requires four point measurements.

To measure the resistance of metallized C-shape Au nanowires on DNA origami tiles, the input voltage was scanned from 0 to 1 V. Figure 13A shows a typical two point I-V curve, measured between leads 1 and 4 in Figure 12A. Figure 13B was obtained by measuring the voltage drop between the inner electrodes (leads 2 and 3 in Figure 12A) for each data point. Electrical resistances for five different C-shape nanowires on two separate Si wafers were characterized by both two- and four-point measurement as shown in Table 1. The two point resistance was calculated by taking the slope of the IV curve while four point took the slope of the voltage drop vs current graph. To verify that leads two and three did not impact resistance measurements standalone two point measurements were conducted and gave similar values with and without leads two and three. The resistivities of the nanowires measured ranged from 0.124 to 4.24 x 10^{-5} Ω m. The 5 nanowires studied had widths of 10-20 nm, which are among the narrowest DNA templated Au nanowires characterized to date. These nanowires are more resistive than those made by Uprety et al.[25] who measured resistivities between 6.7 x 10^{-5} and 8.9 x 10^{-7} Ω m for Au nanowires with widths between 13-29 nm. Ongaro et al.[36] reported a resistivity of 10^{-4} Ω m for Au nanowires with a mean width of 40 nm, while Pearson et al.[17] reported 6.2 x 10^{-6} Ω m for 33 nm wide wires. Other values have been reported with lower resistivities but with larger widths.[86]

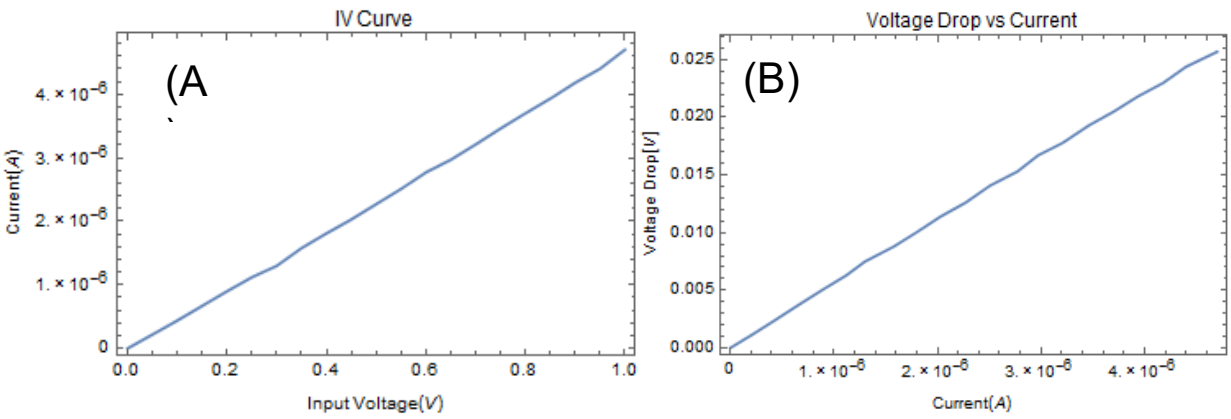

Figure 13. *Four-point electrical characterization of a single nanowire on a DNA origami tile. (A) I-V curve from a C-shape nanowire with input voltages spanning 0 to 1 V. (B) Measured voltage drop between inner electrodes on the C shape.*

Sample #	2 Point (MΩ)	4 Point (MΩ)	Resistivity (Ω m)
1	3.31	0.934	9.79×10^{-3}
2	1.01	0.0849	9.03×10^{-4}
3	273	11.7	0.124
4	76.4	2.61	0.0283
5	.221	0.00558	4.24×10^{-5}

Table 1. *Two- and four-point resistances, as well as calculated resistivities, for 5 different C-shape Au nanowires.*

Possible reasons for the higher resistivity values reported here (compared to other publications) include the smaller nanowire diameters in this study, and differences in the processing of the nanowires after electroless plating. Electron beam lithography patterning has a resist prebake step that Uprety et al.[25] found caused a change in the morphology of the nanowires. This morphological change appeared to smooth edges, reducing surface roughness and potentially resulting in fewer gaps or lower conduction barriers between grains, which would increase conductivity. Importantly, EBID allows electrical measurements on as-formed nanowires. Furthermore, since EBID is a

direct write technique, it allows facile connection to randomly oriented structures, and the <25 nm width traces enable multiple connections to ~100 nm scale devices.

Conclusion

In this paper, we have examined the fabrication yield and electrical properties of different Au nanowire structures created on DNA origami tiles by site-specific attachment of Au nanorods to molecularly programmed sites. A careful assessment of the structures formed showed that yields of plated nanowires were limited to a degree by the seeding process. Consequently, additional attachment sites were added to the DNA tiles to provide more effective linking of DNA-functionalized Au nanorods to the desired sites. As a result, the measured yields improved by a factor of six over recently published studies. The improved yields combined with anisotropic plating on the Au nanorods enabled successful fabrication of the desired nanowire structures. In addition, we demonstrated, for the first time, the ability to perform a four-point resistance measurement on an individual metal nanostructure formed on a single 70 nm x 90 nm DNA origami tile. The measurement was made possible through the use of electron beam induced deposition to form conductive connecting leads to the Au nanowire. Electrical measurements on thin C-shaped Au nanowires 130 nm long and 10 nm in diameter with 40 nm spacing between measurement points were carried out, and nanowires were found to have resistivities as low as 4.24×10^{-5} Ω m.

These advances offer great promise for future nanoelectronics studies on biological templates. Subsequent work on the reproducibility and scalability of bottom-up nanofabrication of conductive inorganic nanostructures should be feasible with this new toolset. Additionally, it may be possible

to study the effects of sample preparation processes on nanowire electrical properties. Finally, this platform provides opportunities for electrical characterization of more complex self-assembled nanostructures involving junctions between different materials, an important endeavor for future studies.

ASSOCIATED CONTENT

Supporting Information: AFM images of DNA tiles, SEM and AFM images of DNA tiles seeded with Au nanorods, and staple strand DNA sequences utilized for assembling DNA templates.

ACKNOWLEDGEMENTS

Funding for the work was provided by the National Science Foundation (1562729) and the Semiconductor Research Corporation (2013-RJ-2487). We would like to thank Dr. J. K Farrer, M. Standing and P. Minson for their technical assistance on SEM instruments. We are grateful to the BYU Department of Chemistry and Biochemistry, and Department of Physics and Astronomy for letting us use available resources.

Supplementary information for Four-Point Probe Electrical Measurements on Templated Gold Nanowires Formed on Single DNA Origami Tiles Paper

Supporting Information for:

Four Point Probe Electrical Measurements on Templated Gold Nanowires Formed on Single DNA Origami Tiles

Basu R. Aryal[a,*], Tyler R. Westover[b,*], Dulashani R. Ranasinghe[a], Diana G. Calvopiña[a], Bibek Uprety[c], John N. Harb[c], Robert C. Davis[b], Adam T. Woolley[a]

[a] Department of Chemistry and Biochemistry, Brigham Young University, Provo, UT 84602

[b] Department of Physics and Astronomy, Brigham Young University, Provo, UT 84602

[c] Department of Chemical Engineering, Brigham Young University, Provo, UT 84602

[*]Equal author contribution

Correspondence: Adam T. Woolley, phone: 801-422-1701; email: atw@byu.edu

- The DNA origami sequence used for this work can be found at the end of the appendix

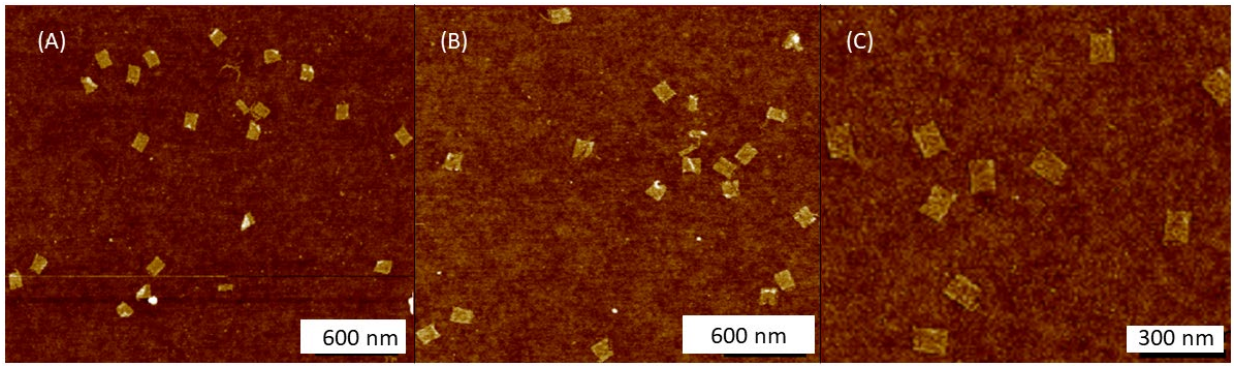

Figure 14. *AFM images of the tile DNA templates utilized to create (A) plus, (B) cross and (C) C shapes. The height scale is 5 nm.*

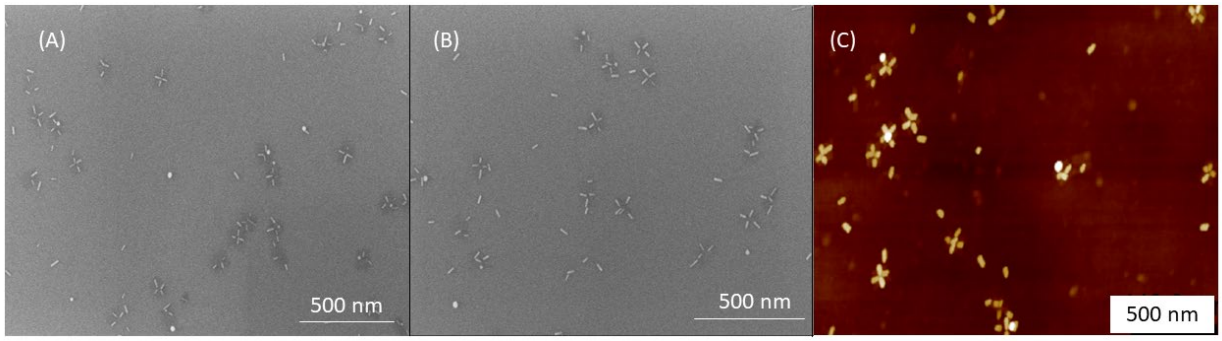

Figure 15. *(A-B) SEM images and (C) AFM images of plus structures on tile DNA templates after seeding with Au nanorods. The height scale in (C) is 25 nm.*

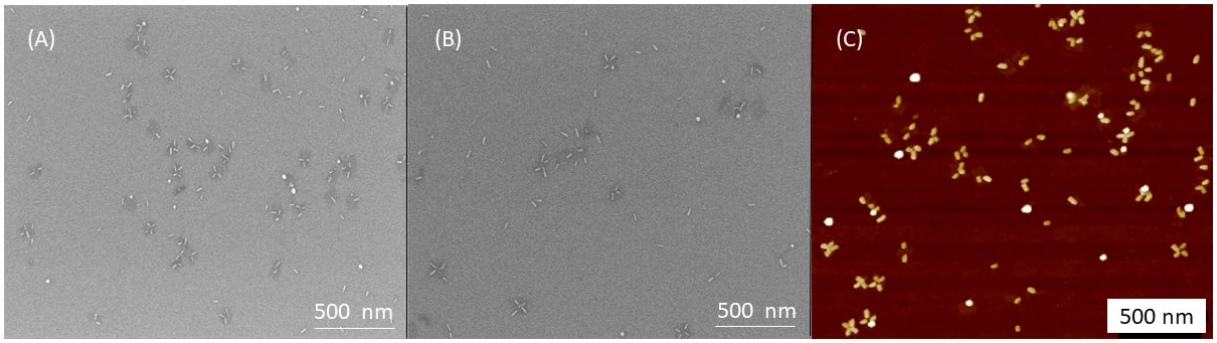

Figure 16. *(A-B) SEM images and (C) AFM image of tile DNA templates seeded with Au nanorods to create cross structures. The height scale in (C) is 25 nm.*

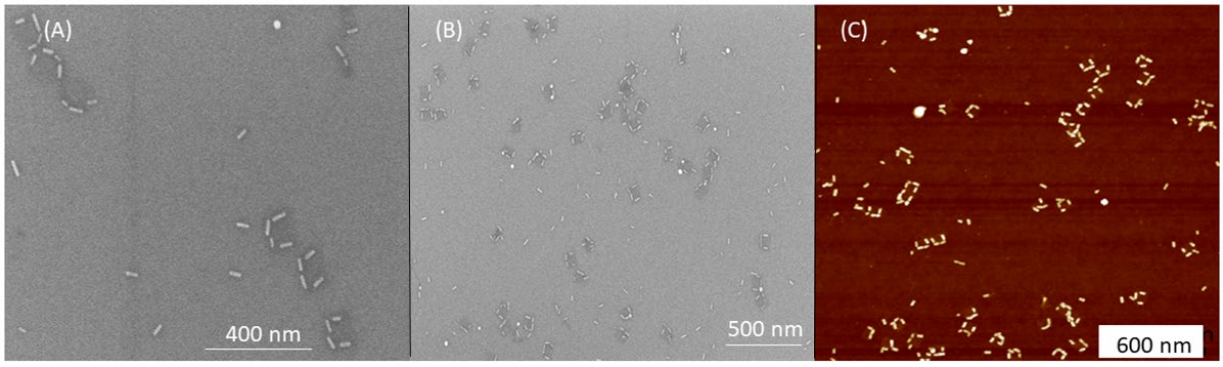

Figure 17. *(A-B) SEM images and (C) AFM image of C shapes on tile DNA templates after seeding with Au nanorods. The height scale in (C) is 20 nm.*

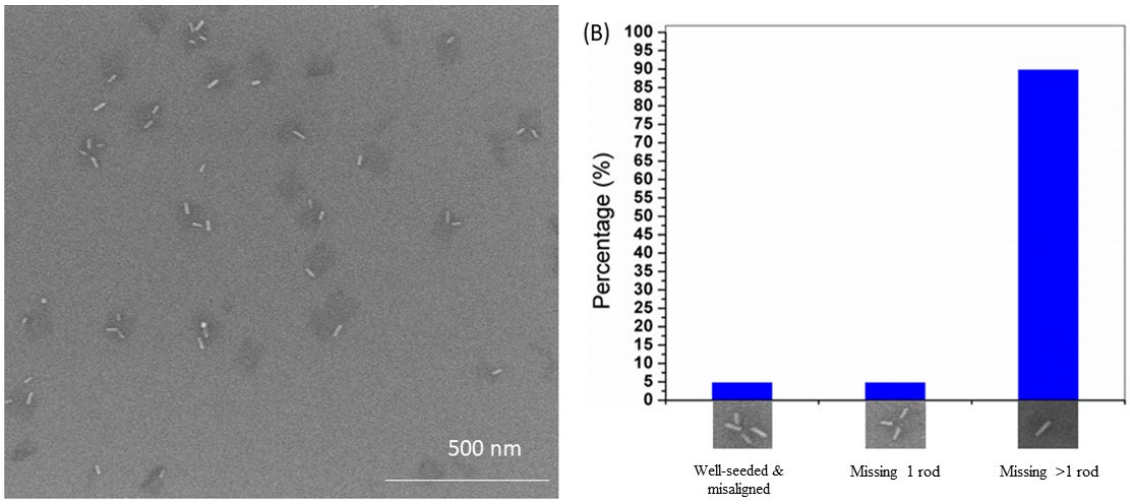

Figure 18. *(A) SEM image of Au nanorod seeded cross structures on DNA tiles that have a single attachment sequence row for each Au nanorod. (B) Seeding yield of the cross structures in (A).*

Chapter 3: Impact of Polymer-Constrained Annealing on the Properties of DNA Origami Templated Gold Nanowires

The following is taken from a paper submitted for publication in Langmuir authored by Tyler R. Westover, Basu R. Aryal, Dulashani R. Ranasinghe, Bibek Uprety, John N. Harb, Adam T. Woolley and Robert C. Davis. Reproduced with permission from Langmuir, submitted for publication. Unpublished work copyright 2020 American Chemical Society.

Impact of Polymer-Constrained Annealing on the Properties of DNA Origami Templated Gold Nanowires

Tyler R. Westover[1], Basu R. Aryal[2], Dulashani R. Ranasinghe[2], Bibek Uprety[3], John N. Harb[3], Adam T. Woolley[2] and Robert C. Davis[1] (✉)

[1] Department of Physics and Astronomy, Brigham Young University, Provo, UT 84602, USA

[2] Department of Chemistry and Biochemistry, Brigham Young University, Provo, UT 84602, USA

[3] Department of Chemical Engineering, Brigham Young University, Provo, UT 84602, USA

Abstract

DNA origami templated fabrication enables bottom-up fabrication of nanoscale structures from a variety of functional materials, including metal nanowires. We studied the impact of low temperature annealing on the morphology and conductance of DNA templated nanowires. Nanowires were formed by selective seeding of gold nanorods on DNA origami and gold electroless plating of the seeded structures. At low annealing temperatures (160° C for seeded-only and 180° C for plated) the wires broke up and separated into multiple, isolated islands. Through the use of polymer-constrained annealing, the island formation in plated wires was suppressed up to annealing temperatures of 210° C. Four-point electrical measurements showed that wires remained conductive after a polymer-constrained anneal at 200° C.

Keywords: annealing, DNA origami, Rayleigh instability, polymer coating, gold nanowires

Introduction

DNA origami is a promising bottom up manufacturing technique that allows for the formation of unique two- and three-dimensional shapes.[2-4, 87-88] Due to the natural complementary base pairing of DNA molecules, self-assembly occurs readily in an easily pre-determined fashion. Rothemund[1] demonstrated this using one long single-stranded DNA and several short oligonucleotides called staple strands that were selected to cause folding; since then others have made complex two dimensional and three dimensional[6-8] shapes. DNA nanofabrication has been exploited to make complex building blocks including tiles[11-12], tubes[13, 89], cages[6, 15], and components including switches[16-18] and logic[19]. These works demonstrate the unique properties of DNA as an alternative to traditional top-down manufacturing techniques. Taking advantage of the site-specific nature of DNA binding, various materials can be attached to form continuous functional structures, such as wires for electronic or plasmonic applications.[20, 90] Materials can be attached to DNA via chemical and electrostatic interactions or through base paring to specific locations.[22, 27] Electronic materials that have been successfully attached to DNA include Au[3, 22, 24-28], Ag[4, 21], Cu[21, 24, 29-30], Ni[31], Pd[32-33], Te[23, 34] and carbon nanotubes[35, 91]. Despite these advancements, making electrically conductive, thin, continuous nanowires still proves to be a challenge, as formed wires usually have a resistivity 2-3 orders of magnitude greater than that of the bulk materials.[22, 26, 36-37]

Due to the size of nanowires electron beam lithography (EBL) is commonly employed to make contact pads that connect to the nanowires, allowing for resistance measurements to be performed.[3, 13, 22, 24-26, 34, 36] Uprety et al.[23] commented on an observed morphological change in nanowires upon heating during EBL processing. The EBL processing involves coating with a

polymer electron beam resist (ZEP 520A), and a 200° C bake step prior to electron exposure. An alternative, lower temperature method to contact these nanowires using electron beam induced deposition (EBID) was recently demonstrated by Aryal et al.[12] This technique is based on local electron-induced decomposition of precursor gas molecules that have been locally injected into a scanning ion/electron system.[39-40] A primary challenge associated with EBID is the high carbon content deposited along with the desired metal, resulting in high resistance in the deposited conductor.[39, 43, 92] There have been numerous efforts to improve the quality of the EBID lines, through both *in situ* and post processing.[42-47] The resistance of EBID lines is also directly correlated with the precursor gas chosen; as new precursors are being developed, the quality of the lines is also improving.[43, 93-94]

Temperature-driven morphological changes in nanowires have been observed and attributed to the Rayleigh instability.[48-51] This theory was initially developed in reference to long liquid cylinders, where the surface area can be minimized by separating into a series of equally spaced spheres. For nanowires this morphology change results in loss of conductivity. The size and quality of a nanowire influence the required temperatures and times for the Rayleigh instability to take effect.[51-53] To integrate DNA origami templated nanowires into electronic systems, further processing will generally be required. Understanding and increasing the temperature stability of DNA origami patterned nanowires will aid in future integration.

In this work we performed annealing studies on DNA origami templated nanowires. The nanowires were formed by seeding DNA origami with gold nanorods , and by plating these seeded origami structures described by Uprety et al[25] illustrated in Figure 19A-C. We observed morphological changes at temperatures as low as 160° C for seeded-only nanowires and 180° C for nanowires that had also been plated to fill in gaps between seeds. These morphological changes

progress to the eventual disassociation of the wires into multiple separate islands illustrated in Figure 19E. By applying a polymer coating to the nanowires we suppress the separation of the nanowires into islands until temperatures exceed 210° C as illustrated in Figure 19D. This could allow for the wires to undergo additional manufacturing steps at this higher temperature. Nanowires were characterized through scanning electron microscopy and four-lead transport measurements, where electrical contacts were made through low temperature tungsten EBID.

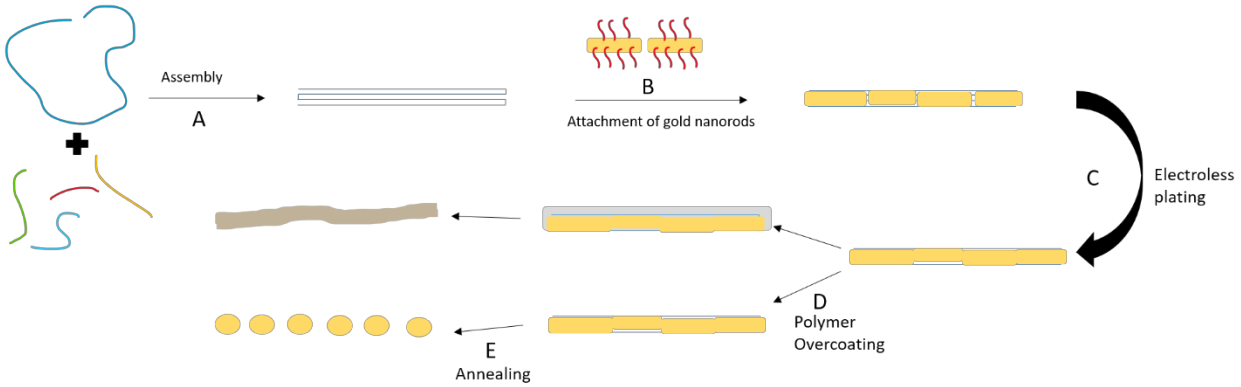

Figure 19. *Process Diagram (A) Scaffold plus staple strand DNA solution is placed on a SiO_2 substrate allowing for the formation of a predesigned bar DNA origami pattern. (B) DNA-functionalized gold nanorods are added to the substrate and attach to the bar DNA origami. (C) Anisotropic electroless plating grows seeded nanorods, connecting the structures. (D) PMMA is spin cast onto the structures (E) Structures are annealed, and depending on temperature and presence of a polymer template, wires can have: no change, nanorods can fuse or nanowires can separate into isolated islands.*

Experimental Methods

Chemicals and materials for the preparation of DNA origami templated gold nanowires were same as those used by Uprety et al.[25] The polymer used to coat the nanowires was 6% polymethyl methacrylate (PMMA) in Anisol (MW 950,000) purchased from MicroChem (Newton, MA).

Preparation of DNA origami templated gold nanowires followed the procedure described by Uprety et al. [25] Briefly, bar DNA origami templates were fabricated and folded as illustrated in Figure 19A. Bar DNA origami are seeded with gold nanorods as illustrated in Figure 19B. Gold electroless plating of the seeded structures was performed as illustrated in Figure 19C. We seeded

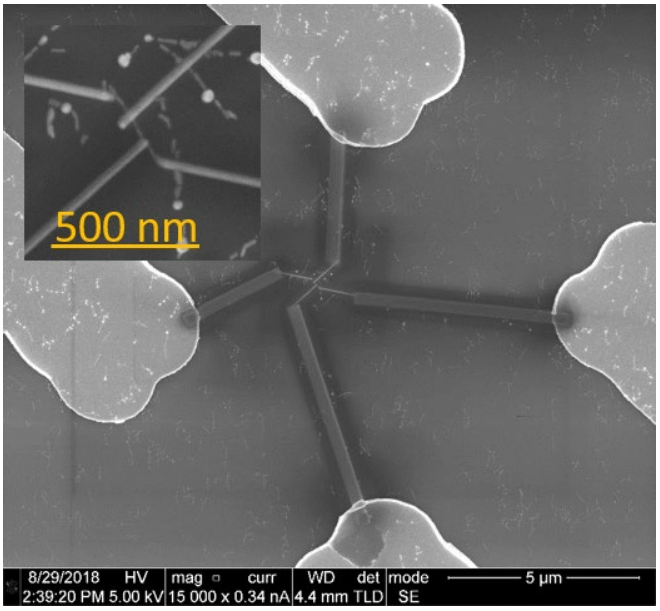

Figure 20. *Electron micrograph of EBID of tungsten connecting to a gold nanowire. A gold nanowire was contacted in a four-point configuration using EBID of tungsten using a line dose. Using an area dose, traces were patterned to connect the lines to large gold pads which could be contacted using micromanipulator probes to perform electrical characterization.*

Au nanorods onto DNA origami deposited on surfaces, rather than seeding in solution[95] and then depositing the seeded DNA origami on surfaces, to avoid having the nanorods crosslink multiple DNA origami structures.

Gold contacts were formed using a lift-off process as described in Aryal et al.[12] Metal contact traces were made from the metalized DNA origami to the 100 micron gold pads using EBID of tungsten in a FEI Helios Nanolab 600 (Figure 20). Tungsten traces were written at 10 kV and 86 pA. The writing parameters were tuned to yield conductive traces while minimizing conductive

overspray. Fine tungsten traces (~25 nm wide) were written to make direct contact to the metalized origami structure (using the line dose setting for a height of 200 nm). Larger traces were written to connect the fine tungsten traces to the 100 um gold pads (using the area dose setting for 250 nm width and 250 nm height).

Nanowire samples were spin coated at room temperature for 1 minute at 5000 rpm with PMMA. This yields an approximate thickness of 350 nm. Heating was performed on a hotplate at the desired temperature, which was measured with a surface thermometer placed directly onto the hotplate. All samples were heated for 2 minutes. The resist was removed by placing the sample in acetone for 10 minutes with light stirring.

All seeded only and plated DNA samples with Au nanorods were imaged by scanning electron microscopy (SEM) in ultra-high-resolution mode on a FEI Helios Nanolab 600, and on a Thermo Scientific Verios UC G4 SEM. On each sample, up to 10 unique locations were imaged before and after annealing to get a clear representation of the morphological changes. The images shown in this paper were selected to be representative of the types of changes seen at each annealing temperature.

A micromanipulator probe station was used to contact the 100 um gold pads for two-point and four-point resistance measurements. A DL Instruments 1211 current preamplifier was used to detect current and data was collected using a national instrument DAQ and a custom LabVIEW program. were used to conduct. Applied voltages were between 0 and 1 volt. After annealing the resist was removed prior to measurements.

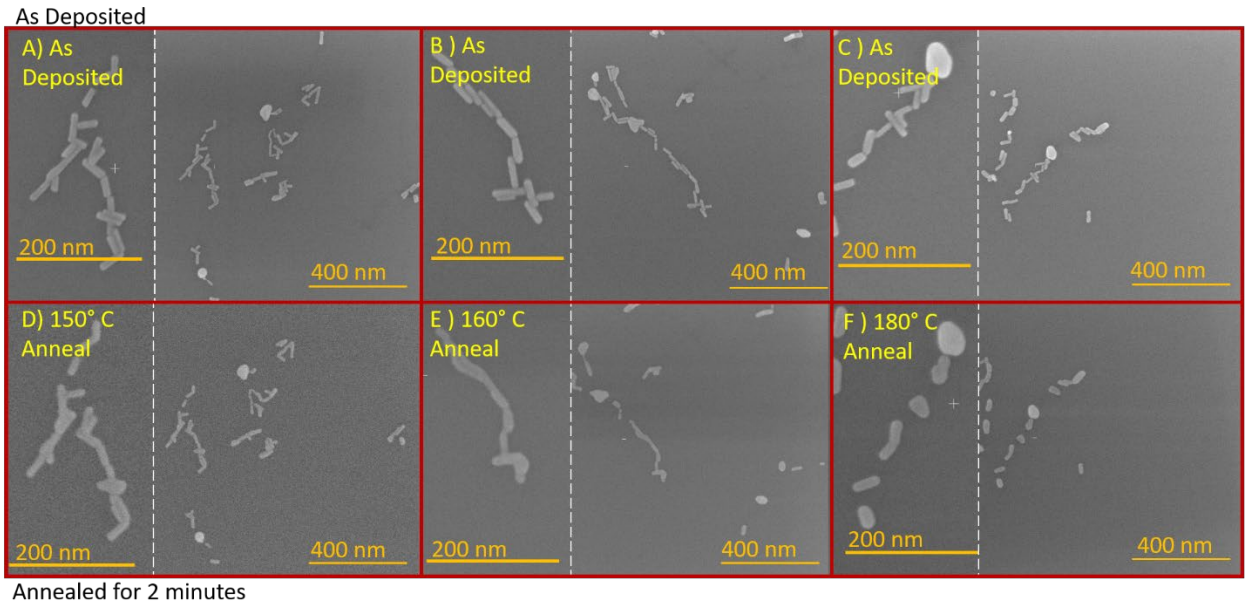

Figure 21 *Electron micrographs of seeded-only gold nanowires before and after annealing without a polymer coating. (A, B) Seeded-only gold nanowires before annealing. (C) After anneal no significant change in morphology is observed. (D) After anneal the nanorods have separated into isolated islands.*

Annealing studies were performed on nanowires formed by seeding DNA origami with gold nanorods followed by electroless plating (defined as plated nanowires), and on nanowires that were formed by seeding only with no plating (defined as seeded-only nanowires). The reason for including the seeded only nanowires was to explore whether individual nanorod seeds would be connected through annealing. Annealing studies were performed at several temperatures ranging from 120–250° C. Annealing induced changes in the nanowire morphology were observed using before and after SEM imaging (at a constant magnification of 250,000× for straightforward comparison). Figure 21 shows the morphological changes observed in plated nanowires when annealed at various temperatures. Figure 21 A-C shows plated nanowires that form continuous structures; these plated nanowires were annealed on a hotplate for two minutes in air at the

specified temperatures. Figure 21A and 21D are images of a plated wire before and after annealing at 150° C; no change in morphology was observed. At temperatures of 160° C (Figure 21E) and 170° C we saw a morphological change compared to the unannealed sample (Figure 21B); the nanowires appeared to fuse as the junctions between the segments became less distinct and, in some cases, disappeared. At temperatures of 180° C and above, more pronounced morphological changes were observed as the nanowires separated into a series of isolated segments (Figure 21F).

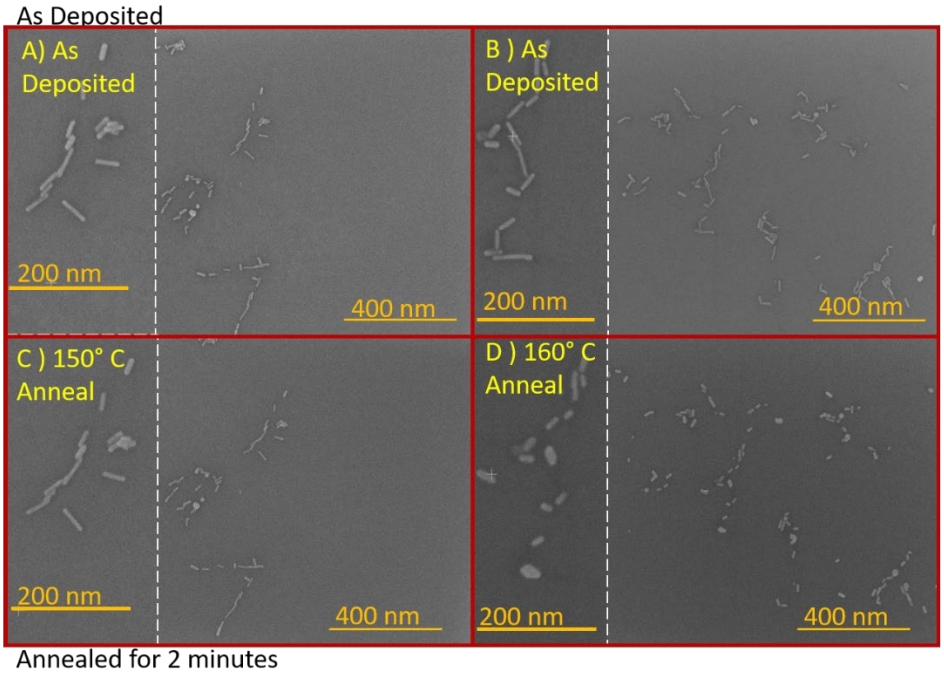

Figure 22. *Electron micrographs of seeded-only gold nanowires before and after annealing without a polymer coating. (A, B) Seeded-only gold nanowires before annealing. (C) After a 2 minute anneal no significant change in morphology is observed. (D) After anneal for 2 minutes the nanorods have separated into isolated islands.*

Seeded-only nanowires showed no morphological change for annealing temperatures at or below 150° C (Figure 22 A,C), but at annealing temperatures of 160° C and above, isolated island formation was observed (Figure 22B,D). In contrast to what was seen for plated nanowires, seeded-only nanowires exhibited no temperature range where fusing was observed.

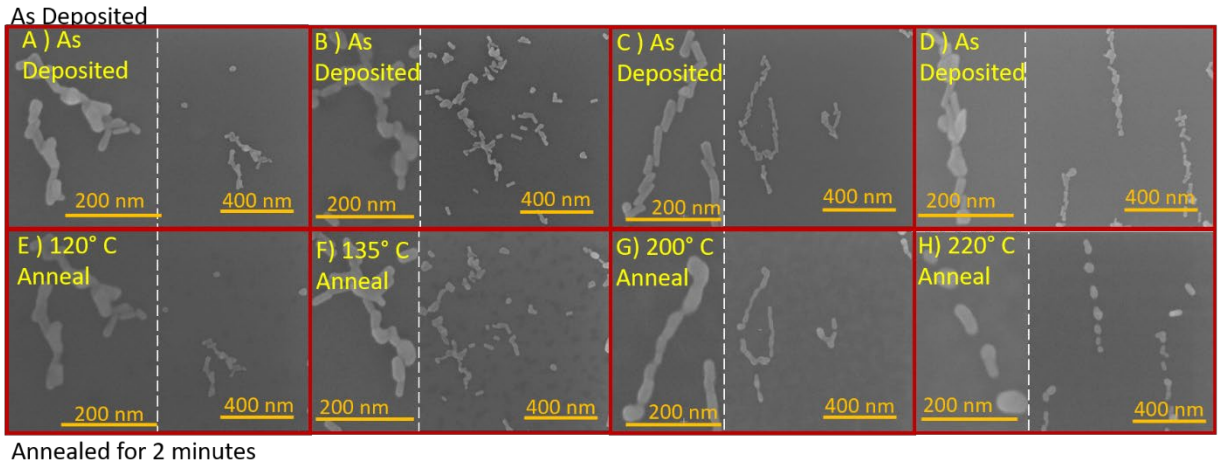

Figure 23. *Electron micrographs of plated gold nanowires before and after annealing with polymer coating. (A)-(D) Plated gold nanowires imaged before annealing. (E) After a 2 minute anneal with a PMMA coating there is no significant change. (F) After a 2 minute anneal with PMMA coating, a morphological change is observed as the nanorods appear to fuse. (G) After a 2 minute anneal with PMMA coating the nanorods are fusing. (H) After a 2 minute anneal with PMMA coating, the nanowires have separated into a series of isolated islands.*

Experiments with PMMA coated nanowires were performed to explore the impact of polymer at stabilizing the overall shape and continuity of the nanowires at elevated temperature. For these experiments, PMMA was spin cast over plated nanowires (we will call these coated plated nanowires) and seeded-only nanowires (we will call these coated seeded-only nanowires) the nanowires prior to annealing. Figure 23 shows examples of the impact of annealing on four coated plated nanowires at temperatures of 120 ° C, 135° C, 200 ° C and 210° C. At annealing

temperatures below 135° C, there was no observed morphological change. At temperatures at or above 135° C the junctions became less distinct and, in some cases disappeared. This apparent fusing occurred at temperatures 25° C lower than without the polymer coating. No further morphological change was readily observed at increasing temperature up to 210° C, as seen in Figure 23G. At 210° C and above the nanowires began to form isolated segments (Figure 23H); this transition occurred at a temperature 30° C higher than for the uncoated nanowires.

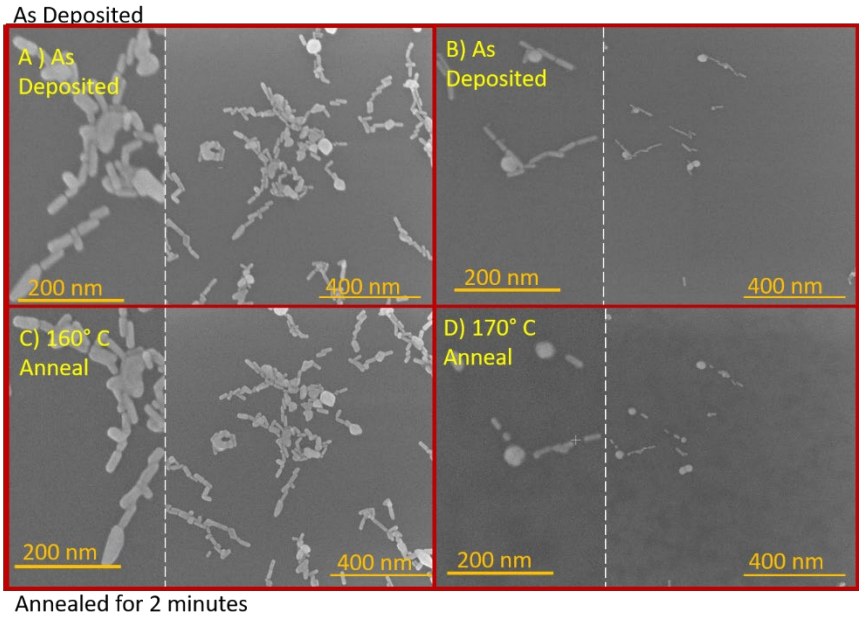

Figure 24. *Electron micrographs of seeded-only gold nanowires before and after annealing with a polymer coating. (A, B) Seeded-only gold nanowires before annealing. (C) After a 2 minute anneal with PMMA coating, no significant change is observed. (D) After a 2 minute anneal with PMMA coating the nanowires have separated in isolated islands.*

The images in Figure 24 represent the effect of annealing on coated seeded-only nanowires. The nanowires remained unchanged when heated to temperatures lower than 160° C and began to

segment at temperatures of 170° C or above. There was no observed region where the nanowires fused without separating.

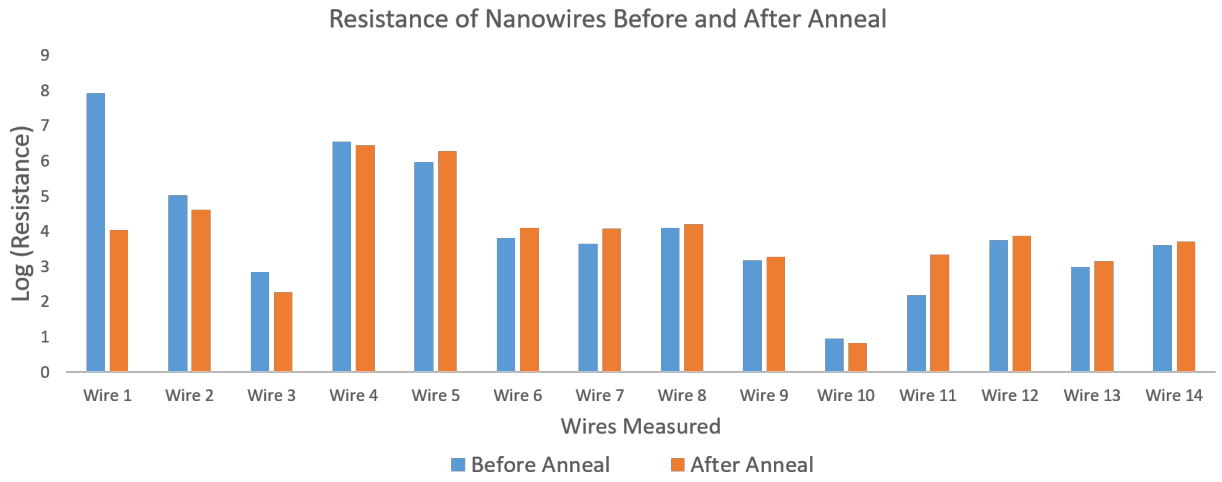

Figure 25. *Nanowire resistance before and after annealing. Log of the resistance of individual nanowires before and after a 2 minute, 200° C anneal with PMMA coating.*

Using four-point micromanipulator probes, electrical characterization was performed before and after annealing nanowires with a PMMA coating at a temperature of 200° C. 200° C was chosen because it was within the transition region, where we observed fusing of wire segments upon anneal. Nanowires were electrically connected to the gold pads using EBID tungsten in the configuration shown in Figure 20. Measured resistance values before and after annealing of individual nanowires are shown in Figure 25. The average wire resistance change was not statistically significant. Due to the lack of heterogeneity of the nanowire resistances before annealing, individual before and after measurements were performed. Individual nanowires were found to have both increased and decreased resistances after annealing. These individual nanowire resistance changes ranged from only a few percent to several orders of magnitude. When uncoated

nanowires were processed in the same manner the resistance was found to be greater than 100 Gohms after annealing.

Discussion

We identified three different annealing regimes based on the observed morphological changes.

1. At lower annealing temperatures no changes are observed in nanowire morphology.
2. At moderate temperatures plated nanowires begin to fuse.
3. At higher temperatures nanowires begin to separate into isolated islands.

The temperatures at which one regime transitions to the next depends upon whether the nanowires are seeded-only, plated, or polymer coated. A summary of the annealing regimes for this range of conditions is shown in Table 2.

	Temperature Range Annealing Regime 1 (No Observed Change)	**Temperature Range Annealing Regime 2 (Fusing Observed)**	**Temperature Range Annealing Regime 3 (Isolated Island Formed)**
Seeded Plated (57 Samples)	<160° C	160-180° C	>180° C
Seeded-Only (26 Samples)	<160° C	-	>160° C
Coated Seeded Plated (106 Samples)	<135° C	135-210° C	>210° C
Coated Seeded-Only (101 Samples)	<170° C	-	>170° C

Table 2. *Summary of observed morphological changes. Threshold temperatures for different annealing regimes with seeded-only, plated and coated nanowires. Regime 1: at lower temperatures no morphological change is observed. Regime 2: at moderate temperatures the nanorods appear to fuse. Regime 3: at higher temperatures nanorods separate into isolated islands*

Polymer coating of the nanowires was seen to significantly delay the segmentation of nanowires until higher annealing temperatures. As plating is typically used to produce conductive nanowires, annealing of plated nanowires is highly relevant to fabrication processes for nanowire electronics. The transition point from regime 2 to regime 3, where nanowires become non-contiguous, was

raised with the addition of the polymer coating from 180° C to 210° C. This increase could allow for other processing steps (like PECVD) to take place to integrate these nanowires into more complex devices.

We hypothesize that in regime 2 polymer-constrained annealing imposes a mechanical constraint on the movement of gold that restricts the formation of islands. Without this mechanical constraint during annealing, the nanowires follow a pattern consistent with the Rayleigh instability, wherein to minimize surface area, a long, thin cylinder will decay into a series of isolated spheres. The resulting spheres have a diameter that is significantly larger than that of the original nanowire. We propose that the diameter of the annealed structure is constrained by the PMMA coating, inhibiting the Rayleigh instability to some degree. This would increase the temperature stability of the nanowires, at least in a temperature regime where the PMMA has significant mechanical stiffness. As the temperature increases, the PMMA becomes more flexible, allowing island formation and loss of continuity. The glass transition temperature of PMMA is 125° C, meaning it becomes more flexible as the temperature increases, allowing for island formation and loss of continuity.

We note that a thermal bake step at 90° C is part of the photolithography process, which occurs before pre-annealing conductivity measurements are made. However, the bake step temperature is significantly lower than that required to generate an observable morphological change and is not expected to impact the conductance of nanowires. The thermal properties of the EBID metal are not expected in influence the annealing of the gold due to the entire substrate being heated uniformly and quickly. Tungsten EBID was chosen over the more common platinum because tungsten deposits do not require a subsequent purification step. A concern with platinum deposit purification is that additional carbon is deposited, which could interfere with conductance

measurements. Four-point probe measurements of the nanowires were required due to the contact resistance of the test leads formed through EBID. A challenge with before and after conductance measurements of the same wire was resist removal could damage the tungsten leads. If the leads had clear breaks or cracks away from the test nanowire it could be repaired through EBID of additional tungsten; however, if the break was close to the nanowire, measurements were not performed.

In conclusion, significant morphological changes were seen in seeded-only and plated nanowires for annealing temperatures as low as 160° C. At 200° C both seeded-only nanowires as well as plated nanowires separated into individual islands, resulting in non-continuous, non-conductive nanowires. We observed that polymer-constrained annealing resulted in suppression of island formation from plated coated nanowires until temperatures exceeded 210° C. We performed a study of plated coated nanowires that had been annealed at 200° C and found that the nanowires remained continuous and conductive. By coating DNA origami templated gold plated nanowires with PMMA, a broader temperature process window is available for subsequent fabrication steps. The mechanical constraints that self-aligned polymer coatings place on nanowires during annealing open up new nanowire morphologies that can result in improved functionality and integration possibilities.

Corresponding Author

Robert Davis

Acknowledgements

We would like to thank Brigham Young University's microscopy facility, and BYU's IML lab for access to facilities. We thank the National Science Foundation (CMMI-1562729) and BYU's Simmons Research Endowment for partial support of this work. Basu Aryal acknowledges

the BYU Department of Chemistry and Biochemistry for a Roland K. Robins Graduate Research Fellowship.

Chapter 4: Preliminary Characterization of Electron Beam Induced Deposition of Tungsten

Experiments were performed to discover the limits of EBID tungsten as a method for four-point electrical contacts. Tungsten was thoroughly tested as the "halo" appeared to be more prevalent than seen with platinum. The results of the testing are shown in Table 3. As the height of the patterned structure increases the halo becomes conductive. This is expected because with the same beam parameters increased height is achieved through longer write times, allowing for more scattering events to occur. As the current of the electron beam increases the halo becomes more conductive, because the beam has more energy to cause scattering events.

Height / **Beam Current**	**500 nm**	**600 nm**	**700 nm**	**800 nm**	**900 nm**	**1000 nm**
5kV .086 nA	NC					
5kV .17 nA	NC	NC				
5kV .34 nA	NC	C	C	C	C	C
5kV .69 nA	NC	C				

Table 3. *Experiments performed using Tungsten EBID to examine the conductive "halo". Traces were patterned with a 5kV accelerating voltage and beam current from .086nA to .69nA. With a constant spacing of 50 nm various heights were patterned and determined if there was a conductive path or not. Wires with no conductive "halo" are labeled "NC" and wires with a conductive "halo" are labeled "C"*

Chapter 5: Conclusions and Suggestions for Future Work

This work explores electrical characteristics of DNA origami templated gold nanowires formed through metallization of nanorod seeds. High resolution electrical contact patterning was developed using EBID for electrical transport measurements. Electrical properties of nanowires are highly influenced by surface roughness and junctions between nanowire grains. Metal atoms have high surface mobilities causing changes in surface roughness and metal grain junctions during modest thermal processes.

Nanowires in this work were patterned on two different origami structures: DNA origami bars that were approximately 400 nm long and 20 nm wide and DNA origami tiles that were 70 nm by 90 nm. Nanowires on the DNA origami bar were straight allowing four linear equally spaced electrical contacts. A “C” shaped nanowire was designed and formed on the DNA origami tile. The “C” shaped geometry was used to facilitate four-point electrical measurements (using EBID contacts) on the shortest possible nanowire, by placing the leads in each corner. The result was four-point electrical characterization of the shortest DNA origami templated nanowire that has been reported.

A chief objective of this work was to gain understanding of the impact of seeded nanowire formation and processing, on wire morphology and conductivity. DNA origami nanowires were shown to be especially susceptible to nanoscale phenomenon like the Rayleigh instability. The result we observed is moderate temperature processing above 180° C, cause the nanowires to separate into individual islands resulting in loss of conductivity. A PMMA overcoating on the DNA nanowires was shown to suppress the nanowire separation into isolated islands up to 210° C.

There are further questions to be answered with regards to annealing and resistivity. SEM analysis after constrained annealing at temperatures of 200° C showed a reduction in the number of visible grain junctions and surface roughness, but no change in the average resistance of the nanowires. We have hypothesized that the gold surface mobility could be used to reduce the resistivity of the nanowires by eliminating or reducing grain junction resistance and in some nanowires the resistance was reduced by several orders of magnitude. To clearly identify junction size and changes in junction morphology, higher resolution imaging like transmission electron microscopy (TEM) may be helpful. Studying grain junctions between nanorod seeds after annealing for different times and temperatures could potentially lead to a predictive model, of how long and at what temperatures the wires can be annealed while retaining their shape, and if there is a correlation to a change in resistivity. If the resistance between grains could be consistently reduced it would be valuable not only for the understanding of the seeded nanowires but also potentially for junctions with other materials for integration into functional electronic devices.

In this work PMMA was used as the polymer overcoat partly because it is non-conductive reducing overcoat interference in electrical measurements. We hypothesize that the eventual island formation of the nanowires above 210° C is related to the softening of the polymer with increased temperature. It is possible that a higher melting temperature, possibly harder, polymer would allow the wires to retain continuity at even higher temperatures than those shown in this work. In conjunction with a better understanding of grain junction behavior, studying overcoats with different material properties could yield valuable knowledge in how to use the mobility of metal atoms to improve the electrical properties of nanowires while suppressing the Rayleigh instability.

An alternative form of Rayleigh instability suppression may involve the use of more temperature stable seed particles. Gold has a high surface mobility even at relatively low temperatures and thus exhibits the effects of the Rayleigh instability at lower temperatures compared to many other metals. We hypothesize that metallic seed rods, with a higher surface melting temperature (but that gold wets to) could be attached to the DNA origami template alongside the gold (or electroplated by gold). Annealing then could lead to wicking of the gold into densely seeded regions and filling small gaps between seeds instead of gold island formation. This may result in suppression of the Rayleigh instability with a different mechanism that opens new possibilities in terms of geometry, temperature and additional materials. Instead of forcing a geometrical constraint upon the nanowire, suppressing it from reaching an energetically favorable state as islands, we may use the wetting properties of metals to design the pattern to be an energetically favorable state.

By starting with the work done here, it could be possible to develop a more complicated system incorporating DNA origami templated nanowires. The versatility of DNA origami to form two and three dimensional shapes with site specific attachments can open frontiers not accessible with typical top down manufacturing. Higher stability DNA template nanowires could be more readily combined with top down processes like lithography, thin film deposition, and etching. This combination will enable more geometrically complex devices for real world applications.

Bibliography

1. Rothemund, P. W., Folding DNA to create nanoscale shapes and patterns. *Nature* **2006,** *440* (7082), 297-302.
2. Matthies, M.; Agarwal, N. P.; Schmidt, T. L., Design and synthesis of triangulated DNA origami trusses. *Nano letters* **2016,** *16* (3), 2108-2113.
3. Helmi, S.; Ziegler, C.; Kauert, D. J.; Seidel, R., Shape-controlled synthesis of gold nanostructures using DNA origami molds. *Nano letters* **2014,** *14* (11), 6693-6698.
4. Pilo-Pais, M.; Goldberg, S.; Samano, E.; Labean, T. H.; Finkelstein, G., Connecting the nanodots: programmable nanofabrication of fused metal shapes on DNA templates. *Nano Lett* **2011,** *11* (8), 3489-92.
5. Anderson, E. H.; Ha, D.; Liddle, J. A., Sub-pixel alignment for direct-write electron beam lithography. *Microelectronic Engineering* **2004,** *73-74*, 74-79.
6. Andersen, E. S.; Dong, M.; Nielsen, M. M.; Jahn, K.; Subramani, R.; Mamdouh, W.; Golas, M. M.; Sander, B.; Stark, H.; Oliveira, C. L., Self-assembly of a nanoscale DNA box with a controllable lid. *Nature* **2009,** *459* (7243), 73.
7. Douglas, S. M.; Dietz, H.; Liedl, T.; Högberg, B.; Graf, F.; Shih, W. M., Self-assembly of DNA into nanoscale three-dimensional shapes. *Nature* **2009,** *459* (7245), 414.
8. Han, D.; Pal, S.; Nangreave, J.; Deng, Z.; Liu, Y.; Yan, H., DNA origami with complex curvatures in three-dimensional space. *Science* **2011,** *332* (6027), 342-346.
9. Wang, P.; Meyer, T. A.; Pan, V.; Dutta, P. K.; Ke, Y., The Beauty and Utility of DNA Origami. *Chem* **2017,** *2* (3), 359-382.
10. Said, H.; Schüller, V. J.; Eber, F. J.; Wege, C.; Liedl, T.; Richert, C., M1. 3–a small scaffold for DNA origami. *Nanoscale* **2013,** *5* (1), 284-290.
11. Ke, Y.; Ong, L. L.; Shih, W. M.; Yin, P., Three-dimensional structures self-assembled from DNA bricks. *science* **2012,** *338* (6111), 1177-1183.
12. Aryal, B. R.; Westover, T. R.; Ranasinghe, D. R.; Calvopiña, D. G.; Uprety, B.; Harb, J. N.; Davis, R. C.; Woolley, A. T., Four-Point Probe Electrical Measurements on Templated Gold Nanowires Formed on Single DNA Origami Tiles. *Langmuir* **2018,** *34* (49), 15069-15077.
13. Ding, B.; Wu, H.; Xu, W.; Zhao, Z.; Liu, Y.; Yu, H.; Yan, H., Interconnecting gold islands with DNA origami nanotubes. *Nano letters* **2010,** *10* (12), 5065-5069.
14. Mohammed, A. M.; Schulman, R., Directing self-assembly of DNA nanotubes using programmable seeds. *Nano Lett* **2013,** *13* (9), 4006-13.
15. Zhao, Z.; Jacovetty, E. L.; Liu, Y.; Yan, H., Encapsulation of gold nanoparticles in a DNA origami cage. *Angewandte Chemie International Edition* **2011,** *50* (9), 2041-2044.
16. Olejko, L.; Cywiński, P. J.; Bald, I., An ion-controlled four-color fluorescent telomeric switch on DNA origami structures. *Nanoscale* **2016,** *8* (19), 10339-10347.
17. Marini, M.; Piantanida, L.; Musetti, R.; Bek, A.; Dong, M.; Besenbacher, F.; Lazzarino, M.; Firrao, G., A revertible, autonomous, self-assembled DNA-origami nanoactuator. *Nano letters* **2011,** *11* (12), 5449-5454.
18. Wang, F.; Liu, X.; Willner, I., DNA switches: from principles to applications. *Angewandte Chemie International Edition* **2015,** *54* (4), 1098-1129.
19. Yang, J.; Jiang, S.; Liu, X.; Pan, L.; Zhang, C., Aptamer-Binding Directed DNA Origami Pattern for Logic Gates. *ACS Appl Mater Interfaces* **2016,** *8* (49), 34054-34060.
20. Shen, X.; Song, C.; Wang, J.; Shi, D.; Wang, Z.; Liu, N.; Ding, B., Rolling up gold nanoparticle-dressed DNA origami into three-dimensional plasmonic chiral nanostructures. *Journal of the American Chemical Society* **2011,** *134* (1), 146-149.

21. Shen, B.; Linko, V.; Tapio, K.; Kostiainen, M. A.; Toppari, J. J., Custom-shaped metal nanostructures based on DNA origami silhouettes. *Nanoscale* **2015,** *7* (26), 11267-72.
22. Pearson, A. C.; Liu, J.; Pound, E.; Uprety, B.; Woolley, A. T.; Davis, R. C.; Harb, J. N., DNA origami metallized site specifically to form electrically conductive nanowires. *J Phys Chem B* **2012,** *116* (35), 10551-60.
23. Aryal, B. R.; Ranasinghe, D. R.; Westover, T. R.; Calvopiña, D. G.; Davis, R. C.; Harb, J. N.; Woolley, A. T., DNA origami mediated electrically connected metal—semiconductor junctions. *Nano Research* **2020**.
24. Uprety, B.; Gates, E. P.; Geng, Y.; Woolley, A. T.; Harb, J. N., Site-specific metallization of multiple metals on a single DNA origami template. *Langmuir* **2014,** *30* (4), 1134-41.
25. Uprety, B.; Westover, T.; Stoddard, M.; Brinkerhoff, K.; Jensen, J.; Davis, R. C.; Woolley, A. T.; Harb, J. N., Anisotropic Electroless Deposition on DNA Origami Templates To Form Small Diameter Conductive Nanowires. *Langmuir* **2017,** *33* (3), 726-735.
26. Geng, Y.; Pearson, A. C.; Gates, E. P.; Uprety, B.; Davis, R. C.; Harb, J. N.; Woolley, A. T., Electrically conductive gold- and copper-metallized DNA origami nanostructures. *Langmuir* **2013,** *29* (10), 3482-90.
27. Uprety, B.; Jensen, J.; Aryal, B. R.; Davis, R. C.; Woolley, A. T.; Harb, J. N., Directional Growth of DNA-Functionalized Nanorods to Enable Continuous, Site-Specific Metallization of DNA Origami Templates. *Langmuir* **2017,** *33* (39), 10143-10152.
28. Bayrak, T. r.; Helmi, S.; Ye, J.; Kauert, D.; Kelling, J.; Schönherr, T.; Weichelt, R.; Erbe, A.; Seidel, R., DNA-mold templated assembly of conductive gold nanowires. *Nano letters* **2018,** *18* (3), 2116-2123.
29. Watson, S. M.; Wright, N. G.; Horrocks, B. R.; Houlton, A., Preparation, characterization and scanned conductance microscopy studies of DNA-templated one-dimensional copper nanostructures. *Langmuir* **2010,** *26* (3), 2068-75.
30. Monson, C. F.; Woolley, A. T., DNA-templated construction of copper nanowires. *Nano letters* **2003,** *3* (3), 359-363.
31. Arora, A. A.; de Silva, C., Beyond the smiley face: applications of structural DNA nanotechnology. *Nano reviews & experiments* **2018,** *9* (1), 1430976.
32. Geng, Y.; Liu, J.; Pound, E.; Gyawali, S.; Harb, J. N.; Woolley, A. T., Rapid metallization of lambda DNA and DNA origami using a Pd seeding method. *Journal of Materials Chemistry* **2011,** *21* (32), 12126.
33. Richter, J.; Seidel, R.; Kirsch, R.; Mertig, M.; Pompe, W.; Plaschke, J.; Schackert, H. K., Nanoscale palladium metallization of DNA. *Advanced Materials* **2000,** *12* (7), 507-510.
34. Liu, J.; Uprety, B.; Gyawali, S.; Woolley, A. T.; Myung, N. V.; Harb, J. N., Fabrication of DNA-templated Te and Bi2Te3 nanowires by galvanic displacement. *Langmuir* **2013,** *29* (35), 11176-11184.
35. Eskelinen, A. P.; Kuzyk, A.; Kaltiaisenaho, T. K.; Timmermans, M. Y.; Nasibulin, A. G.; Kauppinen, E. I.; Torma, P., Assembly of single-walled carbon nanotubes on DNA-origami templates through streptavidin-biotin interaction. *Small* **2011,** *7* (6), 746-50.
36. Ongaro, A.; Griffin, F.; Beecher, P.; Nagle, L.; Iacopino, D.; Quinn, A.; Redmond, G.; Fitzmaurice, D., DNA-Templated Assembly of Conducting Gold Nanowires between Gold Electrodes on a Silicon Oxide Substrate. *Chemistry of Materials* **2005,** *17* (8), 1959-1964.
37. Teschome, B.; Facsko, S.; Schönherr, T.; Kerbusch, J.; Keller, A.; Erbe, A., Temperature-dependent charge transport through individually contacted DNA origami-based Au nanowires. *Langmuir* **2016,** *32* (40), 10159-10165.

38. van Dorp, W. F.; Hagen, C. W., A critical literature review of focused electron beam induced deposition. *Journal of Applied Physics* **2008,** *104* (8), 081301.
39. Utke, I.; Moshkalev, S.; Russell, P., *Nanofabrication using focused ion and electron beams: principles and applications*. Oxford University Press: 2012.
40. Winkler, R.; Fowlkes, J.; Szkudlarek, A.; Utke, I.; Rack, P. D.; Plank, H., The nanoscale implications of a molecular gas beam during electron beam induced deposition. *ACS applied materials & interfaces* **2014,** *6* (4), 2987-2995.
41. Rykaczewski, K.; Hildreth, O. J.; Kulkarni, D.; Henry, M. R.; Kim, S.-K.; Wong, C. P.; Tsukruk, V. V.; Fedorov, A. G., Maskless and resist-free rapid prototyping of three-dimensional structures through electron beam induced deposition (EBID) of carbon in combination with metal-assisted chemical etching (MaCE) of silicon. *ACS applied materials & interfaces* **2010,** *2* (4), 969-973.
42. Botman, A.; Hesselberth, M.; Mulders, J., Improving the conductivity of platinum-containing nano-structures created by electron-beam-induced deposition. *Microelectronic Engineering* **2008,** *85* (5-6), 1139-1142.
43. Botman, A.; Mulders, J.; Hagen, C., Creating pure nanostructures from electron-beam-induced deposition using purification techniques: a technology perspective. *Nanotechnology* **2009,** *20* (37), 372001.
44. Botman, A.; Mulders, J.; Weemaes, R.; Mentink, S., Purification of platinum and gold structures after electron-beam-induced deposition. *Nanotechnology* **2006,** *17* (15), 3779.
45. Geier, B.; Gspan, C.; Winkler, R.; Schmied, R.; Fowlkes, J. D.; Fitzek, H.; Rauch, S.; Rattenberger, J.; Rack, P. D.; Plank, H., Rapid and Highly Compact Purification for Focused Electron Beam Induced Deposits: A Low Temperature Approach Using Electron Stimulated H2O Reactions. *The Journal of Physical Chemistry C* **2014,** *118* (25), 14009-14016.
46. Gopal, V.; Radmilovic, V. R.; Daraio, C.; Jin, S.; Yang, P.; Stach, E. A., Rapid prototyping of site-specific nanocontacts by electron and ion beam assisted direct-write nanolithography. *Nano Letters* **2004,** *4* (11), 2059-2063.
47. Langford, R.; Wang, T.-X.; Ozkaya, D., Reducing the resistivity of electron and ion beam assisted deposited Pt. *Microelectronic Engineering* **2007,** *84* (5-8), 784-788.
48. Karim, S.; Toimil-Molares, M. E.; Balogh, A. G.; Ensinger, W.; Cornelius, T. W.; Khan, E. U.; Neumann, R., Morphological evolution of Au nanowires controlled by Rayleigh instability. *Nanotechnology* **2006,** *17* (24), 5954-5959.
49. Toimil Molares, M.; Balogh, A.; Cornelius, T.; Neumann, R.; Trautmann, C., Fragmentation of nanowires driven by Rayleigh instability. *Applied physics letters* **2004,** *85* (22), 5337-5339.
50. Li, H.; Biser, J. M.; Perkins, J. T.; Dutta, S.; Vinci, R. P.; Chan, H. M., Thermal stability of Cu nanowires on a sapphire substrate. *Journal of Applied Physics* **2008,** *103* (2), 024315.
51. Shin, H. S.; Yu, J.; Song, J. Y., Size-dependent thermal instability and melting behavior of Sn nanowires. *Applied Physics Letters* **2007,** *91* (17), 173106.
52. Xu, S.; Li, P.; Lu, Y., In situ atomic-scale analysis of Rayleigh instability in ultrathin gold nanowires. *Nano Research* **2018,** *11* (2), 625-632.
53. Karim, S.; Toimil-Molares, M.; Ensinger, W.; Balogh, A.; Cornelius, T.; Khan, E.; Neumann, R., Influence of crystallinity on the Rayleigh instability of gold nanowires. *Journal of Physics D: Applied Physics* **2007,** *40* (12), 3767.
54. Suchaneck, G.; Norkus, V.; Gerlach, G., Low-temperature PECVD-deposited silicon nitride thin films for sensor applications. *Surface and Coatings Technology* **2001,** *142*, 808-812.

55. Danaie, K.; Bosseboeuf, A.; Clerc, C.; Gousset, C.; Julie, G., Fabrication of UV-transparent SixOyNz membranes with a low frequency PECVD reactor. *Sensors and Actuators A: Physical* **2002,** *99* (1-2), 78-81.
56. Tong, M.; Dai, G.; Wu, Y.; He, X.; Gao, D., WO3 thin film prepared by PECVD technique and its gas sensing properties to NO2. *Journal of materials science* **2001,** *36* (10), 2535-2538.
57. Löffler, J.; Groenen, R.; Linden, J.; Van de Sanden, M.; Schropp, R., Amorphous silicon solar cells on natively textured ZnO grown by PECVD. *Thin Solid Films* **2001,** *392* (2), 315-319.
58. Hofmann, S.; Ducati, C.; Robertson, J.; Kleinsorge, B., Low-temperature growth of carbon nanotubes by plasma-enhanced chemical vapor deposition. *Applied Physics Letters* **2003,** *83* (1), 135-137.
59. Liu, P.; Chen, J.; Sun, W., Characterizations of SnO2 and SnO2: Sb thin films prepared by PECVD. *Vacuum* **2004,** *76* (1), 7-11.
60. Biswas, A.; Bayer, I. S.; Biris, A. S.; Wang, T.; Dervishi, E.; Faupel, F., Advances in top–down and bottom–up surface nanofabrication: Techniques, applications & future prospects. *Advances in colloid and interface science* **2012,** *170* (1-2), 2-27.
61. Qin, D.; Xia, Y.; Whitesides, G. M., Soft lithography for micro- and nanoscale patterning. *Nat Protoc* **2010,** *5* (3), 491-502.
62. Austin, M. D.; Ge, H.; Wu, W.; Li, M.; Yu, Z.; Wasserman, D.; Lyon, S. A.; Chou, S. Y., Fabrication of 5nm linewidth and 14nm pitch features by nanoimprint lithography. *Applied Physics Letters* **2004,** *84* (26), 5299-5301.
63. Cheng, J. Y.; Ross, C.; Chan, V. H.; Thomas, E. L.; Lammertink, R. G.; Vancso, G. J., Formation of a cobalt magnetic dot array via block copolymer lithography. *Advanced Materials* **2001,** *13* (15), 1174-1178.
64. Mijatovic, D.; Eijkel, J. C.; van den Berg, A., Technologies for nanofluidic systems: top-down vs. bottom-up—a review. *Lab on a Chip* **2005,** *5* (5), 492-500.
65. Ozin, G. A.; Hou, K.; Lotsch, B. V.; Cademartiri, L.; Puzzo, D. P.; Scotognella, F.; Ghadimi, A.; Thomson, J., Nanofabrication by self-assembly. *Materials Today* **2009,** *12* (5), 12-23.
66. Li, H.; Carter, J. D.; LaBean, T. H., Nanofabrication by DNA self-assembly. *Materials Today* **2009,** *12* (5), 24-32.
67. Nummelin, S.; Kommeri, J.; Kostiainen, M. A.; Linko, V., Evolution of structural DNA nanotechnology. *Advanced Materials* **2018**, 1703721.
68. Douglas, S. M.; Dietz, H.; Liedl, T.; Hogberg, B.; Graf, F.; Shih, W. M., Self-assembly of DNA into nanoscale three-dimensional shapes. *Nature* **2009,** *459* (7245), 414-8.
69. Xu, A.; Harb, J. N.; Kostiainen, M. A.; Hughes, W. L.; Woolley, A. T.; Liu, H.; Gopinath, A., DNA Origami: The Bridge from Bottom to Top. *MRS Bull.* **2017,** *42*, 943-950.
70. Kuzyk, A.; Jungmann, R.; Acuna, G. P.; Liu, N., DNA Origami Route for Nanophotonics. *ACS Photonics* **2018,** *5* (4), 1151-1163.
71. Tørring, T.; Voigt, N. V.; Nangreave, J.; Yan, H.; Gothelf, K. V., DNA origami: a quantum leap for self-assembly of complex structures. *Chemical Society Reviews* **2011,** *40* (12), 5636-5646.
72. Jones, M. R.; Seeman, N. C.; Mirkin, C. A., Programmable materials and the nature of the DNA bond. *Science* **2015,** *347* (6224), 1260901.
73. LaBean, T. H.; Li, H., Constructing novel materials with DNA. *Nano Today* **2007,** *2* (2), 26-35.

74. Douglas, S. M.; Dietz, H.; Liedl, T.; Hogberg, B.; Graf, F.; Shih, W. M., Self-assembly of DNA into nanoscale three-dimensional shapes. *Nature* **2009,** *459* (7245), 414-418.
75. Sherman, W. B.; Seeman, N. C., A precisely controlled DNA biped walking device. *Nano letters* **2004,** *4* (7), 1203-1207.
76. Seelig, G.; Soloveichik, D.; Zhang, D. Y.; Winfree, E., Enzyme-free nucleic acid logic circuits. *science* **2006,** *314* (5805), 1585-1588.
77. Chen, Z.; Liu, C.; Cao, F.; Ren, J.; Qu, X., DNA metallization: principles, methods, structures, and applications. *Chem Soc Rev* **2018**.
78. Liu, J.; Geng, Y.; Pound, E.; Gyawali, S.; Ashton, J. R.; Hickey, J.; Woolley, A. T.; Harb, J. N., Metallization of branched DNA origami for nanoelectronic circuit fabrication. *Acs Nano* **2011,** *5* (3), 2240-2247.
79. Bayrak, T.; Helmi, S.; Ye, J.; Kauert, D.; Kelling, J.; Schonherr, T.; Weichelt, R.; Erbe, A.; Seidel, R., DNA-Mold Templated Assembly of Conductive Gold Nanowires. *Nano Lett* **2018,** *18* (3), 2116-2123.
80. Chen, Z.; Liu, C.; Cao, F.; Ren, J.; Qu, X., DNA metallization: principles, methods, structures, and applications. *Chemical Society Reviews* **2018,** *47* (11), 4017-4072.
81. Liu, J.; Uprety, B.; Gyawali, S.; Woolley, A. T.; Myung, N. V.; Harb, J. N., Fabrication of DNA-templated Te and Bi2Te3 nanowires by galvanic displacement. *Langmuir* **2013,** *29* (35), 11176-84.
82. Xin, H.; Woolley, A. T., DNA-Templated Nanotube Localization. *J Am Chem Soc* **2003,** *125*, 8710-8711.
83. Ali, M. R.; Snyder, B.; El-Sayed, M. A., Synthesis and optical properties of small Au nanorods using a seedless growth technique. *Langmuir* **2012,** *28* (25), 9807-15.
84. Liu, K.; Zheng, Y.; Lu, X.; Thai, T.; Lee, N. A.; Bach, U.; Gooding, J. J., Biocompatible gold nanorods: one-step surface functionalization, highly colloidal stability, and low cytotoxicity. *Langmuir* **2015,** *31* (17), 4973-80.
85. Woo, S.; Rothemund, P. W., Self-assembly of two-dimensional DNA origami lattices using cation-controlled surface diffusion. *Nature communications* **2014,** *5*, 4889.
86. Satti, A.; Aherne, D.; Fitzmaurice, D., Analysis of Scattering of Conduction Electrons in Highly Conducting Bamboolike DNA-Templated Gold Nanowires. *Chemistry of Materials* **2007,** *19* (7), 1543-1545.
87. Pound, E.; Ashton, J. R.; Becerril, H. A.; Woolley, A. T., Polymerase chain reaction based scaffold preparation for the production of thin, branched DNA origami nanostructures of arbitrary sizes. *Nano letters* **2009,** *9* (12), 4302-4305.
88. Andersen, E. S.; Dong, M.; Nielsen, M. M.; Jahn, K.; Lind-Thomsen, A.; Mamdouh, W.; Gothelf, K. V.; Besenbacher, F.; Kjems, J., DNA origami design of dolphin-shaped structures with flexible tails. *ACS nano* **2008,** *2* (6), 1213-1218.
89. Mohammed, A.; Velazquez, L.; Chisenhall, A.; Schiffels, D.; Fygenson, D.; Schulman, R., Self-assembly of precisely defined DNA nanotube superstructures using DNA origami seeds. *Nanoscale* **2017,** *9* (2), 522-526.
90. Shen, X.; Asenjo-Garcia, A.; Liu, Q.; Jiang, Q.; García de Abajo, F. J.; Liu, N.; Ding, B., Three-dimensional plasmonic chiral tetramers assembled by DNA origami. *Nano letters* **2013,** *13* (5), 2128-2133.
91. Xin, H.; Woolley, A. T., DNA-templated nanotube localization. *Journal of the American Chemical Society* **2003,** *125* (29), 8710-8711.

92. Botman, A.; Hesselberth, M.; Mulders, J. J. L., Improving the conductivity of platinum-containing nano-structures created by electron-beam-induced deposition. *Microelectronic Engineering* **2008,** *85* (5), 1139-1142.
93. Fernández-Pacheco, A.; De Teresa, J.; Córdoba, R.; Ibarra, M., Metal-insulator transition in Pt-C nanowires grown by focused-ion-beam-induced deposition. *Physical Review B* **2009,** *79* (17), 174204.
94. Klein, K.; Randolph, S.; Fowlkes, J.; Allard, L.; Meyer Iii, H.; Simpson, M.; Rack, P., Single-crystal nanowires grown via electron-beam-induced deposition. *Nanotechnology* **2008,** *19* (34), 345705.
95. Meyer, T. A.; Zhang, C.; Bao, G.; Ke, Y., Programmable Assembly of Iron Oxide Nanoparticles Using DNA Origami. *Nano Letters* **2020,** *20* (4), 2799-2805.

Appendix

S.O.P. for Thermal Evaporation

SOP of Jim

Note: The system should always be left in standby when not in use. This means that the chamber is under vacuum.

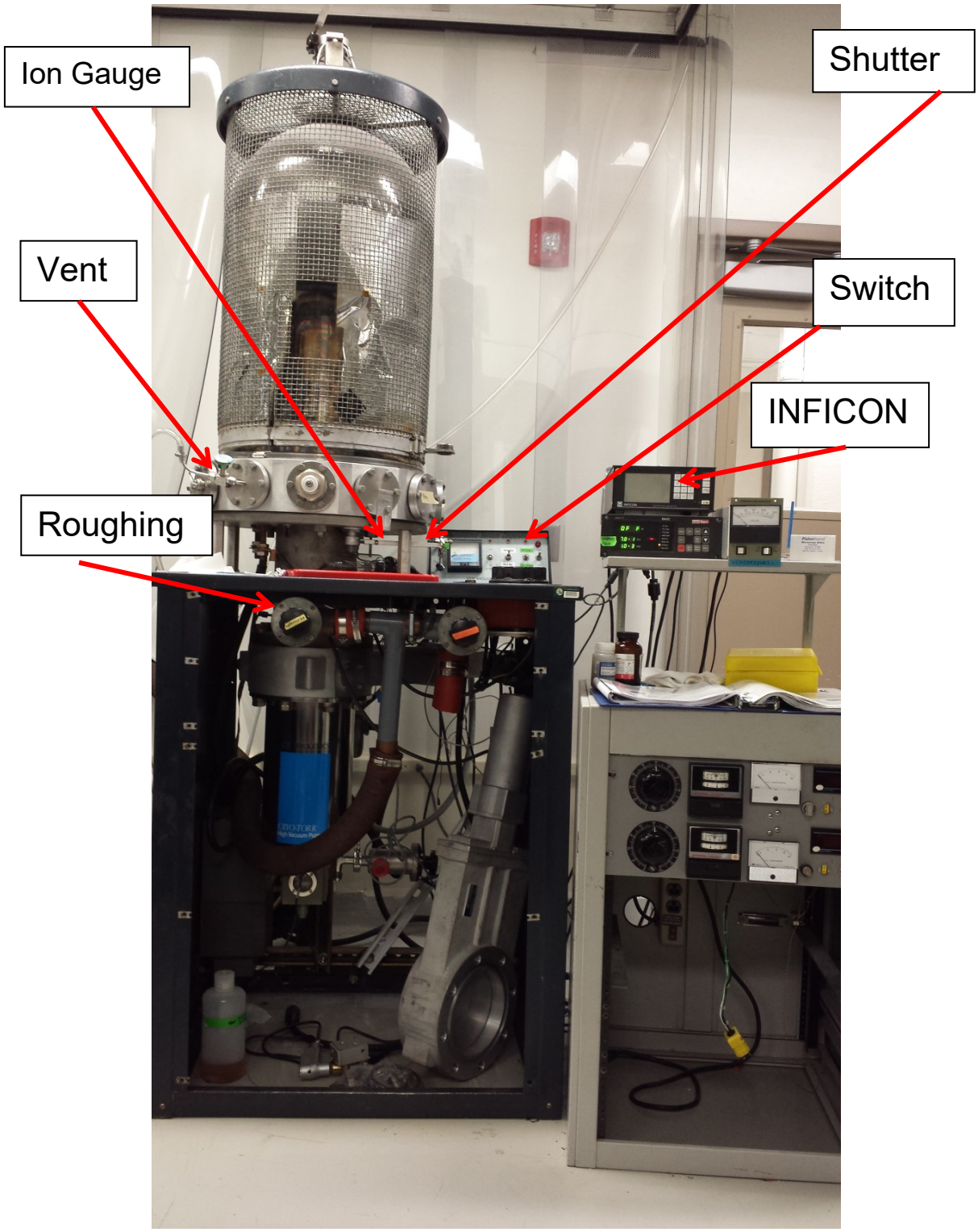

***Figure 26**. Image of JIM with labels of the important pieces of equipment*

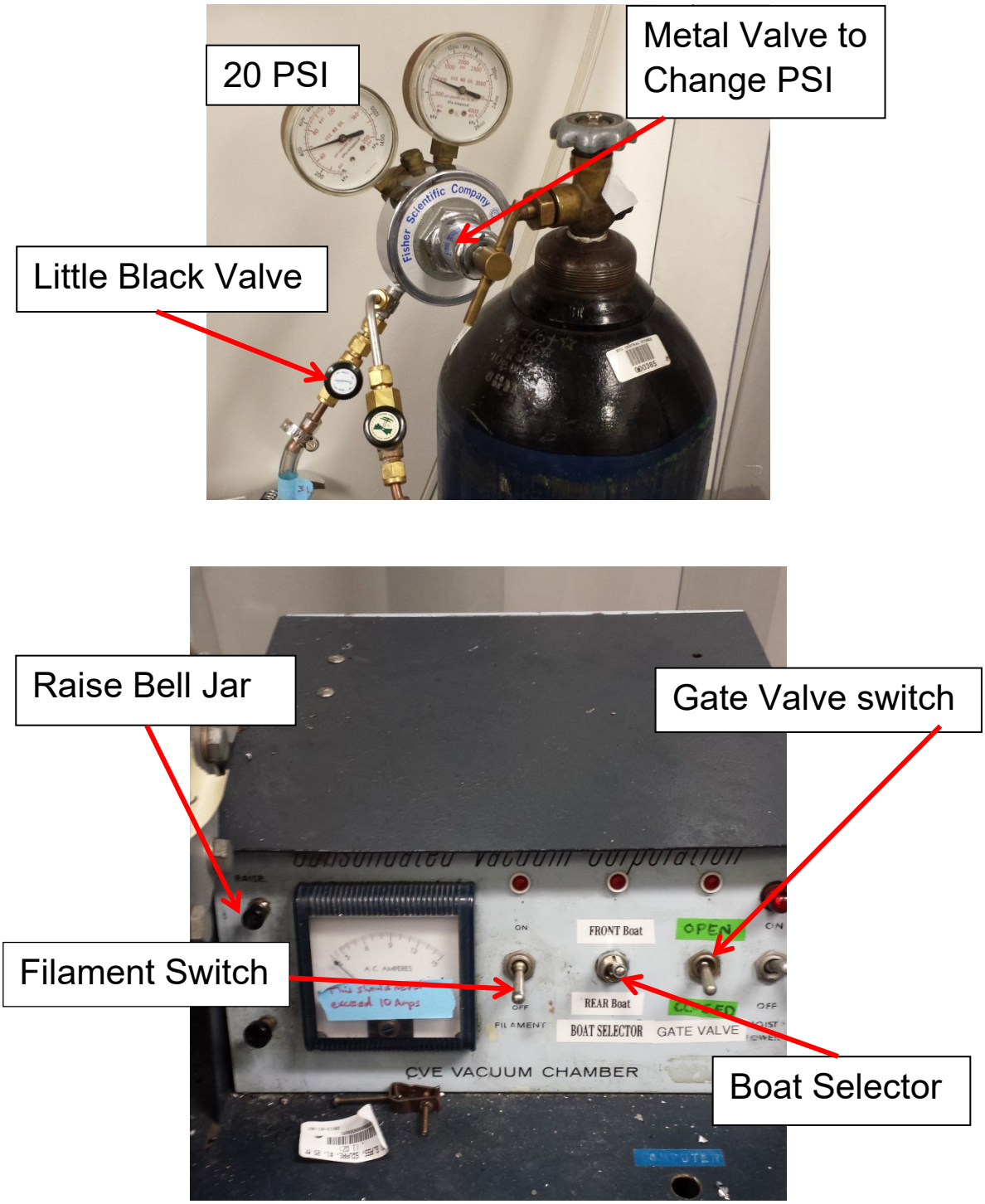

Figure 27. *Images of the nitrogen gas cylinder and control panel for JIM*

1. **Vent the chamber**
   1.1. Double check to make sure that the chamber is ready to be vented.

1.1.1. The ION GAUGE should be OFF (the bulb is NOT lit). If the bulb is ON, turn it off with the EMIS button.

1.1.2. Make sure the GATE VALVE is CLOSED.

1.2. Open the Nitrogen tank in the corner; record the pressure on the log sheet. Then open the back little black valve on the regulator.

1.2.1. Make sure the left gauge is around 20 psi. The metal valve opens when rotated clockwise.

1.2.2. Make sure that you close the nitrogen tank when you are done.

1.3. Open the VENT VALVE.

1.4. Wait until the chamber pressure reads 7.6 +2 (760 torr, this is atmospheric pressure)

1.5. Raise the bell jar a little bit using the RAISE button, and then turn of the VENT VALVE.

1.6. Raise the jar the rest of the way.

2. Prepare your sample

2.1. Look for a location on the plate where your sample will be shielded from the Gold AND Chrome when the SHUTTER is closed, and exposed to the Gold AND Chrome when SHUTTER is open.

2.2. Tape your sample to that location using the VACUUM TAPE

2.3. Obtain both the GOLD BOAT and CHROME ROD located in the top drawer of a black shelf box.

2.4. Place the boats in their respective holders. Chrome in the back holder under the nut. Gold in the front holder under the wing nuts.

2.5. Make sure there is chrome on the tungsten rod, if it has been previously used it will have a green tint. If new it will be distinct coloration from the tungsten ends.

2.6. Add 2-3 gold beads to the gold boat each time.

2.7. If needed, replace the GLASS SLIDE WINDOW.

3. Check the CRYSTAL MONITOR (XTAL)

3.1. Turn on the INFICON monitor if it is not already on.

3.2. Push the XTAL button (button number 1), if the XTAL reading is 100%, change the CRYSTAL.

4. Pump down the CHAMBER

4.1. Lower the bell jar slowing using the LOWER button, make sure that the coating of the jar does not get caught on the sample holder. Make sure it makes a good seal.

4.2. Make sure the VENT VALVE is CLOSED.

4.3. SLOWLY open the ROUGHING PUMP VALVE, and start a timer for T_{ROUGH} in the JIM logbook.

4.3.1. Keep the foreline pressure BELOW 3.0 +2.

4.4. When the pressure reads 5 -2 (50 mtorr) CLOSE the ROUGHING PUMP VALVE and record T_{ROUGH}.

4.5. Open the GATE VALVE, and start T_{CRYO}.

4.6. Wait for ~30 seconds and turn on the ION GAUGE by pressing the EMIS button.

4.6.1. The filament should turn on, looking like a light bulb.

4.7. Wait until the chamber reaches 2.0 -6 ($2*10^{-6}$ torr), this usually takes around 120 minutes or so.

5. Deposition of Chrome

5.1. Make sure that the INFICON monitor is on.

5.2. Chrome should be program 7 and gold program 8

5.3. Change the settings of DENISTY, Z-RATIO, and TOOLING FACTOR.

5.3.1. Press the PROG button.

5.3.2. Use the button that has a C with a triangle around it to go up in the menu, and the E with a triangle around it to go down until you are over the desired parameter.

5.3.3. To change the parameter, just type in the numbers. When the numbers are what they should be, hit the E triangle button.

Material	Density	Z-Ratio	Tooling
Chrome	7.200	0.305	63.0
Gold	19.30	.381	63.0

Table 4. *Table of relevant values to input into the crystal monitor control panel for Chrome and Gold*

5.4. Flip the BOAT SELECTION toggle switch to the REAR BOAT.

5.5. Flip the FILAMENT toggle switch to on. This turns on the power supply.

5.6. Ramp up the voltage with a maximum rate of 20 V/Min (5 V/15 Sec) using the VARIAC.

5.6.1. You should not exceed 10 Amps.

5.6.2. Go until you have a deposition rate of around 1Å/s. This can be seen on the INFICON monitor.

5.6.3. The voltage will usually be around 60-80 V.

5.7. OPEN the SHUTTER, and ZERO the crystal monitor (hit the 3 button that has the word ZERO over it).

5.8. Record the everything in the logbook.

5.9. Wait until the INFICON monitor reads the desired thickness, usually around 0.070 kÅ (this is going to be 7 nm), then CLOSE the SHUTTER.

5.10. Ramp down the voltage at a rate LESS than 20 V/min.

5.11. Turn off the FILAMENT toggle switch.

6. Deposition of Gold

6.1. Flip the BOAT SELECTION toggle switch to the FRONT BOAT.

6.2. Flip the FILAMENT toggle switch to on.

6.3. Ramp up the voltage with a maximum rate of 20 V/Min (5 V/15 Sec) using the VARIAC.

6.3.1. You should not exceed 10 Amps.

6.3.2. Go until you have a deposition rate of around 1Å/s.

6.3.3. The voltage will usually be around 180 V.

6.4. OPEN the SHUTTER, and ZERO the crystal monitor.

6.5. Record everything in the logbook

6.6. Wait until the INFICON monitor reads the desired thickness, usually around 0.500 kÅ (this is going to be 50 nm), then CLOSE the SHUTTER.

6.7. Ramp down the voltage at a rate LESS than 20 V/min.

6.8. Turn off the FILAMENT toggle switch.

7. Vent the chamber and remove sample

7.1. Get the chamber ready to be vented.

7.1.1. Turn OFF the ION GAUGE by hitting the EMIS button.

7.1.2. CLOSE the GATE VALVE toggle switch!

7.2. Open the Nitrogen Tank.

7.3. Open the VENT VALVE.

7.4. Wait until the chamber pressure reads 7.6 +2 (760 torr, this is atmospheric pressure)

7.5. Raise the bell jar a little bit using the RAISE button, and then turn of the VENT VALVE.

7.6. Raise the jar the rest of the way.

8. Get the system into standby

8.1. Lower the bell jar slowing using the LOWER button, make sure that the coating of the jar does not get caught on the sample holder. Make sure it makes a good seal.

8.2. Make sure the VENT VALVE is CLOSED.

8.3. SLOWLY open the ROUGHING PUMP VALVE

8.3.1. Keep the foreline pressure BELOW 3.0 +2.

8.4. When the pressure reads 5.0 -1 (0.5 torr) CLOSE the ROUGHING PUMP VALVE.

8.5. The system is now in standby.

9. REMEMBER TO MAKE SURE THE NITROGEN TANK IS TRUNED OFF!! This includes the main valve on the far right, and the little black valve on the far left.

S.O.P. Electron Beam Induced Deposition

Figure 28. *The Helios Scanning Electron Microscope*

All electron beam induced deposition (EBID) is currently performed on the Helios SEM due to it being the only scope with gas injection systems (GIS).

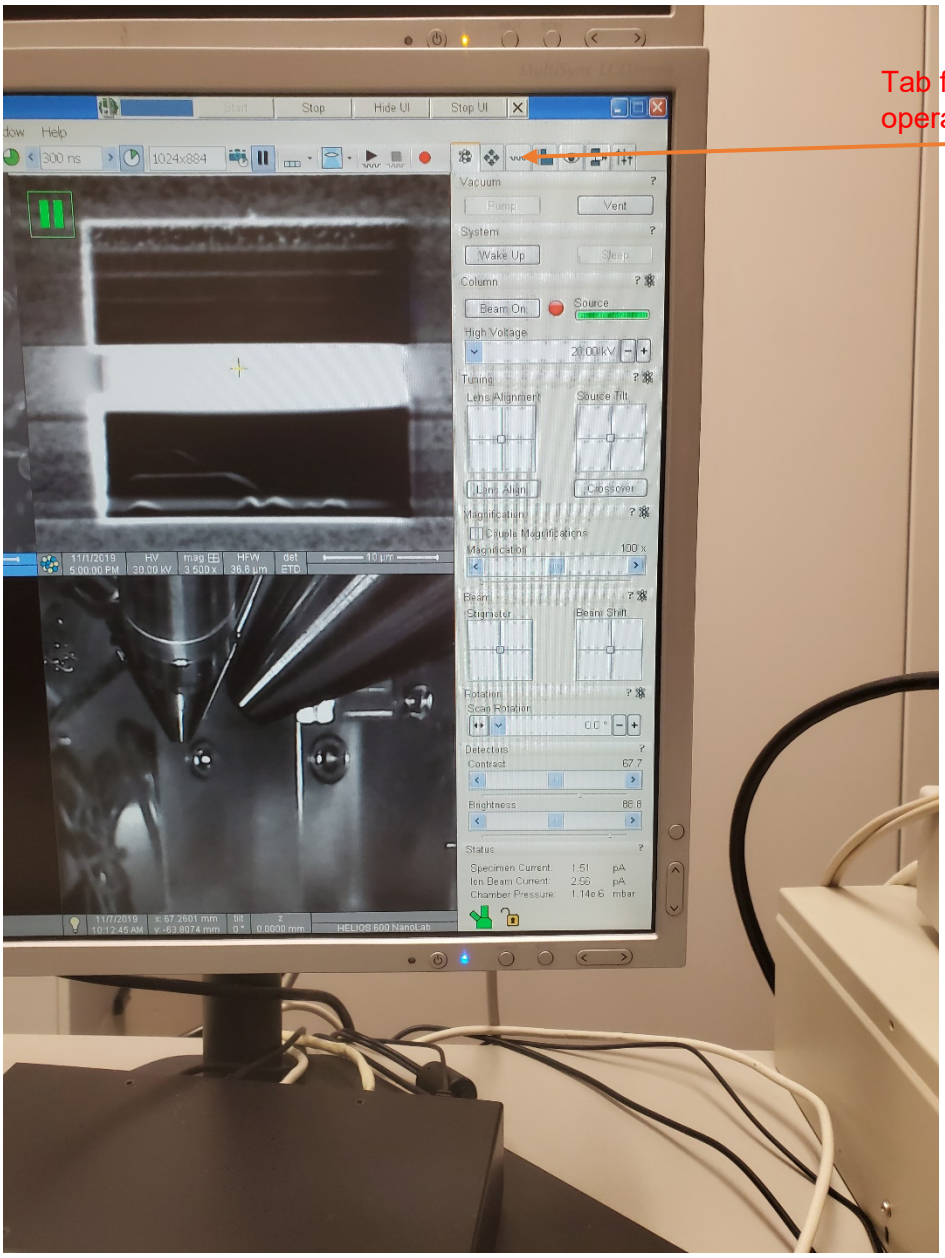

Figure 29. *The left microscope computer, clicking on the third tab allows for EBID control.*

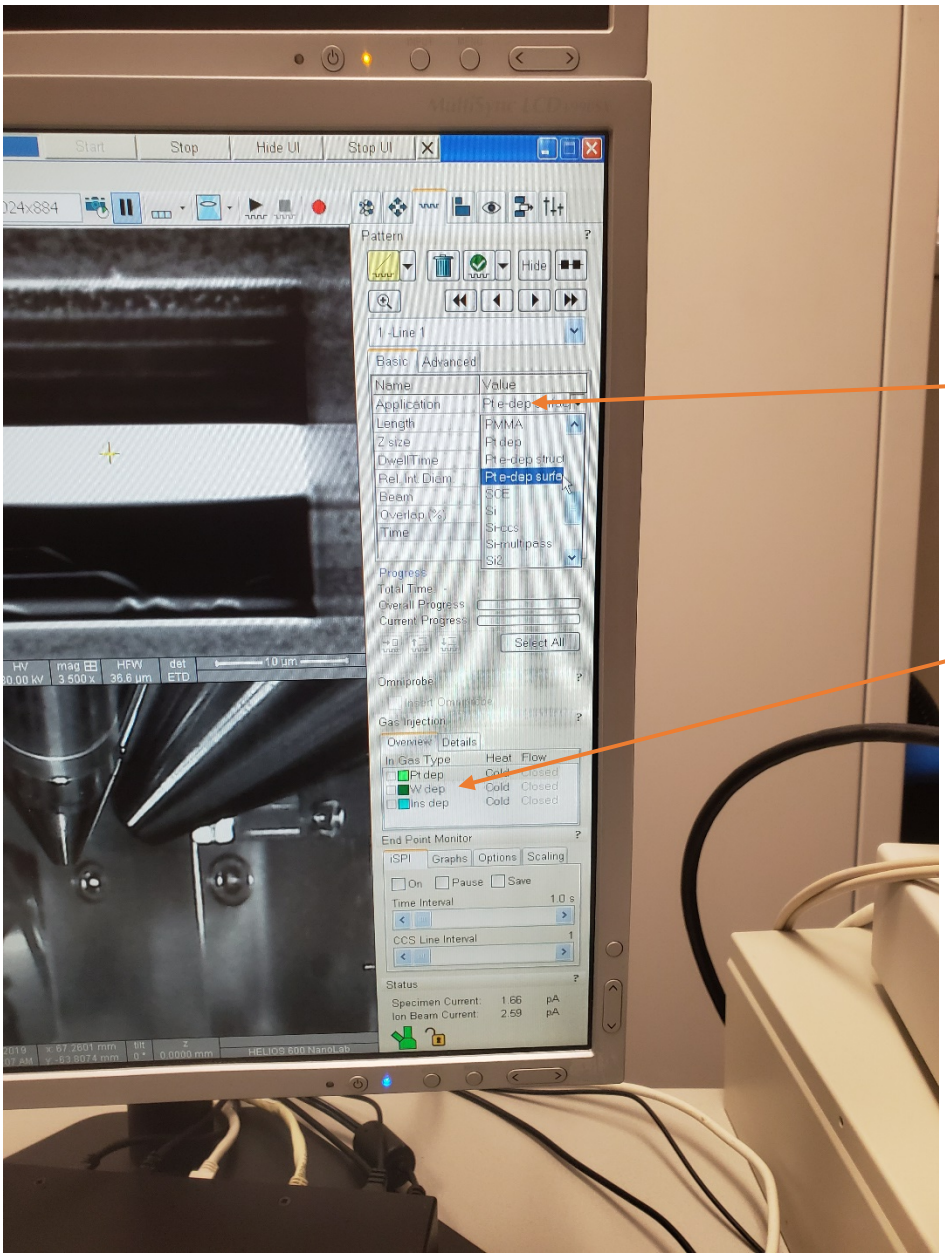

Figure 30. *Electron beam induced deposition control panel. Arrow indicate where gas injection systems can be controlled and metal type selected.*

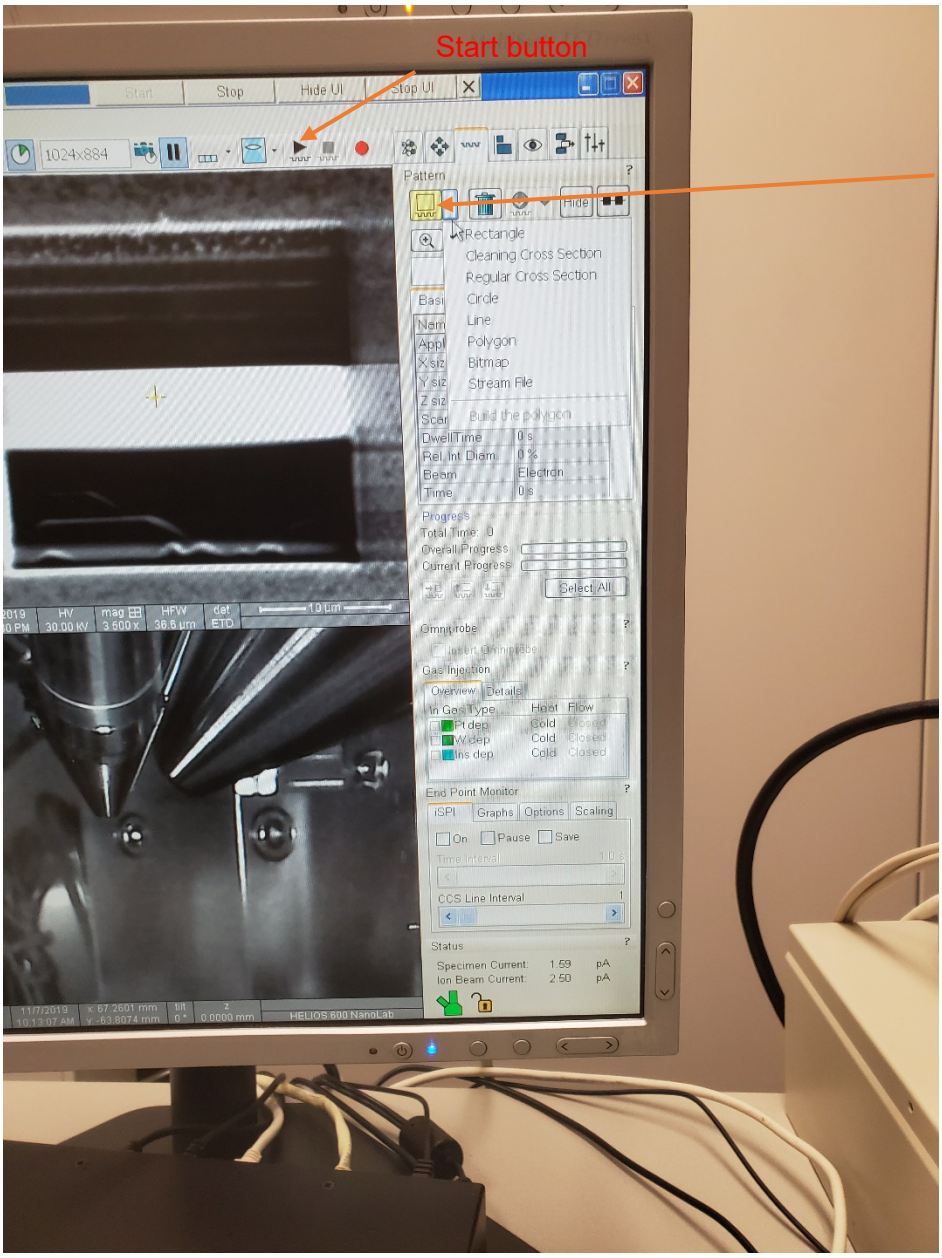

Figure 31. *Electron beam induced deposition control panel. Arrows indicate patterning options and how to begin patterning.*

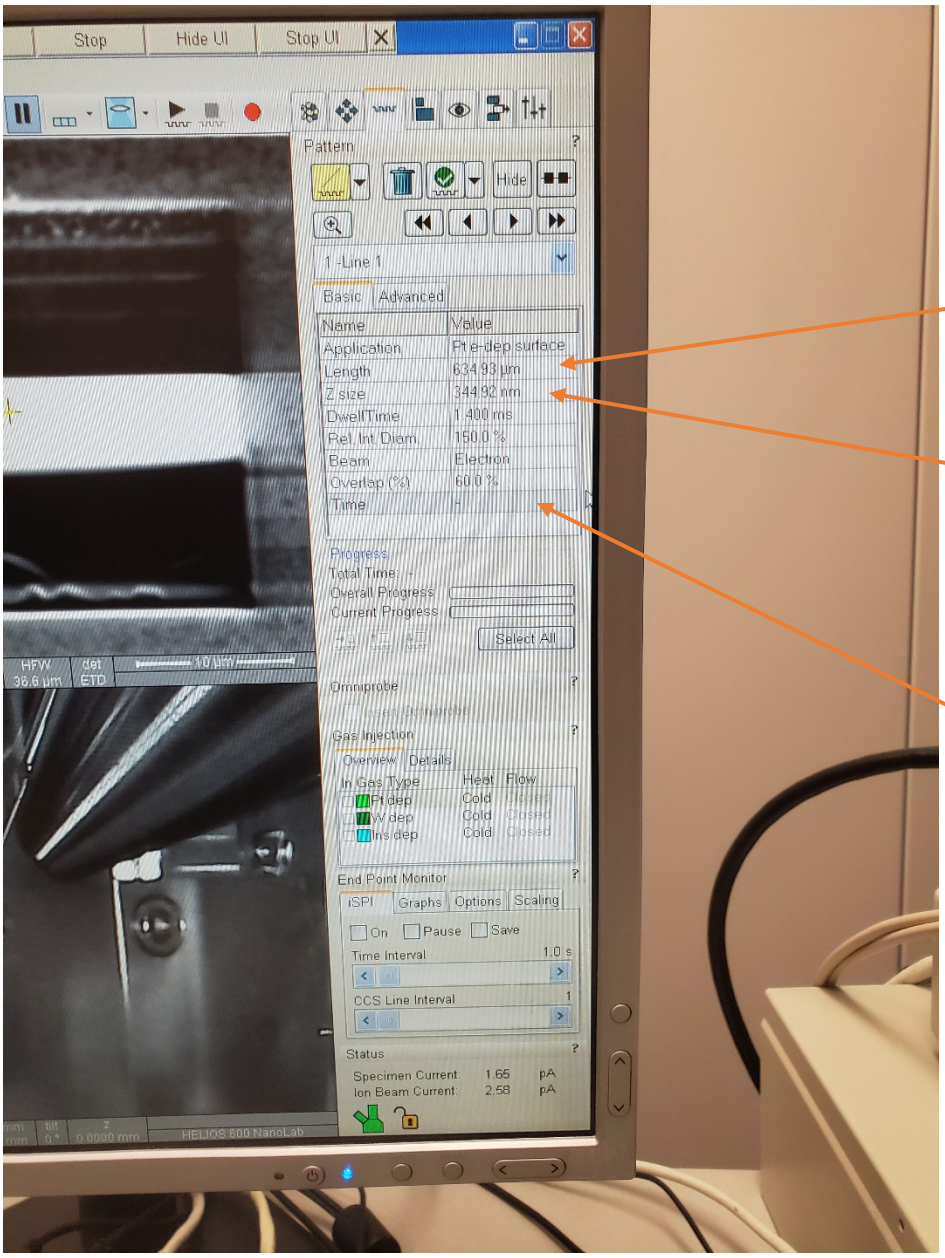

Figure 32. *Electron beam induced deposition control panel. Arrows indicate where to specify dimensions of pattern and resulting time expected till completion.*

ELECTRON BEAM INDUCED DEPOSITION

1. Startup Helios SEM
    a. Following Helios Training get the microscope sample inserted
    b. Pump down
    c. Perform alignments (Focus, Sitgmate, Get to eucentric height for Pt, or 5 mm for W)
    d. Find desired location on sample
2. Prepare GIS
    a. Turn on the GIS heater, (ideally as soon as the microscope is at pressure)
        i. Located in patterning tab (3rd tab)
    b. Once at temperature ideally wait 5-10 more minutes before use.
3. Software
    a. The patterning tab is the 3rd tab
    b. Select what patterning technique you want to use
        i. W or Pt e-dep
    c. Select what type of pattern you want to write a line or an area
        i. In the viewing screen patterns can be drawn once selected
        ii. Fine adjustments can be made on the right and the z height must be inputed
            1. Actual height was usually about 1/3 the desired height
    d. You can write more than one pattern at a time
        i. They must all be in the same viewing window
        ii. I don't recommend writing more than one area at a time in case of drift
    e. Start Run
        i. Insert the GIS
        ii. Make sure your still where you want to be
        iii. Press start button
        iv. Time will reflect progress
4. Other Notes
    a. Drift
        i. Drift is a big issue , make sure your focus and sigmation is as good as you can get it to minimize drift
        ii. You can add more material to a section that didn't quite turn out right due to drift
    b. Overspray
        i. Overspray occurs because of scattering causing the breakdown of the gas in other locations
        ii. This becomes an issue if there is enough metal deposited to create a conductive path
        iii. Line dose has less overspray than area dose
    c. Pt vs W
        i. I have been able to write finer features with Pt with out overspray being a problem, but Pt needs purified if being used for electrical transport
        ii. Due to the location of the GIS Pt can be operated at normal eucentric height but W must be lower or it will crash into the stage

d. Immersion mode
    i. I did all my writing in immersion mode
    ii. It is easier to write in normal mode but there is some more overspray so features are not as small
e. Tungsten
    i. Sometimes the W GIS will knock the vacuum out of green when opened
    ii. Let it come back to green and then manually flow the gas make sure it stays open for a couple minutes without issue
    iii. Close it and then it should work normally

S.O.P. Purification of Platinum

Purification of Platinum EBID through electron irradiation in water atmosphere modified from a paper[45]

This is performed in the ESEM electron microscope by FEI

1. SETUP
    a. The end of the pole piece needs replaced with the low vac piece
    b. The GSM detector needs installed into the back on the chamber
        i. Both of these are part of the training for low vac mode
    c. Pump down in low vac mode to .5 Torr
    d. Choose the 2nd largest spot size
        i. This allows for faster purification
2. Purification
    a. Typical setup of SEM with focus/stigmation etc
    b. Find area of platinum that needs to be purified
    c. Expose the area by just imaging one area
        i. The typical times are 8min/um^2
            1. The size is your exposure window
    d. Once one area has completed move the exposed window along Pt lines and repeat
    e. Continue until completion of all structures
3. Other facts
    a. The Pt traces will reduce in volume throughout the purification process
    b. There will be a visible change in some of the traces but the overall shape usually remains the same

S.O.P. Four point probe station

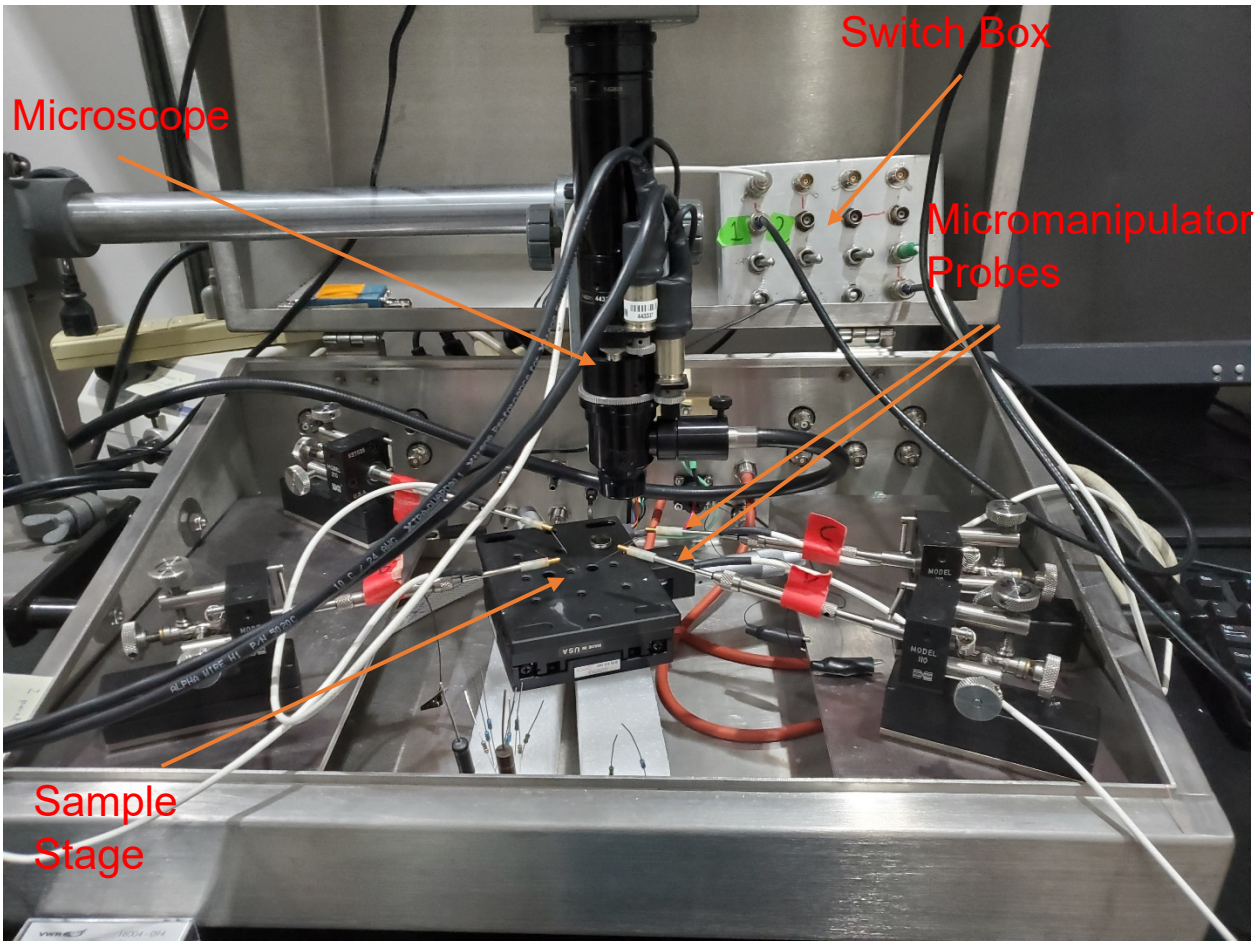

Figure 33. *Four-Point probe station. Key components are indicated.*

The four-point probe station is a simple station designed for controlled placement of 2 or 4 electrical leads for the purpose of conductivity measurements.

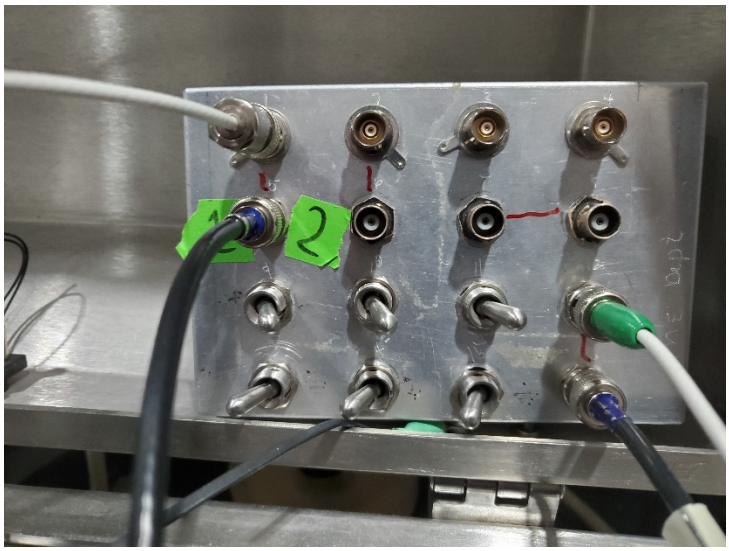

Figure 34. *Switch box for four-point probe station. Box is used to convert from tri-ax cables to coax cables.*

Switch box is designed to act as a transition box between the tri-ax cables coming from the probes and coax in the equipment. Two of the cables are already co-ax but the box is still used for consistency. The connected ports are denoted by the red lines

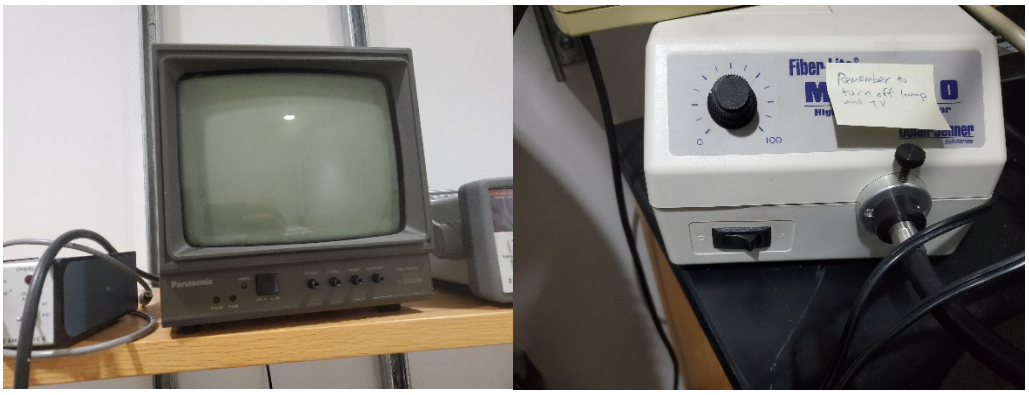

Figure 35. *Left image is small TV used as output for four-point probe microscope. Right image is the light control box for the microscope of four-point probe.*

For smaller structures there is a microscope in the middle of the station. To use the microscope the TV and the sight source both need turned on.

***Figure 36**. Preamp for four-point probe station.*

Pico-ammeter is used to scale you current to make it detectable. The input comes from the switch box and the output going into the DAQ to measure the current. The only knob that should be changed is the sensitivity knob.

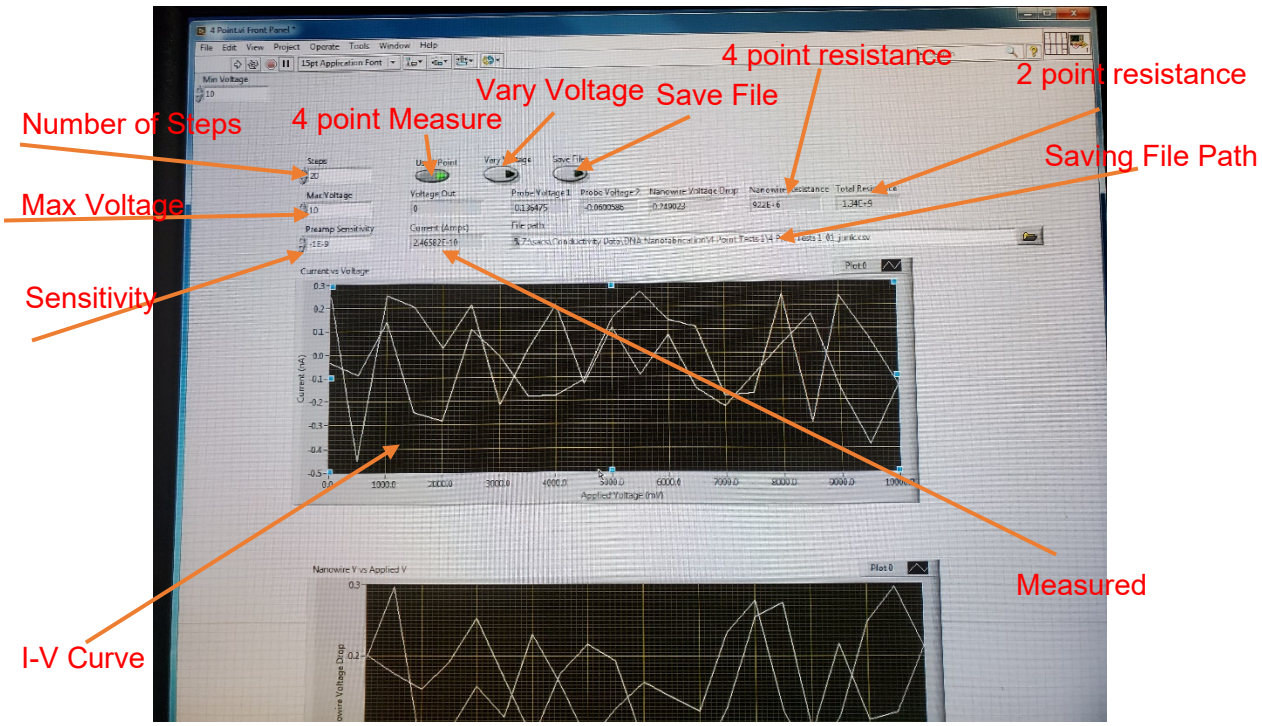

***Figure 37.** Image of the Labview program used for the four-point probe station. Key features are indicated.*

1. Sample Connections
    a. Place test sample on xy stage
    b. Turn on Microscope light and the TV
    c. Move stage to see desired test area on TV
        i. Focus microscope on sample
    d. Move micromanipulator probes to desired location
        i. They are connecting once the tip is in focus
2. Software setup
    a. Open labview
        i. Open 4 point probe file
    b. Enter the number of steps
        i. The number of steps is divided by the max voltage and determines the amount of each step size
    c. Enter max voltage
    d. Set the sensitivity to match what the pico ammeter is set to
    e. Click buttons to specify if performing 2 or 4 point measurement
        i. Can chose to vary voltage or keep a steady voltage
        ii. Specify if going to have the file saved
            1. File path needs specified
            2. It will save over the file if you don't change the name
3. Run software
    a. While running watch the pico-ammeter if the red light comes on the sensitivity needs lowered
    b. The display shows current and voltage
        i. If the current is negative it is indicating that there is no detectable current
            1. Sensitivity needs increased or the sample is non conductive
    c. Once completed an IV curve will be displayed
    d. The display will give an estimated resistance for the 2 and 4 point measurements
        i. This is simply the slope from the lowest and highest point on the graph
        ii. If the graph is no linear it will not be reliable
4. Troubleshooting
    a. Nothing seems conductive
        i. Try placing the two current leads on a known conductive site like a large metal pad. The red light on the ammeter should illuminate even if no voltage is applied
    b. Connections
        i. There are 4 connections 2 current and 2 voltage drop
        ii. The current driving cable comes from the output on the DAQ
        iii. The return goes into the pico ammeter then into an input on the DAQ
        iv. Those two are the only ones used in 2 point measurements
        v. The two voltage drop cables just go into the inputs on the DAQ
    c. Sample Stage
        i. The stage is just an xy stage on some foam

ii. To move just slide around on the foam

List of Staple Strand DNA Sequences

All are given 5' → 3'. Sequences in blue font have a protruding poly(A)$_{10}$ for DNA-coated Au nanorod capture.

(A) 'Plus' design

TGAACGGTCGCGTCTGGCCTTCCTGGGATGTG

AAGCCTGGGCCAGCTGGCGAAAGGGTAGCCAGAAAAAAAAAA

ATGCTGATGCAACCAAGTACCG

TACTGGTAACCGTTCCAGTAAGCGTAAATATT

GCCCGAAACAGTCAGGACGTTGGGAGAAACAC

TAACAATTAAGAAGATGATGAAACCTAAAATA

TTTGGAACAAGAGTCCACTATTAAAGCTGTTT

GCACAGACAATTATAATCCTGA

TTGAGTAAAAGCCAGAATGGAAAGAATTATCA

TACTTAGCCGGGAGAGGCTTTT

CCGTCACCTAGAAAATTCATATGGGTTTAACG

AATGCCACATCAACGTAACAAAGCGGAACAAC

CATTTTTGATTTCAACGCAAGGATCGTTCTAG

TTAATTTCATCGGAACGAGGGTAGCTTTTGCG

AATAACATGCTATTTTGCACCCAGAATTCTGT

GCAAAAGAAGTTTAGCTATATT

GCAAATCAGAATTGAGTTAAGCCCAACGGAAT

ACCTTTTACCCTTAGAATCCTTGAGCGTTAAAAAAAAAAAAA

ACATTAATAGGGCGATCGGTGCGGGAGTAACA

AATGCGCGTTCCTGATTATCAGATGAAGGGTT

AGAACCGCGGCGGATAAGTGCCGTATTTTCAGAAAAAAAAAA

CCGGAACCAGTATAGCCCGGAATATCAGAACCAAAAAAAAAA

TTACCGAAAACAAGCAAGCCGTTTCAAGAACG

GAGCAAGAAATCATTACCGCGCCCAATCAATA

CAAAGCGCGAAACCTGTCGTGCCACTGAGAGA

GAAAAGGTATGGTCAATAACCTGTTTTGCCAG

ATTACGCAAGCACCGTAATCAGTAACCCTCAGAAAAAAAAAA

CGCCTGATGCTTCTGTAAATCGTCTTACTAGA

CTGATTGCCCTTCACCGCCTGGCCGCTGCATT

GATTGACCTTAATGCCGGAGAGGGTGCGGGAG

GCCTGAGAAACATTAAATGTGAGCGCCTCTTCAAAAAAAAAA

TTCATTTGGGGAAATATTTAAA

TTTGAGAGGATTCTCCGTGGGAACTGCGCAAC

ATCACCATCGCATCGTAACCGTGCAGCCAGCT

TTTGACCCGCGCATAGGCTGGCTGATGCAGAT

ACCCAAAATGCCTTTAGCGTCAGACCACCCTCAAAAAAAAAA

GGATCGTCCTCAGAACCGCCACCCGGTGTATCAAAAAAAAAA

CCGCCTGCATCCTTTGCCCGAACGGTAACAGTAAAAAAAAAA

CAGAAAACATACCACATTCAACTAACCTTCATAAAAAAAAAA

CGAAAGACAGCAACTTTAATCA

AATGCAGAAACACCGGAATCATAAGCTATTAAAAAAAAAAAA

TTATTAGCAGATAGCCGAACAAAGTAGCTATC

ATTATTACACCCTGACTATTATAGTAATTGCT

CAGCCATATTACAACCGATTGA

CTTTCCAGTAAGAAACGATTTTTTTTTACCAG

GATTAGTTAAAAACAGGGAAGCGCAAAGAAAC

TTACCCAATACGAAGGCACCAACCGCTTGATA

CATTATACGACTTCAAATATCGCGGATTAGAG

TTTCATCTCGAGCATGTAGAAACCAATAGCAA

ATCGGCTGCTTTTTCAAATATATTGGTCTGAG

GGATTTTGGAATTGCGAATAATAAATCGCCTG

AAGAGCAATACTGCGGAATCGTCAATTCTGCG

CTTTCGAGTAGCATTCCACAGACATATTCTGA

ATTACCGCCAGCCATTGCAACAGGGAGCCAGC

GAGGAAGTAAGGCTTGCCCTGACGAAGAAAAA

ATCGTAGGAACAATGAAATAGCAATTACCAGA

GGTTTAACTAGATTAAGACGCTGATGGTTTGA

ACCAGTCACACGACCAGTAATAAAACATCGCC

CTGCAAGGTACGAGCCGGAAGCATTCAAAAGA

AGGAAACCTCGGCATTTTCGGTCAAGCCACCAAAAAAAAAAA

GAGGATCCCCGACCGTCTATCA

AAGAGAAGCCAGAACCACCACCAGTGAAACCA

AGGAAGGTTATAAACATCAAGA

AGCCGCCAGATTAGGATTAGCGGGATGTACCGAAAAAAAAAA

ATTAAAAAAAACCACCAGAAGGAGTGCACGTA

AGCATTAAGATTTAGTTTGACCATACTGGATA

TAACATCACTTGCCTGAGTAGAAGTCAATATC

TAAGAATAACGCGCCTGTTTATCAAACCTCCCAAAAAAAAAA

TAGATGGGCAATATGATATTCAACAAAAATTT

CGAGCTTCCTTATGCGATTTTAAGGAGATGGT

CCTCATTACAGTGCCCGTATAAACTGTCGTCTAAAAAAAAAA

AGGCTTGCCAGAGCCACCACCCTCCGAGAGGGAAAAAAAAAA

GCCACCCTAGGGAGTTAAAGGCCGCAACGGCT

CTAAGAACTTGAGCGCTAATATCAGACTCCTT

AACTAAAGCTAAACAACTTTCAACCAGGAGTGAAAAAAAAAA

CGATAGCTGTCAGATGAATATACATTATTAAT

GAAATCGGCAAAATCCCTTATAAAAAAGTGTAAAAAAAAAAA

GGGAGGGAAGGTCATACATGGCAAAAAAAAAA

AATAGTGAATAAAGAAATTGCGTAATTTTGCG

CCAACTTTAACGGAGATTTGTATCTTTTTTCA

GTCTGAAATGGATTATTTACATTGAGCAGAAG

AGAACCTATTTTTAACCTCCGGCTAAAGAACG

CAAAAACATCGCATTAAATTTTTGACGACGGC

TAACACTGTGCGCCGACAATGACAAAATACGT

AATGAATCCCGCTTCTGGTGCCGGCGTTGGTG

ATCAAGTTGAACTGGCATGATTAAGAGAGATA

AATCCAAAAGCCTAATTTGCCAGTATTTAGGC

AGCAAATGGACTTTACAAACAATTAACGGATT

CTTTCATCGTCTGGAGCAAACAAGATAAAGCCAAAAAAAAAA

TTCCGGCAGGCCAACGCGCGGGGAGGCAACAG

CAGTACCACACCCTCAGAGCCACCGCGACAGA

ACATAACGCCCCCTCAAATGCTTTGAAGTTTC

ACAGAGGCGTAGTAAATTGGGCTTAACTGGCT

TTCCAGACATCTCCAAAAAAAAGGGCGCGAAA

TAGCAAGGAAGGTGGCAACATATAATTAGACGAAAAAAAAAA

TCATCATAAACTGATAGCCCTAAAAGGGACAT

CGCCAAAGTTATTCATTAAAGGTGCGCAGTCTAAAAAAAAAA

AAGTATTAAAAAATCTAAAGCATCAGAACAAT

TTATCCTGGAAAATAGCAGCCTTTATTTTGTC

TTTAAAAGGAGGTGAGGCGGTCAGGCTCAATC

AAGCCTTTCGGATGGCTTAGAGCTTCAGAAGC

ACCCACAAGATATAGAAGGCTTATATCCCATC

GTACCGCCACCACCCTCAGCAG

CCGATAGTAGTTTCGTCACCAGTAGACTCCTC

GCCGTCAAAATATCAAACCCTCAAAACTCAAA

TGAGTAATAACTCCAACAGGTCAGTTTTAATT

GTATCGGCCTCTGGGCGCCAGG

GTGGTTTTTCTTTTCACCAGTGAGACGGAGGCGGT

CAGACCAGCCAGCGATTATACCAACTCCAAAA

GCGTCCAACACTATCATAACCCTCCGAACTGA

CCCCCTGCCTTGATATTCACAAACGAATTAGA

GAAAGCGTAAGAATACGTG

TATGCAACTAAAGCTAAATCGGTTAGGTCATTAAAAAAAAAA

CCAGACGAGTTTAGTATCATATGCGTGAGTGA

ATATGTACTTTAACCAATAGGAACCGCCAGGG

TTCATCAAATTTTTGAATGGCTATTCTGACCT

ACACAACACGATTAAGTTGGGTAAGCCATCAA

GAAAAGTAAGCGTTTGCCATCT

TTTCGCAAGGCATCAATTCTACTAAAAAGCCC

ATTCCATATTAGCAAAATTAAGCAAGAATCGA

TTAGAACCTAATTGCTCCTTTTGAAAGAGGAA

GCCAGCAAACCACGGAATAAGTTTACAGAGAG

GTTATATAATACTTCTGAATAATGGATGGCAA

GCTATTACGGTGCCTAATGAGTGAGTGGTTCCAAAAAAAAAA

ACCGTACTAAATCACCGGAACCAGTAGCCCCC

GATTCAAAAGGGGACGACGACA

CAGTGAATTTCCATTAAACGGGTAACAACCAT

CGAGAAAATCTTTCCTTATCATTCTTATTTTC

TCGCGCAGACATAAATCAATATATGTTATACA

CGTTGAAAGTTAGTAAATGAATTTTCAGTGCCAAAAAAAAAA

AGCAGGCGAAAATCCTGTTTGATGGCTAACTC

CATACATACCGGAAACGTCACCAAAGCCGCCG

CCAGCATTAGTATTAAGAGGCTGACAAACTAC

AGTTAGCGTAATTGTATCGGTTTACACTCATC

AAACAAAATTATATTTAACAAC

CGATTGGCCTATTTCGGAACCTATGCCCTCAT

GACGGAAAACAAAAGGGCGACATTTTTATCCC

GACTTGCGAACTGAACACCCTGAAAGAAAATAAAAAAAAAAA

ATAGCCCGAGATAGGGTTGAGTGTACAATTCC

TTGTTTGGATTACTATATGTAA

TTAATTTTCATCGGGAGAAACAATCGACAACTAAAAAAAAAA

TTGTGAATTACAAAGCGAACCA

GCCAACATGTATACAAAATAAA

CGTTTTCAGAGGAAACGCAATAATAATAATAA

GCAGACGGTGTCGAAATCCGCGACAAAGGAAC

TCTACGTTTTGCATCAAAAAGATTTAAGAGGT

AGTACCTTCTCATATATTTTAAATACAGTCAA

CACTCATCGAGGCCCTTTTTAA

TTTTCCCAAAATTGTTATCCGCTCTGTTCCAG

TCTTTAGGTGGCAAATCAACAGTTATTAGTAA

AAAGCGGAAATAAAACGAACTAACTGCTCATT

AATACCGAGAACAAGAAAAATAATCCGGTATT

AGTGAGAATAGCTGCTCCATGT

GAACCTCATAGATAATACATTTGATTACAAAA

CTGAATTTATAAGTTTTAACGGGGTCTGTATGAAAAAAAAAA

AACATGAAGACAGGAGGTTGAGGCATTACCAT

GAATATAAGACCCTGTAATACTTTTAGCTATT

CATTGAATCCAAAAGGAATTACGAACGGTGTA

CAGAACGATTTGAGGACTAAAGACGGTCGCTG

GTTTGAGGGTGAGAAAGGCCGGAGGCAATGCC

TTTTGATGATAAGTTTCAGCGGAAAAAAAAAA

ACAATCAAGACTTGAGCCATTTGGAAATAAATAAAAAAAAAA

TGGTCAGTAGCACTAACAACTAATTCAATTAC

ATAAATTGTCAATCATAAGGGAACGTTTACCA

AAACAGAAATTTATCAAAATCATATTAGTTAA

AGGGGGTATAAAAACCAAAATAGCAACGAGGC

GAAACAGTAGGCGAATTATTCATTAGATTAGA

GTTAAAATGGAAGATTGTATAAGCCGCGAGCT

AAATAATTAATCGTAAAACTAGCACAGGCAAG

AGGTCTTTAGGTAGAAAGATTCATGATATTCA

ATAACCTTTGCTTTGAATACCAAGGGATTTAG

GACTCCAACGTCAAAGGGCGAAAAGGTACCGA

GCTCGAATAGCTTGCATGCCTGCAAATATTTT

CTGAGCAATCATTTGAATTACCTTGCTCAACA

ATAAAACATTTGAGTAACATTATCGATTTTCA

TTGCGTATAGGAAGATCGCACTCCATCTGCCA

GGAGAATTGGAGGTTTTGAAGCCTGTTCAGCTAAAAAAAAAA

TGTTGGGATGCGTTGCGCTCACTGTTTGCCCC

CTGATAAAGTAATGGGATAGGTCAAAACCAGG

TCATGGAAATACCTACATTTTGACTATTAACAAAAAAAAAAA

CAAAGTACGAAAGAGGACAGATGAGGCATAGT

ATACTTCTTTGGAAAGGAATTG

GGTATTAAAATCCAATCGCAAGACTAGGTTGG

TTGTAAACGTTGGTCGACTCTA

AATTCTTACGACAAAAGGTAAAGTCTACAATT

TTTCATAATCACAGGAGGTTTAAAAAAAAAAA

GCAAAGAATAACAGTTGATTCCCATAAATATT

CGCCCACGAGCCCAATAGGAACCCGTTTTGCTAAAAAAAAAA

CTATCGGCCTTGCTGGTAATATCCACCTTGCT

CTAATTTATCTGACCTAAATTTAAGAAGAGTC

GAACAAAGTACCGAACGAACCACCGCAGATTC

TAAAGTACCCAGTATAAAGCCAACTTTTAATG

AGAGGCATTAATTGAGAATCGCCAATTACATT

GTTGCAGCAAGCGGTCCACGCTGGCCCGCTTT

GTAGGGCTTTTCGAGCCAGTAATAACGAGCGT

GACGACGAATAGTAAAATGTTTAGTAGATACA

ATTTAGGAGAGAATGACCATAAATGTTTTAAAAAAAAAAAA

AAAAGCCTCGACAATAAACAACATTAAATCAA

TCTGGCCAACAGAGATAGAACCCTTAGTCTTT

AACGAGTACATCCAATAAATCATATGTCAATC

CAAGAGTAAAAGAATACACTAAAATCAGCTTG

CCAGTCGGCATTCGCCATTCAGGCAAACGGCG

TAAGTCCTCCGTGTGATAAATAAGAAACATAG

GAGGGTAAGCGAGGCGTTTTAGCGACAATAGA

TCGATAGCGTATGTTAGCAAACGTCAAAGTCA

AAGAGGCAATCTTGACAAGAACCGCAGTTGAGAAAAAAAAAA

GGATAGCACATAACCGATATATTCTTTTTCAT

GGAGCCTTTAACGATCTAAAGTTTAGTTAATGAAAAAAAAAA

AGACTACCCCATATCAAAATTATTCGGAATTA

TCAAAAATAATCTTACCAACGCTAAGAGAATA

ACCCGTCGATCTACAAAGGCTATCGTACCAAA

CAGTGCCATCGTAATCATGGTCATAGAACGTG

TTGATATAGCCTCCCTCAGAGCCGCTGTAGCG

TCAGAGCATAAAGTACGGTGTCTGAAACAGTTAAAAAAAAAA

AACGCCTGGTGAATTTCTTAAACATAAAACGA

AACATTATTGCTGTAGCTCAACATCAAAAATC

CGTATTAAAACAGTGCCACGCTGAAAAAACGCAAAAAAAAAA

GCTCATTTCCCGGTTGATAATCAGATAGTAGT

GCAAAGACAATCACCAGTAGCACCAGGTCAGA

GACCGGAAGCAGTGTAGGTAAA

CCTGTGTGGTCACGACGTTGTAAATTAAATCA

(B) 'Cross' design

TGAACGGTCGCGTCTGGCCTTCCTGGGATGTG

AAGCCTGGGCCAGCTGGCGAAAGGGTAGCCAGAAAAAAAAAA

ATGCTGATGCAACCAAGTACCG

TACTGGTAACCGTTCCAGTAAGCGTAAATATT

GCCCGAAACAGTCAGGACGTTGGGAGAAACAC

TAACAATTAAGAAGATGATGAAACCTAAAATA

TTTGGAACAAGAGTCCACTATTAAAGCTGTTT

GCACAGACAATTATAATCCTGA

TTGAGTAAAAGCCAGAATGGAAAGAATTATCA

TACTTAGCCGGGAGAGGCTTTT

CCGTCACCTAGAAAATTCATATGGGTTTAACG

AATGCCACATCAACGTAACAAAGCGGAACAACAAAAAAAAAA

CATTTTTGATTTCAACGCAAGGATCGTTCTAGAAAAAAAAAA

TTAATTTCATCGGAACGAGGGTAGCTTTTGCG

AATAACATGCTATTTTGCACCCAGAATTCTGT

GCAAAAGAAGTTTAGCTATATT

GCAAATCAGAATTGAGTTAAGCCCAACGGAATAAAAAAAAAA

ACCTTTTACCCTTAGAATCCTTGAGCGTTAAA

ACATTAATAGGGCGATCGGTGCGGGAGTAACA

AATGCGCGTTCCTGATTATCAGATGAAGGGTTAAAAAAAAAA

AGAACCGCGGCGGATAAGTGCCGTATTTTCAG

CCGGAACCAGTATAGCCCGGAATATCAGAACC

TTACCGAAAACAAGCAAGCCGTTTCAAGAACG

GAGCAAGAAATCATTACCGCGCCCAATCAATAAAAAAAAAAA

CAAAGCGCGAAACCTGTCGTGCCACTGAGAGA

GAAAAGGTATGGTCAATAACCTGTTTTGCCAG

ATTACGCAAGCACCGTAATCAGTAACCCTCAGAAAAAAAAAA

CGCCTGATGCTTCTGTAAATCGTCTTACTAGA

CTGATTGCCCTTCACCGCCTGGCCGCTGCATT

GATTGACCTTAATGCCGGAGAGGGTGCGGGAG

GCCTGAGAAACATTAAATGTGAGCGCCTCTTC

TTCATTTGGGGAAATATTTAAA

TTTGAGAGGATTCTCCGTGGGAACTGCGCAAC

ATCACCATCGCATCGTAACCGTGCAGCCAGCTAAAAAAAAAA

TTTGACCCGCGCATAGGCTGGCTGATGCAGATAAAAAAAAAA

ACCCAAAATGCCTTTAGCGTCAGACCACCCTC

GGATCGTCCTCAGAACCGCCACCCGGTGTATC

CCGCCTGCATCCTTTGCCCGAACGGTAACAGT

CAGAAAACATACCACATTCAACTAACCTTCAT

CGAAAGACAGCAACTTTAATCA

AATGCAGAAACACCGGAATCATAAGCTATTAA

TTATTAGCAGATAGCCGAACAAAGTAGCTATC

ATTATTACACCCTGACTATTATAGTAATTGCT

CAGCCATATTACAACCGATTGA

CTTTCCAGTAAGAAACGATTTTTTTTTACCAG

GATTAGTTAAAAACAGGGAAGCGCAAAGAAACAAAAAAAAAA

TTACCCAATACGAAGGCACCAACCGCTTGATA

CATTATACGACTTCAAATATCGCGGATTAGAG

TTTCATCTCGAGCATGTAGAAACCAATAGCAAAAAAAAAAAA

ATCGGCTGCTTTTTCAAATATATTGGTCTGAGAAAAAAAAAA

GGATTTTGGAATTGCGAATAATAAATCGCCTG

AAGAGCAATACTGCGGAATCGTCAATTCTGCGAAAAAAAAAA

CTTTCGAGTAGCATTCCACAGACATATTCTGA

ATTACCGCCAGCCATTGCAACAGGGAGCCAGC

GAGGAAGTAAGGCTTGCCCTGACGAAGAAAAAAAAAAAAAA

ATCGTAGGAACAATGAAATAGCAATTACCAGA

GGTTTAACTAGATTAAGACGCTGATGGTTTGA

ACCAGTCACACGACCAGTAATAAAACATCGCC

CTGCAAGGTACGAGCCGGAAGCATTCAAAAGA

AGGAAACCTCGGCATTTTCGGTCAAGCCACCAAAAAAAAAAA

GAGGATCCCCGACCGTCTATCA

AAGAGAAGCCAGAACCACCACCAGTGAAACCA

AGGAAGGTTATAAACATCAAGA

AGCCGCCAGATTAGGATTAGCGGGATGTACCGAAAAAAAAAA

ATTAAAAAAAACCACCAGAAGGAGTGCACGTA

AGCATTAAGATTTAGTTTGACCATACTGGATA

TAACATCACTTGCCTGAGTAGAAGTCAATATCAAAAAAAAAA

TAAGAATAACGCGCCTGTTTATCAAACCTCCC

TAGATGGGCAATATGATATTCAACAAAAATTT

CGAGCTTCCTTATGCGATTTTAAGGAGATGGT

CCTCATTACAGTGCCCGTATAAACTGTCGTCT

AGGCTTGCCAGAGCCACCACCCTCCGAGAGGG

GCCACCCTAGGGAGTTAAAGGCCGCAACGGCT

CTAAGAACTTGAGCGCTAATATCAGACTCCTTAAAAAAAAAA

AACTAAAGCTAAACAACTTTCAACCAGGAGTG

CGATAGCTGTCAGATGAATATACATTATTAAT

GAAATCGGCAAAATCCCTTATAAAAAAGTGTA

GGGAGGGAAGGTCATACATGGC

AATAGTGAATAAAGAAATTGCGTAATTTTGCG

CCAACTTTAACGGAGATTTGTATCTTTTTTCA

GTCTGAAATGGATTATTTACATTGAGCAGAAG

AGAACCTATTTTTAACCTCCGGCTAAAGAACGAAAAAAAAAA

CAAAAACATCGCATTAAATTTTTGACGACGGCAAAAAAAAAA

TAACACTGTGCGCCGACAATGACAAAATACGTAAAAAAAAAA

AATGAATCCCGCTTCTGGTGCCGGCGTTGGTGAAAAAAAAAA

ATCAAGTTGAACTGGCATGATTAAGAGAGATAAAAAAAAAAA

AATCCAAAAGCCTAATTTGCCAGTATTTAGGC

AGCAAATGGACTTTACAAACAATTAACGGATT

CTTTCATCGTCTGGAGCAAACAAGATAAAGCCA

TTCCGGCAGGCCAACGCGCGGGGAGGCAACAG

CAGTACCACACCCTCAGAGCCACCGCGACAGAAAAAAAAAAA

ACATAACGCCCCCTCAAATGCTTTGAAGTTTC

ACAGAGGCGTAGTAAATTGGGCTTAACTGGCT

TTCCAGACATCTCCAAAAAAAAAGGGCGCGAAA

TAGCAAGGAAGGTGGCAACATATAATTAGACG

TCATCATAAACTGATAGCCCTAAAAGGGACAT

CGCCAAAGTTATTCATTAAAGGTGCGCAGTCT

AAGTATTAAAAAATCTAAAGCATCAGAACAAT

TTATCCTGGAAAATAGCAGCCTTTATTTTGTCAAAAAAAAAA

TTTAAAAGGAGGTGAGGCGGTCAGGCTCAATC

AAGCCTTTCGGATGGCTTAGAGCTTCAGAAGCAAAAAAAAAA

ACCCACAAGATATAGAAGGCTTATATCCCATC

GTACCGCCACCACCCTCAGCAG

CCGATAGTAGTTTCGTCACCAGTAGACTCCTC

GCCGTCAAAATATCAAACCCTCAAAACTCAAA

TGAGTAATAACTCCAACAGGTCAGTTTTAATT

GTATCGGCCTCTGGGCGCCAGG

GTGGTTTTTCTTTTCACCAGTGAGACGGAGGCGGT

CAGACCAGCCAGCGATTATACCAACTCCAAAA

GCGTCCAACACTATCATAACCCTCCGAACTGA

CCCCCTGCCTTGATATTCACAAACGAATTAGAAAAAAAAAAA

GAAAGCGTAAGAATACGTG

TATGCAACTAAAGCTAAATCGGTTAGGTCATT

CCAGACGAGTTTAGTATCATATGCGTGAGTGA

ATATGTACTTTAACCAATAGGAACCGCCAGGG

TTCATCAAATTTTTGAATGGCTATTCTGACCT

ACACAACACGATTAAGTTGGGTAAGCCATCAA

GAAAAGTAAGCGTTTGCCATCT

TTTCGCAAGGCATCAATTCTACTAAAAAGCCCAAAAAAAAAA

ATTCCATATTAGCAAAATTAAGCAAGAATCGA

TTAGAACCTAATTGCTCCTTTTGAAAGAGGAA

GCCAGCAAACCACGGAATAAGTTTACAGAGAGAAAAAAAAAA

GTTATATAATACTTCTGAATAATGGATGGCAA

GCTATTACGGTGCCTAATGAGTGAGTGGTTCC

ACCGTACTAAATCACCGGAACCAGTAGCCCCC

GATTCAAAAGGGGACGACGACA

CAGTGAATTTCCATTAAACGGGTAACAACCAT

CGAGAAAATCTTTCCTTATCATTCTTATTTTC

TCGCGCAGACATAAATCAATATATGTTATACAAAAAAAAAAA

CGTTGAAAGTTAGTAAATGAATTTTCAGTGCC

AGCAGGCGAAAATCCTGTTTGATGGCTAACTC

CATACATACCGGAAACGTCACCAAAGCCGCCG

CCAGCATTAGTATTAAGAGGCTGACAAACTAC

AGTTAGCGTAATTGTATCGGTTTACACTCATCAAAAAAAAAA

AAACAAAATTATATTTAACAAC

CGATTGGCCTATTTCGGAACCTATGCCCTCAT

GACGGAAAACAAAAGGGCGACATTTTTATCCC

GACTTGCGAACTGAACACCCTGAAAGAAAATA

ATAGCCCGAGATAGGGTTGAGTGTACAATTCC

TTGTTTGGATTACTATATGTAA

TTAATTTTCATCGGGAGAAACAATCGACAACT

TTGTGAATTACAAAGCGAACCA

GCCAACATGTATACAAAATAAA

CGTTTTCAGAGGAAACGCAATAATAATAATAA

GCAGACGGTGTCGAAATCCGCGACAAAGGAAC

TCTACGTTTTGCATCAAAAAGATTTAAGAGGTAAAAAAAAAA

AGTACCTTCTCATATATTTTAAATACAGTCAAAAAAAAAAAA

CACTCATCGAGGCCCTTTTTAA

TTTTCCCAAAATTGTTATCCGCTCTGTTCCAG

TCTTTAGGTGGCAAATCAACAGTTATTAGTAA

AAAGCGGAAATAAAACGAACTAACTGCTCATTAAAAAAAAAA

AATACCGAGAACAAGAAAAATAATCCGGTATT

AGTGAGAATAGCTGCTCCATGT

GAACCTCATAGATAATACATTTGATTACAAAA

CTGAATTTATAAGTTTTAACGGGGTCTGTATG

AACATGAAGACAGGAGGTTGAGGCATTACCAT

GAATATAAGACCCTGTAATACTTTTAGCTATT

CATTGAATCCAAAAGGAATTACGAACGGTGTAAAAAAAAAAA

CAGAACGATTTGAGGACTAAAGACGGTCGCTG

GTTTGAGGGTGAGAAAGGCCGGAGGCAATGCC

TTTTGATGATAAGTTTCAGCGG

ACAATCAAGACTTGAGCCATTTGGAAATAAAT

TGGTCAGTAGCACTAACAACTAATTCAATTACAAAAAAAAAA

ATAAATTGTCAATCATAAGGGAACGTTTACCA

AAACAGAAATTTATCAAAATCATATTAGTTAAAAAAAAAAAA

AGGGGGTATAAAAACCAAAATAGCAACGAGGC

GAAACAGTAGGCGAATTATTCATTAGATTAGA

GTTAAAATGGAAGATTGTATAAGCCGCGAGCT

AAATAATTAATCGTAAAACTAGCACAGGCAAG

AGGTCTTTAGGTAGAAAGATTCATGATATTCA

ATAACCTTTGCTTTGAATACCAAGGGATTTAG

GACTCCAACGTCAAAGGGCGAAAAGGTACCGA

GCTCGAATAGCTTGCATGCCTGCAAATATTTT

CTGAGCAATCATTTGAATTACCTTGCTCAACAAAAAAAAAAA

ATAAAACATTTGAGTAACATTATCGATTTTCA

TTGCGTATAGGAAGATCGCACTCCATCTGCCA

GGAGAATTGGAGGTTTTGAAGCCTGTTCAGCT

TGTTGGGATGCGTTGCGCTCACTGTTTGCCCC

CTGATAAAGTAATGGGATAGGTCAAAACCAGG

TCATGGAAATACCTACATTTTGACTATTAACA

CAAAGTACGAAAGAGGACAGATGAGGCATAGTAAAAAAAAAA

ATACTTCTTTGGAAAGGAATTG

GGTATTAAAATCCAATCGCAAGACTAGGTTGG

TTGTAAACGTTGGTCGACTCTA

AATTCTTACGACAAAAGGTAAAGTCTACAATTAAAAAAAAAA

TTTCATAATCACAGGAGGTTTA

GCAAAGAATAACAGTTGATTCCCATAAATATTAAAAAAAAAA

CGCCCACGAGCCCAATAGGAACCCGTTTTGCT

CTATCGGCCTTGCTGGTAATATCCACCTTGCT

CTAATTTATCTGACCTAAATTTAAGAAGAGTC

GAACAAAGTACCGAACGAACCACCGCAGATTC

TAAAGTACCCAGTATAAAGCCAACTTTTAATGAAAAAAAAAA

AGAGGCATTAATTGAGAATCGCCAATTACATT

GTTGCAGCAAGCGGTCCACGCTGGCCCGCTTT

GTAGGGCTTTTCGAGCCAGTAATAACGAGCGT

GACGACGAATAGTAAAATGTTTAGTAGATACA

ATTTAGGAGAGAATGACCATAAATGTTTTAAA

AAAAGCCTCGACAATAAACAACATTAAATCAA

TCTGGCCAACAGAGATAGAACCCTTAGTCTTT

AACGAGTACATCCAATAAATCATATGTCAATCAAAAAAAAAA

CAAGAGTAAAAGAATACACTAAAATCAGCTTG

CCAGTCGGCATTCGCCATTCAGGCAAACGGCG

TAAGTCCTCCGTGTGATAAATAAGAAACATAG

GAGGGTAAGCGAGGCGTTTTAGCGACAATAGA

TCGATAGCGTATGTTAGCAAACGTCAAAGTCA

AAGAGGCAATCTTGACAAGAACCGCAGTTGAG

GGATAGCACATAACCGATATATTCTTTTTCAT

GGAGCCTTTAACGATCTAAAGTTTAGTTAATG

AGACTACCCCATATCAAAATTATTCGGAATTA

TCAAAAATAATCTTACCAACGCTAAGAGAATAAAAAAAAAAA

ACCCGTCGATCTACAAAGGCTATCGTACCAAA

CAGTGCCATCGTAATCATGGTCATAGAACGTG

TTGATATAGCCTCCCTCAGAGCCGCTGTAGCG

TCAGAGCATAAAGTACGGTGTCTGAAACAGTT

AACGCCTGGTGAATTTCTTAAACATAAAACGA

AACATTATTGCTGTAGCTCAACATCAAAAATC

CGTATTAAAACAGTGCCACGCTGAAAAAACGC

GCTCATTTCCCGGTTGATAATCAGATAGTAGTAAAAAAAAAA

GCAAAGACAATCACCAGTAGCACCAGGTCAGAAAAAAAAAAA

GACCGGAAGCAGTGTAGGTAAA

CCTGTGTGGTCACGACGTTGTAAATTAAATCAAAAAAAAAAA

(C) 'C' design

TGAACGGTCGCGTCTGGCCTTCCTGGGATGTG

AAGCCTGGGCCAGCTGGCGAAAGGGTAGCCAG

ATGCTGATGCAACCAAGTACCG

TACTGGTAACCGTTCCAGTAAGCGTAAATATTAAAAAAAAAA

GCCCGAAACAGTCAGGACGTTGGGAGAAACAC

TAACAATTAAGAAGATGATGAAACCTAAAATA

TTTGGAACAAGAGTCCACTATTAAAGCTGTTT

GCACAGACAATTATAATCCTGA

TTGAGTAAAAGCCAGAATGGAAAGAATTATCA

TACTTAGCCGGGAGAGGCTTTT

CCGTCACCTAGAAAATTCATATGGGTTTAACG

AATGCCACATCAACGTAACAAAGCGGAACAAC

CATTTTTGATTTCAACGCAAGGATCGTTCTAG

TTAATTTCATCGGAACGAGGGTAGCTTTTGCGAAAAAAAAAA

AATAACATGCTATTTTGCACCCAGAATTCTGT

GCAAAAGAAGTTTAGCTATATT

GCAAATCAGAATTGAGTTAAGCCCAACGGAAT

ACCTTTTACCCTTAGAATCCTTGAGCGTTAAA

ACATTAATAGGGCGATCGGTGCGGGAGTAACA

AATGCGCGTTCCTGATTATCAGATGAAGGGTT

AGAACCGCGGCGGATAAGTGCCGTATTTTCAG

CCGGAACCAGTATAGCCCGGAATATCAGAACCAAAAAAAAAA

TTACCGAAAACAAGCAAGCCGTTTCAAGAACG

GAGCAAGAAATCATTACCGCGCCCAATCAATA

CAAAGCGCGAAACCTGTCGTGCCACTGAGAGA

GAAAAGGTATGGTCAATAACCTGTTTTGCCAGAAAAAAAAAA

ATTACGCAAGCACCGTAATCAGTAACCCTCAG

CGCCTGATGCTTCTGTAAATCGTCTTACTAGA

CTGATTGCCCTTCACCGCCTGGCCGCTGCATT

GATTGACCTTAATGCCGGAGAGGGTGCGGGAG

GCCTGAGAAACATTAAATGTGAGCGCCTCTTC

TTCATTTGGGGAAATATTTAAA

TTTGAGAGGATTCTCCGTGGGAACTGCGCAAC

ATCACCATCGCATCGTAACCGTGCAGCCAGCT

TTTGACCCGCGCATAGGCTGGCTGATGCAGAT

ACCCAAAATGCCTTTAGCGTCAGACCACCCTC

GGATCGTCCTCAGAACCGCCACCCGGTGTATCAAAAAAAAAA

CCGCCTGCATCCTTTGCCCGAACGGTAACAGT

CAGAAAACATACCACATTCAACTAACCTTCAT

CGAAAGACAGCAACTTTAATCA

AATGCAGAAACACCGGAATCATAAGCTATTAAAAAAAAAAA

TTATTAGCAGATAGCCGAACAAAGTAGCTATCAAAAAAAAAA

ATTATTACACCCTGACTATTATAGTAATTGCT

CAGCCATATTACAACCGATTGA

CTTTCCAGTAAGAAACGATTTTTTTTTACCAGAAAAAAAAAA

GATTAGTTAAAAACAGGGAAGCGCAAAGAAAC

TTACCCAATACGAAGGCACCAACCGCTTGATA

CATTATACGACTTCAAATATCGCGGATTAGAGAAAAAAAAAA

TTTCATCTCGAGCATGTAGAAACCAATAGCAA

ATCGGCTGCTTTTTCAAATATATTGGTCTGAGAAAAAAAAAA

GGATTTTGGAATTGCGAATAATAAATCGCCTGAAAAAAAAAA

AAGAGCAATACTGCGGAATCGTCAATTCTGCG

CTTTCGAGTAGCATTCCACAGACATATTCTGA

ATTACCGCCAGCCATTGCAACAGGGAGCCAGCAAAAAAAAAA

GAGGAAGTAAGGCTTGCCCTGACGAAGAAAAA

ATCGTAGGAACAATGAAATAGCAATTACCAGAAAAAAAAAAA

GGTTTAACTAGATTAAGACGCTGATGGTTTGA

ACCAGTCACACGACCAGTAATAAAACATCGCCAAAAAAAAAA

CTGCAAGGTACGAGCCGGAAGCATTCAAAAGA

AGGAAACCTCGGCATTTTCGGTCAAGCCACCAAAAAAAAAAA

GAGGATCCCCGACCGTCTATCA

AAGAGAAGCCAGAACCACCACCAGTGAAACCA

AGGAAGGTTATAAACATCAAGA

AGCCGCCAGATTAGGATTAGCGGGATGTACCG

ATTAAAAAAAAACCACCAGAAGGAGTGCACGTAAAAAAAAAA

AGCATTAAGATTTAGTTTGACCATACTGGATA

TAACATCACTTGCCTGAGTAGAAGTCAATATCAAAAAAAAAA

TAAGAATAACGCGCCTGTTTATCAAACCTCCC

TAGATGGGCAATATGATATTCAACAAAAATTT

CGAGCTTCCTTATGCGATTTTAAGGAGATGGTAAAAAAAAAA

CCTCATTACAGTGCCCGTATAAACTGTCGTCT

AGGCTTGCCAGAGCCACCACCCTCCGAGAGGG

GCCACCCTAGGGAGTTAAAGGCCGCAACGGCTAAAAAAAAAA

CTAAGAACTTGAGCGCTAATATCAGACTCCTT

AACTAAAGCTAAACAACTTTCAACCAGGAGTGAAAAAAAAAA

CGATAGCTGTCAGATGAATATACATTATTAATAAAAAAAAAA

GAAATCGGCAAAATCCCTTATAAAAAAGTGTA

GGGAGGGAAGGTCATACATGGC

AATAGTGAATAAAGAAATTGCGTAATTTTGCGAAAAAAAAAA

CCAACTTTAACGGAGATTTGTATCTTTTTTCA

GTCTGAAATGGATTATTTACATTGAGCAGAAGAAAAAAAAAA

AGAACCTATTTTTAACCTCCGGCTAAAGAACG

CAAAAACATCGCATTAAATTTTTGACGACGGC

TAACACTGTGCGCCGACAATGACAAAATACGT

AATGAATCCCGCTTCTGGTGCCGGCGTTGGTG

ATCAAGTTGAACTGGCATGATTAAGAGAGATA

AATCCAAAAGCCTAATTTGCCAGTATTTAGGC

AGCAAATGGACTTTACAAACAATTAACGGATTAAAAAAAAAA

CTTTCATCGTCTGGAGCAAACAAGATAAAGCC

TTCCGGCAGGCCAACGCGCGGGGAGGCAACAG

CAGTACCACACCCTCAGAGCCACCGCGACAGA

ACATAACGCCCCCTCAAATGCTTTGAAGTTTC

ACAGAGGCGTAGTAAATTGGGCTTAACTGGCTAAAAAAAAAA

TTCCAGACATCTCCAAAAAAAAGGGCGCGAAA

TAGCAAGGAAGGTGGCAACATATAATTAGACG

TCATCATAAACTGATAGCCCTAAAAGGGACATAAAAAAAAAA

CGCCAAAGTTATTCATTAAAGGTGCGCAGTCTAAAAAAAAAA

AAGTATTAAAAAATCTAAAGCATCAGAACAATAAAAAAAAAA

TTATCCTGGAAAATAGCAGCCTTTATTTTGTC

TTTAAAAGGAGGTGAGGCGGTCAGGCTCAATCAAAAAAAAAA

AAGCCTTTCGGATGGCTTAGAGCTTCAGAAGC

ACCCACAAGATATAGAAGGCTTATATCCCATC

GTACCGCCACCACCCTCAGCAG

CCGATAGTAGTTTCGTCACCAGTAGACTCCTC

GCCGTCAAAATATCAAACCCTCAAAACTCAAA

TGAGTAATAACTCCAACAGGTCAGTTTTAATTAAAAAAAAAA

GTATCGGCCTCTGGGCGCCAGG

GTGGTTTTTCTTTTCACCAGTGAGACGGAGGCGGT

CAGACCAGCCAGCGATTATACCAACTCCAAAA

GCGTCCAACACTATCATAACCCTCCGAACTGA

CCCCCTGCCTTGATATTCACAAACGAATTAGA

GAAAGCGTAAGAATACGTG

TATGCAACTAAAGCTAAATCGGTTAGGTCATT

CCAGACGAGTTTAGTATCATATGCGTGAGTGAAAAAAAAAAA

ATATGTACTTTAACCAATAGGAACCGCCAGGG

TTCATCAAATTTTTGAATGGCTATTCTGACCT

ACACAACACGATTAAGTTGGGTAAGCCATCAA

GAAAAGTAAGCGTTTGCCATCT

TTTCGCAAGGCATCAATTCTACTAAAAAGCCCAAAAAAAAAA

ATTCCATATTAGCAAAATTAAGCAAGAATCGA

TTAGAACCTAATTGCTCCTTTTGAAAGAGGAA

GCCAGCAAACCACGGAATAAGTTTACAGAGAG

GTTATATAATACTTCTGAATAATGGATGGCAA

GCTATTACGGTGCCTAATGAGTGAGTGGTTCC

ACCGTACTAAATCACCGGAACCAGTAGCCCCCAAAAAAAAAA

GATTCAAAAGGGGACGACGACA

CAGTGAATTTCCATTAAACGGGTAACAACCAT

CGAGAAAATCTTTCCTTATCATTCTTATTTTC

TCGCGCAGACATAAATCAATATATGTTATACA

CGTTGAAAGTTAGTAAATGAATTTTCAGTGCC

AGCAGGCGAAAATCCTGTTTGATGGCTAACTC

CATACATACCGGAAACGTCACCAAAGCCGCCG

CCAGCATTAGTATTAAGAGGCTGACAAACTAC

AGTTAGCGTAATTGTATCGGTTTACACTCATC

AAACAAAATTATATTTAACAAC

CGATTGGCCTATTTCGGAACCTATGCCCTCAT

GACGGAAAACAAAAGGGCGACATTTTTATCCCAAAAAAAAAA

GACTTGCGAACTGAACACCCTGAAAGAAAATA

ATAGCCCGAGATAGGGTTGAGTGTACAATTCC

TTGTTTGGATTACTATATGTAA

TTAATTTTCATCGGGAGAAACAATCGACAACTAAAAAAAAAA

TTGTGAATTACAAAGCGAACCA

GCCAACATGTATACAAAATAAA

CGTTTTCAGAGGAAACGCAATAATAATAATAA

GCAGACGGTGTCGAAATCCGCGACAAAGGAAC

TCTACGTTTTGCATCAAAAAGATTTAAGAGGT

AGTACCTTCTCATATATTTTAAATACAGTCAA

CACTCATCGAGGCCCTTTTTAA

TTTTCCCAAAATTGTTATCCGCTCTGTTCCAG

TCTTTAGGTGGCAAATCAACAGTTATTAGTAA

AAAGCGGAAATAAAACGAACTAACTGCTCATT

AATACCGAGAACAAGAAAAATAATCCGGTATT

AGTGAGAATAGCTGCTCCATGT

GAACCTCATAGATAATACATTTGATTACAAAAAAAAAAAAAA

CTGAATTTATAAGTTTTAACGGGGTCTGTATGAAAAAAAAAA

AACATGAAGACAGGAGGTTGAGGCATTACCAT

GAATATAAGACCCTGTAATACTTTTAGCTATT

CATTGAATCCAAAAGGAATTACGAACGGTGTA

CAGAACGATTTGAGGACTAAAGACGGTCGCTG

GTTTGAGGGTGAGAAAGGCCGGAGGCAATGCCAAAAAAAAAA

TTTTGATGATAAGTTTCAGCGG

ACAATCAAGACTTGAGCCATTTGGAAATAAATA

TGGTCAGTAGCACTAACAACTAATTCAATTAC

ATAAATTGTCAATCATAAGGGAACGTTTACCA

AAACAGAAATTTATCAAAATCATATTAGTTAA

AGGGGGTATAAAAACCAAAATAGCAACGAGGCAAAAAAAAAA

GAAACAGTAGGCGAATTATTCATTAGATTAGAAAAAAAAAA

GTTAAAATGGAAGATTGTATAAGCCGCGAGCTAAAAAAAAAA

AAATAATTAATCGTAAAACTAGCACAGGCAAG

AGGTCTTTAGGTAGAAAGATTCATGATATTCA

ATAACCTTTGCTTTGAATACCAAGGGATTTAGAAAAAAAAAA

GACTCCAACGTCAAAGGGCGAAAAGGTACCGA

GCTCGAATAGCTTGCATGCCTGCAAATATTTT

CTGAGCAATCATTTGAATTACCTTGCTCAACA

ATAAAACATTTGAGTAACATTATCGATTTTCAAAAAAAAAAA

TTGCGTATAGGAAGATCGCACTCCATCTGCCA

GGAGAATTGGAGGTTTTGAAGCCTGTTCAGCT

TGTTGGGATGCGTTGCGCTCACTGTTTGCCCC

CTGATAAAGTAATGGGATAGGTCAAAACCAGG

TCATGGAAATACCTACATTTTGACTATTAACA

CAAAGTACGAAAGAGGACAGATGAGGCATAGT

ATACTTCTTTGGAAAGGAATTG

GGTATTAAAATCCAATCGCAAGACTAGGTTGG

TTGTAAACGTTGGTCGACTCTA

AATTCTTACGACAAAAGGTAAAGTCTACAATT

TTTCATAATCACAGGAGGTTTA

GCAAAGAATAACAGTTGATTCCCATAAATATT

CGCCCACGAGCCCAATAGGAACCCGTTTTGCTAAAAAAAAAA

CTATCGGCCTTGCTGGTAATATCCACCTTGCTAAAAAAAAAA

CTAATTTATCTGACCTAAATTTAAGAAGAGTC

GAACAAAGTACCGAACGAACCACCGCAGATTCAAAAAAAAAA

TAAAGTACCCAGTATAAAGCCAACTTTTAATG

AGAGGCATTAATTGAGAATCGCCAATTACATT

GTTGCAGCAAGCGGTCCACGCTGGCCCGCTTT

GTAGGGCTTTTCGAGCCAGTAATAACGAGCGT

GACGACGAATAGTAAAATGTTTAGTAGATACAAAAAAAAAAA

ATTTAGGAGAGAATGACCATAAATGTTTTAAA

AAAAGCCTCGACAATAAACAACATTAAATCAA

TCTGGCCAACAGAGATAGAACCCTTAGTCTTT

AACGAGTACATCCAATAAATCATATGTCAATC

CAAGAGTAAAAGAATACACTAAAATCAGCTTG

CCAGTCGGCATTCGCCATTCAGGCAAACGGCG

TAAGTCCTCCGTGTGATAAATAAGAAACATAGAAAAAAAAAA

GAGGGTAAGCGAGGCGTTTTAGCGACAATAGA

TCGATAGCGTATGTTAGCAAACGTCAAAGTCA

AAGAGGCAATCTTGACAAGAACCGCAGTTGAG

GGATAGCACATAACCGATATATTCTTTTTCAT

GGAGCCTTTAACGATCTAAAGTTTAGTTAATG

AGACTACCCCATATCAAAATTATTCGGAATTAAAAAAAAAAA

TCAAAAATAATCTTACCAACGCTAAGAGAATA

ACCCGTCGATCTACAAAGGCTATCGTACCAAA

CAGTGCCATCGTAATCATGGTCATAGAACGTG

TTGATATAGCCTCCCTCAGAGCCGCTGTAGCG

TCAGAGCATAAAGTACGGTGTCTGAAACAGTT

AACGCCTGGTGAATTTCTTAAACATAAAACGA

AACATTATTGCTGTAGCTCAACATCAAAAATC

CGTATTAAAACAGTGCCACGCTGAAAAAACGCAAAAAAAAAA

GCTCATTTCCCGGTTGATAATCAGATAGTAGT

GCAAAGACAATCACCAGTAGCACCAGGTCAGA

GACCGGAAGCAGTGTAGGTAAA

CCTGTGTGGTCACGACGTTGTAAATTAAATCA